

ABSTRACT

Title of dissertation: **TRADING ADVANTAGES OF
STRUCTURED PRODUCTS
AND OPTION IMPLIED LIQUIDITY**

Yun Zhou, Doctor of Philosophy, 2011

Dissertation directed by: **Professor Dilip B. Madan
Department of Finance**

The two-price market theory is based on a new performance measure - acceptability indices, and provides a new way to describe incomplete markets. Unlike the classical option pricing theory, in which the risk-neutral measure is unique and derivatives are bought or sold at the same prices, in two-price markets - the uniqueness of risk-neutral measure is not guaranteed, and derivative prices are determined by the direction of the trade.

Based on the two-price market theory, this dissertation presents an argument for the advantages of trading options spreads and exotic options from investors' point of view. It is shown that from the investors' perspective, the price of buying these products is always lower than the price of trading their-component options separately, and the price of selling these options is always higher than the price of trading their-component options separately. The trading advantages of bull, bear, strangle and butterfly spreads, as well as cliquet options, reverse cliquet options and spread options, are illustrated with mathematical proofs and numerical work. We

also investigated the role of volatility, maturity, stress level and market skewness in the trading benefits of these products. It is observed that the greater the complexity of structured products, the greater packaging benefits of trading them.

Moreover, an investigation of liquidity risk implied by market option bid and ask prices was conducted. The liquidity risk parameter included in option bid and ask prices is modeled as a nonlinear function of strike prices and a linear function of maturities. The Variance Gamma Scaled Self-Decomposable process is used to model the risk-neutral process of the underlying asset. Calibration using market option bid and ask prices could help to reveal the model parameters. The analysis is performed on quarterly SPX, NDX and DJX options for the years 2007-2010. A detailed structure of the implied liquidity parameter suggests that call options are more liquid than put options. The implied liquidity parameter for at-the-money options suggests that great liquidity risk existed during the eruption of the subprime crisis in 2008.

TRADING ADVANTAGES OF STRUCTURED PRODUCTS AND
OPTION IMPLIED LIQUIDITY

by

Yun Zhou

Dissertation submitted to the Faculty of the Graduate School of the
University of Maryland, College Park in partial fulfillment
of the requirements for the degree of
Doctor of Philosophy
2011

Advisory Committee:
Professor Dilip B. Madan, Chair/Advisor
Professor Gerard Hoberg
Professor Doron Levy
Professor Tobias von Petersdorff
Professor Victor Yakovenko

© Copyright by
Yun Zhou
2011

Dedication

To

My uncle

Ni, Zhongming

Acknowledgments

I owe my utmost gratitude to my advisor Professor Dilip B. Madan, who has not just been an extraordinary scholar, but also a caring mentor, a role model, and a dear friend to me. His enthusiasm, wisdom, and depth of knowledge have been the driving forces in my graduate study. His encouragement and patience pulled me out of my frustration. His guidance and intuitions always enlightened me when I was lost. I feel myself extremely lucky to have him as my advisor. This invaluable experience working with him will always motivate me throughout my life.

I would like to thank my committee, Professors Gerard Hoberg, Doron Levy, Tobias von Petersdorff, and Victor Yakovenko for their invaluable time spent reviewing my thesis and giving suggestions. I also benefited from the excellent lecturing of Professors Doron Levy, Tobias von Petersdorff, and Gerard Hoberg. Special thanks go to Professor Steve Heston, who advised me on my very first project in math finance, and Professors Pete Kyle and Mark Lowenstein, who provided helpful discussion and wonderful lectures. My internship supervisors Dr. Violet Lo in Goldman Sachs, Mr. Raymond Zhang in Merrill Lynch, Dr. Jeffery Smith, and Mr. Jason Lindauer in Nasdaq also helped me to hone my skills and better understand my field of work.

Mrs. Alveda McCoy has always been willing to help and gives me the best suggestions. The journey could not be easy without her.

My colleagues and friends have enriched my life in many ways. Drs. Jun Wang, Su li, Huaqiang Ma and Wenqing Hu discussed with me my research and

future career extensively. I also benefited from talks with Pablo Federico, Dr. Lucas Vaczlavik and Scott Smith. Minghao Wu, Sean Rostini and Joespher Paulson have made this journey a joy. Thanks go to my friends in Virginia, who often play Texas Hold' em with me and have helped me to realize that life without risk is just too dull.

I would also like to thank those in OIT and Smith School, who provide great computing and data services, especially Mr. David McNabb and Mr. Chuck LaHaie. Most of my work was performed on the deepthought cluster and option data source is WRDS.

I am indebted to my family and can not find any words to express my feelings toward them. All the wonderful adventures I have had and could ever have are all because of them.

The best thing ever happen to me in the United States was to meet Xiaofei in Maryland. His generosity, optimism and perseverance have helped me get through the most depressing days, and made me stay to continue my American dream. He has lit up my life and turned it from black and white to technicolor. Without him, nothing would be worth doing.

Table of Contents

List of Tables	vii
List of Figures	ix
List of Abbreviations	xi
1 Introduction and Preliminary Background	1
1.1 Overview	1
1.2 Lévy Processes in Finance	7
1.2.1 Definition and Properties	7
1.2.2 Variance Gamma Model	11
1.2.3 Variance Gamma Scaled Self-Decomposable Process	12
1.3 The Fast Fourier Transform Based Methods in Option Pricing	14
1.3.1 Mathematical Statement	15
1.3.2 Numerical Comparison	18
1.3.3 Statistical Fit	20
2 The Conic Two-Price Markets	23
2.1 Introduction	23
2.2 Acceptability Index	26
2.2.1 Definition	26
2.2.2 Weighted Value at Risk (WVAR) Acceptability Indices	27
2.3 Option Pricing in Two-Price Markets	30
2.4 Hedging in Two-Price Markets	32
3 The Trading Advantages of Structured Products	36
3.1 Introduction	36
3.2 The Two-Price Markets	38
3.3 Option Spreads	39
3.3.1 Bull Spread	39
3.3.2 Bear Spread	47
3.3.3 Strangle	53
3.3.4 Straddle	59
3.3.5 Butterfly Spread	65
3.3.6 Risk Reversal	69
3.4 Exotic Options	73
3.4.1 Cliquet Options	73
3.4.2 Reverse Cliquet Options	75
3.4.3 Spread Option	78
3.5 Summary	89

4	Option Implied Liquidity	91
4.1	Introduction	91
4.2	Nonlinear Least Square	93
4.3	Model Estimation Analysis	96
4.4	Summary and Future Work	123
A	Proof of Trading Advantages of Option Spreads	124
	Bibliography	133

List of Tables

1.1	Moments of the Variance Gamma Process	12
1.2	Moments of the Variance Gamma Scaled Self-Decomposable Process	13
1.3	Estimated VG Parameters by MLE	22
3.1	Advantages of Trading a Cliquet (GBM) for 6, 12 and 24 Months	76
3.2	Advantages of Trading a Cliquet (VG) for 6, 12 and 24 Months	77
3.3	Advantages of Trading a Reverse Cliquet (GBM) for 6, 12 and 24 Months	79
3.4	Advantages of Trading a Reverse Cliquet (VG) for 6, 12 and 24 Months	80
3.5	Advantages of Trading a Spread Option with Noncorrelated Assets (Bivariate Normal): Correlation=0	82
3.6	Advantages of Trading a Spread Option with Correlated Assets (Bi- variate Normal): Correlation=0.25	83
3.7	Advantages of Trading a Spread Option with Correlated Assets (Bi- variate Normal): Correlation=0.5	84
3.8	Advantages of Trading a Spread Option with Correlated Assets (Bi- variate Normal): Correlation=0.75	85
3.9	Advantages of Trading a Spread Option with Correlated Assets (Bi- variate Normal): Correlation=-0.25	86
3.10	Advantages of Trading a Spread Option with Correlated Assets (Bi- variate Normal): Correlation=-0.5	87
3.11	Advantages of Trading a Spread Option with Correlated Assets (Bi- variate Normal): Correlation=-0.75	88
4.1	SPX OTM Calibrated Parameters : λ has four parameters.	99
4.2	SPX OTM Calibration Fit Statistics : λ has four parameters.	100
4.3	Standard Error: SPX OTM Calibrated Parameters (basis point)	101
4.4	Parameter Identification: SPX OTM Calibrated Parameters	102
4.5	NDX OTM Calibrated Parameters : λ has four parameters.	103
4.6	NDX OTM Calibration Fit Statistics : λ has four parameters.	104
4.7	Standard Error: NDX OTM Calibrated Parameters (basis point)	105
4.8	Parameter Identification: NDX OTM Calibrated Parameters	106
4.9	DJX OTM Calibrated Parameters : λ has four parameters.	107
4.10	DJX OTM Calibration Fit Statistics : λ has four parameters.	108
4.11	Standard Error: DJX OTM Calibrated Parameters (basis point)	109
4.12	Parameter Identification: DJX OTM Calibrated Parameters	110
4.13	SPX OTM Calibrated Parameters : λ has five parameters.	114
4.14	NDX OTM Calibrated Parameters : λ has five parameters.	115
4.15	DJX OTM Calibrated Parameters : λ has five parameters.	116
4.16	Standard Error: SPX OTM Calibrated Parameters (basis point)	117
4.17	Parameter Identification: SPX OTM Calibrated Parameters	118
4.18	Standard Error: NDX OTM Calibrated Parameters (basis point)	119
4.19	Parameter Identification: NDX OTM Calibrated Parameters	120

4.20	Standard Error: DJX OTM Calibrated Parameters (basis point)	. . .	121
4.21	Parameter Identification: DJX OTM Calibrated Parameters	122

List of Figures

1.1	Recovered density function of the VG model by FFT and COS	19
1.2	Error convergence for recovering the VG density function by FFT and COS	19
1.3	Data Fit by Normal and VG	21
2.1	Hedging strategy comparison of local quadratic error minimization and capital minimization with input variables $S_0 = [50 : 5 : 200]$, $K = 105$, $\sigma = 0.2$, $\theta = -0.3$ and $\nu = 0.5$. The underlying asset follows a Variance Gamma model.	35
3.1	Buy and sell advantages of trading a bull spread using GBM with input variables $S_0 = 100$, $K_2 = 120$, $\sigma = 0.2$ and $\lambda = 0.25$	44
3.2	Buy and sell advantages of trading a bull spread using GBM with input variables $S_0 = 100$, $K_2 = 120$, $\sigma = 0.2$ and $\lambda = 0.25$	45
3.3	Buy and sell advantages of trading a bull spread using VGSSD with input variables $S_0 = 100$, $K_2 = 120$, $\sigma = 0.2$, $\nu = 0.5$, $\gamma = 0.5$ and $\lambda = 0.25$	48
3.4	Buy and sell advantages of trading a bull spread using VGSSD with input variables $S_0 = 100$, $K_1 = 80$, $\sigma = 0.2$, $\nu = 0.5$, $\gamma = 0.5$ and $\lambda = 0.25$	49
3.5	Cumulative distribution function of VGSSD with T=1.	50
3.6	Buy and sell advantages of trading a bear spread using GBM with input variables $S_0 = 100$, $K_2 = 120$, $\sigma = 0.2$ and $\lambda = 0.25$	54
3.7	Buy and sell advantages of trading a bear spread using GBM with input variables $S_0 = 100$, $K_1 = 80$, $\sigma = 0.2$ and $\lambda = 0.25$	55
3.8	Buy and sell advantages of trading a bear spread using VGSSD with input variables $S_0 = 100$, $K_2 = 120$, $\sigma = 0.2$, $\nu = 0.5$, $\gamma = 0.5$ and $\lambda = 0.25$	56
3.9	Buy and sell advantages of trading a bear spread using VGSSD with input variables $S_0 = 100$, $K_1 = 80$, $\sigma = 0.2$, $\nu = 0.5$, $\gamma = 0.5$ and $\lambda = 0.25$	57
3.10	Buy and sell advantages of trading a strangle using GBM with input variables $S_0 = 100$, $K_2 = 120$, $\sigma = 0.2$ and $\lambda = 0.25$	60
3.11	Buy and sell advantages of trading a strangle using GBM with input variables $S_0 = 100$, $K_1 = 80$, $\sigma = 0.2$ and $\lambda = 0.25$	61
3.12	Buy and sell advantages of trading a strangle using VGSSD with input variables $S_0 = 100$, $K_2 = 120$, $\sigma = 0.2$, $\nu = 0.5$, $\gamma = 0.5$ and $\lambda = 0.25$	62
3.13	Buy and sell advantages of trading a strangle using VGSSD with input variables $S_0 = 100$, $K_1 = 90$, $\sigma = 0.2$, $\nu = 0.5$, $\gamma = 0.5$ and $\lambda = 0.25$	63
3.14	Buy and sell advantages of trading a straddle using GBM with input variables $S_0 = 100$, $\sigma = 0.2$ and $\lambda = 0.25$	66

3.15	Buy and sell advantages of trading a butterfly spread using GBM with input variables $S_0 = 100$, $K_2 = 120$, $\sigma = 0.2$ and $\lambda = 0.05$	70
3.16	Buy and sell advantages of trading a butterfly spread using VGSSD with input variables $S_0 = 100$, $K_2 = 120$, $\sigma = 0.2$, $\nu = 0.5$, $\gamma = 0.5$ and $\lambda = 0.05$	71
4.1	Market ask and bid option prices are blue circles and model ask and bid option prices are denoted by red dots. The risk-neutral model is VGSSD and data are OTM option prices on the SPX on December 31, 2008.	111
4.2	Estimated stress level λ is denoted by blue circles. The risk-neutral model is VGSSD and data are OTM option prices on the SPX on December 31, 2008.	112
4.3	Parameter identifications are across different maturities and strike price. The risk-neutral model is VGSSD and data are OTM option prices on the SPX on December 31, 2008.	113

List of Abbreviations

α	alpha
β	beta
VG	Variance Gamma
VGSSD	Variance Gamma Scaled Self-Decomposable
FFT	Fast Fourier Transform
MLE	Maximum Likelihood Estimation
RMSE	Root Mean Squared Error
ATM	at-the-money
OTM	out-of-the-money
ITM	in-the-money
OTC	over-the-counter

Chapter 1

Introduction and Preliminary Background

What you risk reveals what you value.

- Jeanette Winterson (1989)

1.1 Overview

European call and put options were first traded on the exchange market in London in the 17th century. Today, many derivatives are traded on the Over-The-Counter (OTC) market, which give the investors various choices to hedge and speculate. However, the birth of options can be traced back to the 16th century. Those option contracts were mainly for the tulip trade. In 1636, in order to speculate on the soaring price of tulips, extensive trading of options on tulips led to the crisis named tulip mania. History repeated itself in 2008, when the subprime mortgage crisis took place. This time, speculated assets are not tulips but housing prices, and the speculating instruments are not just options but more complicated derivatives. The aftermath of the subprime mortgage crisis has led to derivatives and the OTC market been blamed for the lack of regulations. On the other hand, the deficiencies of models that are used to study today's complex dynamic market invokes the research interest on risk and derivatives.

Risk or the uncertainty in stock prices determines the price of derivatives.

Stochastic processes are just one way to describe uncertainty in the future. The marriage of stochastic processes and finance started in 1900 when the first mathematical model to study the dynamics of stock markets was proposed by the French mathematician Louis Bachelier [4]. In his model, the stock price $S = \{S_t, t \geq 0\}$ at time t could be modeled as $S_t = S_0 + \sigma W_t$, where S_0 is the initial stock price, σ is the volatility of the stock prices and W_t is a Brownian motion or a Wiener process. Simply put, a Brownian motion $\{B_t : t \geq 0\}$ starts from 0 at the initial time with independent increments $B_{t_{i+1}} - B_{t_i}$ following a normal distribution $N(0, t_{i+1} - t_i)$ with zero mean and variance $t_{i+1} - t_i$. The brilliant idea to use a Brownian motion in modeling stock markets opened up a research area applying stochastic processes to stock markets. The major flaw in this model is that stock prices can be negative. During the following decades, a geometric Brownian motion (GBM) was introduced, demonstrating that the log stock price, $\ln S_t$, follows a Brownian motion, i.e.,

$$d\ln(S_t) = \mu dt + \sigma dW_t,$$

where μ is the drift of the process. Then, the stock price at time t , S_t could be written as:

$$S_t = S_0 e^{(\mu - \sigma^2/2)t + \sigma W_t}.$$

Compared with Bachelier's model, the stock price S_t follows a geometric normal distribution, rather than a normal distribution, which solves the problem of the existence of negative stock prices. Option valuation on GBM soon became a hot research topic in 1960s. However, researchers remained mired in the problem of finding the risk premiums of options. In 1970s, Fisher Black and Myron Scholes [11]

proposed the risk-neutral pricing method and dynamic hedging idea; this resulted in the unique analytical solutions of European call and put options, called the "Black-Scholes formula," by solving the stochastic partial differential equation. The story on how they came up with the option formula could be found in [10]. Later, Robert Merton [44] approached the same formula from other angles. Their work on the risk-neutral pricing and dynamic hedging lay down the foundation for asset pricing theory.

According to the asset pricing theory, all derivatives are priced under risk-neutral measure in order to satisfy the non-arbitrage condition. Under the risk-neutral measure Q , the drift μ in the GBM is the risk-free rate. For example, to price a European call option, with the strike price K , the expiration date T , the risk free rate r and the volatility as σ , the price of the European call at time t is given by

$$C(t) = e^{-r(T-t)} E^Q[(S_T - K)^+].$$

This equation states that the option price at time t is the expectation of the terminal payoff under the risk-neutral measure discounted at the risk-free rate.

Under the risk-neutral measure Q , the discounted stock price and the discounted values of derivatives are martingales. Hence, the discounted stock price and the discounted values of derivatives have no tendency to rise or fall during the following time period. The option prices valued under the risk-neutral measure are no different than under other probability measures, for instance, the physical measure. The reason that there is no pricing under the physical measure is that the

discounted rate for the expected payoff under the physical measure could not be easily obtained. On the other hand, the expected log return of any stock and the discounted rate are the risk-free rate r under the risk-neutral measure. Black and Scholes noticed that the option pricing process is independent of the risk preferences; here, this is represented in the model as μ . In other words, the expected rate of log return on the underlying stock in the real world is not involved in the option valuation. Therefore, we can treat the risk-neutral measure as an artificial device for obtaining option prices.

The other major contribution of the Black-Scholes-Merton (BSM) model is dynamic hedging. The option could be replicated by trading the stock and a money market account dynamically in any infinitesimal time interval. In other words, we can build up a riskless portfolio of the stock and the derivative. In a very short time period, the gain or loss from the stock position offsets the gain or loss from the derivative position. This is because the sources of uncertainties in the stock and the option are the same: the movement in stock prices. Hence, the expected return of this portfolio is the risk-free rate during this short time period. The delta hedging states that for a short position in one call option, a long position in δ , number of shares of stock would make this portfolio riskless, where $\delta = \partial C / \partial S$. δ is then defined as the rate of change in the option prices with respect to the stock prices. The dynamic delta-hedging requires that we continuously rebalance the position in stocks in order to make the portfolio riskless in any infinitesimal time interval. We can also see that the δ of the position in the stock offsets the δ of the position in the option. This makes the δ in the riskless portfolio zero. In any infinitesimal time

interval, we have $\Delta C = \delta \Delta S$, and thus, the hedging cost $\delta \Delta S$ is indeed the option price.

The successful BSM model as long as the Greeks became an extraordinary powerful tool in research and trading. Empirical studies also demonstrate the deficiencies in this model [21]. First, the implied volatility obtained by fitting the market option prices by the BSM model is a function of strike price K with a shape called the "volatility smile," whereas the volatility is assumed as a constant in the model. Second, the generic properties of Brownian motion - continuity and scale invariance - are not suitable descriptors for price behavior. Jumps exist in the paths of stock prices over all time scales, especially short horizons (like intraday). Continuity in Brownian motion is insufficient to portray price movement. The scale invariance states that the statistical properties of randomness in stock prices are all the same for all time horizons. Market price behavior shows that jumps dominate the movement in short time scales, and continuities dominate for long time scales. Merton [45] then introduced a jump model into financial modeling. After that, studies of the combination of diffusion and jump processes, i.e., Lévy processes enrich the research of mathematical finance. Popular Lévy processes, will be presented in Section 1.2.

In the BSM world, the market is complete with existence of only one risk-neutral measure. The benefit of being in complete markets is that all derivatives can be perfectly replicated or hedged. This makes derivatives redundant in complete markets. The prices of derivatives are the hedging costs. In a world with jumps, market completeness becomes an exception, derivatives are not redundant, the risk-

neutral measure is not unique and a perfect hedge does not exist. Under the BSM model, a European call option is an instantaneously linear function of the underlying asset in continuous time, resulting in perfect hedging. When jumps come in, the linearity breaks down with positive variance of the jump term, which makes option prices a nonlinear function of the underlying assets. This is the reason why a perfect hedge does not exist in jump diffusion processes [21]. Incomplete markets are a fact of life in the real world. Hedging in incomplete markets is necessary to minimize the risk between the target payoff and its approximation by a trading strategy [26]. Thus, measuring this risk leads to various kinds of hedging approaches. The common ways to hedge in incomplete markets are: superhedging, utility optimization, local quadratic hedging, mean-variance hedging, and etc. Three important theories to price and hedge in incomplete markets are indifference pricing [13], good deal bounds [9] and coherent risk measures [3]. The conic finance theory [18] used in this study is developed based on the coherent risk measures.

Cherny and Madan [18] developed a new performance measure called indices of acceptability. These indices of acceptability are used to evaluate the quality of cash flows, similar to the Sharpe ratio and the Gain Loss ratio, with improved economical properties. The acceptability index, defined as a nonnegative real number, is associated with a collection of random cash flows that are acceptable at this nonnegative real number. They then proposed conic finance theory [19], which described the illiquid market as a counterparty. Bid and ask prices can be valued by the distorted expectation, with acceptability indices as parameters. These closed-form formulas for the bid and ask prices of European options are easily implemented and make

possible the calibration of bid and ask option prices at the same time. The many applications of the conic finance theory include credit, liquid risk modeling [23] [34] using option prices, capital, profit, leverage and rate of return [17], dynamic gamma hedging using nonuniform grids [30], dynamically consistent bid and ask prices using a Markov chain [36], and etc. This two-price market based on the conic finance theory does not only use option surface calibration for the mid-quote, with prices never traded on the market. It also provides a new approach to studying the liquidity risk.

The rest of Chapter 1 will briefly introduce the Lévy processes that will be used in this study, and the Fast Fourier Transform (FFT) based methods widely used for recovering probability density function, distribution function and option pricing. Chapter 2 will present the general idea of conic finance theory and how to carry out option pricing in two-price markets. In Chapter 3, trading advantages of structured products will be studied using the two-price market theory. Analysis on options spreads and exotic options illustrate the benefits of packaging from the investor's perspective. The option implied liquidity will be studied in Chapter 4. Analysis on major index options through the lens of the subprime mortgage crisis offers insight into liquidity risk.

1.2 Lévy Processes in Finance

1.2.1 Definition and Properties

Definition 1.1. *Lévy Process*

Lévy Proces is a "cadlag" (right continuous and left limit) stochastic process $X = \{X_t, t \geq 0\}$ on $(\Omega, \mathcal{F}, \mathbb{P})$ with the following properties:

1. $X_0 = 0$.
2. These random variables $X_{t_{i+1}} - X_{t_i}$, for any $0 \leq t_i \leq t_{i+1}$ are independent.
3. These increments $X_{t_i+\Delta t} - X_{t_i}$ are stationary: the law of $X_{t_i+\Delta t} - X_{t_i}$ is independent of time t .
4. Jumps occur at random times, i.e., $\forall \epsilon > 0, \lim_{\Delta t \rightarrow 0} P(|X_{t+\Delta t} - X_{t_i}| \geq \epsilon) = 0$

One special property of Lévy processes is infinitely divisibility, which states that the random variable X_t has the same distribution of a sum of n i.i.d. random variables whose distribution is that of $X_{t/n}$, for any $t > 0$ and $n > 1$.

Definition 1.2. *Infinitely Divisible*

If the n -th convolution root of a probability distribution F is also a probability distribution, for any integer $n > 1$, the distribution F is said to be infinitely divisible.

Some examples of infinitely divisible laws are the Gaussian distribution, the Gamma distribution, α -stable distribution and the Poisson distribution. The following proposition states the relationship between the infinitely divisibility and Lévy processes.

Proposition 1.3. *For any Lévy processes $X = \{X_t, t \geq 0\}$, for every t , $\{X_t\}$ has an infinitely divisible distribution. Conversely, given any infinitely divisible distribution F , there is a Lévy processes $\{X_t\}$ with the distribution of $\{X_1\}$ given by F .*

This proposition implies that as long as we know the distribution of $\{X_t\}$ at a unit time, then the corresponding Lévy process $\{X_t\}$ is determined. Using

this proposition, the characteristic function of a Lévy process $\{X_t\}$, $\Phi_X(u)$ can be written as:

$$\Phi_X(u) = e^{t\psi_{X_1}(u)},$$

where $\psi_{X_1}(u)$ is called the characteristic exponent of $\{X_t\}$. If we know a general expression for the characteristic function of any infinitely divisible distribution, all Lévy processes could be specified. Lévy-Kinchin formula presents the general expression for the characteristic function of Lévy processes.

Theorem 1.4. *Lévy-Kinchin Representation*

For any Lévy process $X = \{X_t, t \geq 0\}$ with characteristic triplet (A, ν, λ) , its characteristic function can be represented as:

$$\Phi_X(u) = e^{t\psi_{X_1}(u)},$$

with

$$\psi_{X_1}(u) = i\lambda u - \frac{1}{2}Au^2 + \int_{\mathbb{R}} (e^{iux} - 1 - iux1_{x \leq 1})\nu(dx). \quad (1.1)$$

In order to address the problem that how the statistical properties of return $r(\Delta t)$ change with the time resolution Δt , issues on scale invariance and self-similarity were studied during 1990s. In other words, given a stochastic process $X = \{X_t, t \geq 0\}$, we want to study whether the statistical properties change or not at different time resolutions.

Definition 1.5. *Self-similarity*

A stochastic process $X = \{X_t, t \geq 0\}$ is called self-similar if we have:

$$X_t \stackrel{d}{=} t^\lambda X_1,$$

with the self-similar exponent $\lambda > 0$.

This states that the two X_t and $c^\lambda X_1$ have the same distribution. The most famous self-similar process is non-drift Brownian motion with $\lambda = 1/2$, and Brownian motion with drift is not a self-similar process but a self-affine process [21]. The only self-similar processes in Lévy processes are the symmetric α -stable processes with the self-similar exponent $\lambda \in [\frac{1}{2}, \infty]$ [21]. The symmetric α -stable processes include the non-drift Brownian motion and processes with infinite variance. The self-similarity in Lévy processes is due to heavy tailed independent increments.

Self-decomposable laws are associated with limit laws which state the laws of centered sum of n independent random variables scaled by some constants when n goes to infinity. The central limit theorem is a special case of limit laws. Lévy and Khintchine connected self-decomposable laws with limit laws.

Definition 1.6. *Self-decomposable Laws*

For any constant c , $c \in (0, 1)$, a random variable X is said to be self-decomposable if

$$X \stackrel{d}{=} cX + X^{(c)},$$

where the random variable $X^{(c)}$ is independent of X .

The above equation states that the distribution of self-decomposable random variables can be written as the sum of two parts, one is a scale down version of its own cX , and the other is independent residuals $X^{(c)}$. Self-decomposable laws are subclass of infinitely divisible laws. The characteristic function of the self-decomposable

laws has the following form:

$$E[e^{iux}] = \exp\left(ibu - \frac{1}{2}Au^2 + \int_{-\infty}^{\infty}(e^{iux} - 1 - iux1_{|x|<1})\frac{h(x)}{|x|}dx\right),$$

where $A \geq 0$, b is a real constant, $\int_{-\infty}^{\infty}(e^{iux} - 1 - iux1_{|x|<1})\frac{h(x)}{|x|}dx < \infty$. $h(x)$ is called the self-decomposability characteristic (SDC). Carr et al. [15] summarized the special condition for infinitely divisible laws being self-decomposable based on their characteristic functions. If the self-decomposability characteristic (SDC), $h(x)$, is increasing with negative x and decreasing for positive x , this infinitely divisible law is self-decomposable. They then built up the processes associated with a self-decomposable law at unit time.

1.2.2 Variance Gamma Model

The variance gamma process (VG) was first developed by Madan and Seneta [42] as a two-parameter model, which is now called the symmetric variance gamma process. Then Madan and Milne [35], Madan et al. [33] extended this model to a three-parameter variance gamma model. Within the variance gamma process, the Brownian motion at a random time change is given by a gamma process. In other words, the continuously compound return during a unit time is normally distributed, conditional on the realization of a random time, where the random time has a gamma density. These three parameters are: the volatility of the Brownian motion σ , the variance rate of the gamma time change ν and the drift of the Brownian motion θ .

Definition 1.7. *Variance Gamma*

If a random variable $X_{VG}(t; \sigma, \nu, \theta)$ follows a variance gamma process, the process

can be written as

$$X_{VG}(t; \sigma, \nu, \theta) = \theta g(t; \nu) + \sigma W(g(t; \nu)),$$

where $g(t; \nu)$ is a gamma process. The characteristic function is

$$\Psi_{VG}(u) = (1 - i\theta\nu u + \sigma^2 u^2 \nu / 2)^{-\frac{1}{\nu}}. \quad (1.2)$$

Variance gamma can be proved to be self-decomposable since its self-decomposability characteristic $h(x)$ is increasing with negative x and decreasing for positive x . Table 1.1 lists the characteristics of the Variance Gamma distribution.

Table 1.1: Moments of the Variance Gamma Process

$VG(\theta, \sigma, \nu)$	
Mean	θ
Variance	$\sigma^2 + \nu\theta^2$
Skewness	$\theta\nu(3\sigma^2 + 2\nu\theta^2)/(\sigma^2 + \nu\theta^2)^{3/2}$
Kurtosis	$3(1 + 2\nu - \nu\sigma^4/(\sigma^2 + \nu\theta^2)^2)$

1.2.3 Variance Gamma Scaled Self-Decomposable Process

The risk-neutral process for the stock price $S(t)$ of Variance Gamma Scaled Self-Decomposable (VGSSD) model follows:

$$S(t) = S(0)e^{rt} \frac{e^{Y(t)}}{E[e^{Y(t)}]},$$

where $Y(t)$ is a self-similar additive process with $Y(\lambda\mu t) \stackrel{d}{=} a(\lambda)a(\mu)Y(t)$, $a(t) = t^\lambda$, r is the risk free rate. Then the characteristic function of $\ln(S(t))$ is

$$E[e^{iu\ln(S(t))}] = e^{iu(\ln(S(0))+rt-\ln(\Psi_{Y(t)}(-i)))}\Psi_{Y(t)}(u). \quad (1.3)$$

The law of $Y(t)$ as $t^\lambda X(1)$, where $X(1)$ follows a VG process, is

$$\Psi_Y(u, t) = (1 - i\theta\nu ut^\lambda + \sigma^2 u^2 t^{2\lambda} \nu/2)^{-1/\nu}. \quad (1.4)$$

Substitute Eq(1.4) into (1.3), the distribution law of the log stock price at any maturity could be obtained. The moments of VGSSD presented in [47] are listed in Table 1.2.

A recent review on stochastic processes in finance by Madan [31] summarized Lévy processes and Sato processes. More description on jump processes could be found in [21] [48].

Table 1.2: Moments of the Variance Gamma Scaled Self-Decomposable Process

$VGSSD(\theta, \sigma, \nu, \gamma)$	
Mean	θt^γ
Variance	$(\sigma^2 + \nu\theta^2)t^{2\gamma}$
Skewness	$\theta\nu(3\sigma^2 + 2\nu\theta^2)/(\sigma^2 + \nu\theta^2)^{3/2}$
Kurtosis	$3(1 + 2\nu - \nu\sigma^4/(\sigma^2 + \nu\theta^2)^2)$

1.3 The Fast Fourier Transform Based Methods in Option Pricing

Since the development of the famous Black-Scholes option model, more complicated option models have been developed. Unfortunately, unlike the Black-Scholes model, most of them do not have closed-form solutions. Thus, efficient numerical methods are needed to price complex financial derivatives and calibrate various financial models. There are three major types of numerical methods used for option pricing: 1) Monte Carlo simulation, 2) partial integro differential equation, and 3) numerical integration. Carr and Madan's [16] FFT method has been widely used in model calibration and option pricing as a numerical integration method. They compared the numerical results of option pricing with the analytical solution and other traditional methods. The use of FFT is faster and offers considerable accuracy. Later, Fang and Oosterlee [24] [25] proposed the COS method, which is an FFT-based method but focuses on the Fourier-cosine expansion to recover the probability density function (PDF) from the characteristics function of Lévy processes. It was shown that the COS method for recovering PDF converges faster than the Carr and Madan FFT method. The COS method is applied to recover the PDF and the cumulative distribution function (CDF) in this section. Then, the results are compared with the PDF and CDF recovered from the Carr and Madan's FFT method, as well as the analytical solutions. The recovered PDF could be used for model calibration on physical measure, and the recovered CDF could be used for further option pricing.

1.3.1 Mathematical Statement

In Carr and Madan [16] FFT method, the FFT is used to compute European option price from a given characteristic function. Let $f(x)$ be the probability density function and $\Psi(u)$ be the characteristic function. Apply the Fourier transform and the inverse Fourier transform, we have:

$$\Psi(u) = \int_{\mathbf{R}} e^{iux} f(x) dx. \quad (1.5)$$

Nyquist relation to the grid sizes in the two domains gives:

$$dxdu = \frac{2\pi}{N}, \quad (1.6)$$

where N denotes the number of grid points. According to the inverse Fourier transform, we have:

$$f(x) = \frac{1}{\pi} \int_0^{\infty} e^{-iux} \Psi(u) du. \quad (1.7)$$

Then the FFT algorithm is used to compute the following:

$$\Psi(k) = \sum_{j=1}^N e^{-i\frac{2\pi}{N}(j-1)(k-1)} \psi(j). \quad (1.8)$$

Let the truncation range on R be $[-b, b]$, then,

$$x_k = -b + dx(k-1), k = 1, \dots, N.$$

and

$$u_j = du(j-1), j = 1, \dots, N.$$

Thus,

$$f(x_k) = \frac{1}{\pi} \sum_{j=1}^N e^{-i\frac{2\pi}{N}(j-1)(k-1)} e^{ibu_j} \psi(u_j) du. \quad (1.9)$$

Although no explicit derivation of CDF is given in Carr and Madan [16], their way to price options could be adapted to derive the distribution function. Let $f(x)$ be the PDF of the random variable x , and $F(k)$ be the CDF, where $1 - F(k) = \int_k^\infty f(x)dx$. Let $g(k) = e^{\alpha k}(1 - F(k))$, where α is a constant. We have,

$$\begin{aligned}
\psi(u) &= \int_{-\infty}^{\infty} e^{iuk} g(k) dk \\
&= \int_{-\infty}^{\infty} e^{iuk} e^{\alpha k} (1 - F(k)) dk \\
&= \int_{-\infty}^{\infty} e^{iuk} e^{\alpha k} \int_k^\infty f(x) dx dk \\
&= \int_{-\infty}^{\infty} f(x) \int_{-\infty}^x e^{iuk + \alpha k} dk dx \\
&= \int_{-\infty}^{\infty} f(x) \frac{e^{(\alpha + iu)k}}{\alpha + iu} dx \\
&= \frac{\phi(u - i\alpha)}{\alpha + iu}.
\end{aligned}$$

Then,

$$g(k) = \frac{1}{2\pi} \int_{-\infty}^{\infty} e^{-iuk} \frac{\phi(u - i\alpha)}{\alpha + iu} du.$$

Thus,

$$F(k) = 1 - \frac{e^{-\alpha k}}{2\pi} \int_{-\infty}^{\infty} e^{-iuk} \frac{\phi(u - i\alpha)}{\alpha + iu} du. \quad (1.10)$$

Similarly, the inverse form by the cosine transform method could also be obtained. The following part illustrates the inverse Fourier integral by the cosine expansion for recovering the PDF from a given characteristics function. For function $f(\theta)$ on $[0, \pi]$, the cosine expansion reads:

$$f(\theta) = \sum_{k=0}^{\infty'} A_k \cos(k\theta),$$

where $A_k = \frac{2}{\pi} \int_0^\pi f(\theta) \cos(k\theta) d\theta$, and \sum' denotes that the first term is weighted by

0.5. For $x \in [a, b] \in \mathbb{R}$, change of variables gives $x = \frac{b-a}{\pi}\theta + a$. Then, we can get

$$f(x) = \sum_{k=0}^{\infty'} A_k \cos \left(k\pi \frac{x-a}{b-a} \right). \quad (1.11)$$

Given Equation (1.7), we have the coefficients A_k ,

$$A_k = \frac{2}{b-a} \operatorname{Re} \left(\Psi \left(\frac{k\pi}{b-a} \right) e^{-i \frac{k a \pi}{b-a}} \right),$$

where "Re" denotes the real part. Thus, the PDF $f(x)$ is :

$$f(x) = \sum_{k=0}^{N-1'} A_k \cos \left(k\pi \frac{x-a}{b-a} \right). \quad (1.12)$$

In order to get the CDF, the discrete sine transform is used instead. The discrete sine transform of the PDF $f(x)$ can be expressed similarly as the cosine expansion,

$$f(x) = \sum_{k=1}^{N'} B_k \sin \left(k\pi \frac{x-a}{b-a} \right), \quad (1.13)$$

with coefficients

$$B_k = \frac{2}{b-a} \operatorname{Imag} \left(\Psi \left(\frac{k\pi}{b-a} \right) e^{-i \frac{k a \pi}{b-a}} \right).$$

Thus, integrate the equation (1.13), the CDF $F(x)$ in terms of the sine expansion of density function is written as:

$$F(x) = - \sum_{k=1}^{N'} B_k \left(\sin \left(k\pi \frac{x-a}{b-a} \right) - 1 \right) \frac{b-a}{k\pi}. \quad (1.14)$$

The convergence of the series expansion representation of distribution function $F(x)$ can be proved by the following lemma.

Lemma 1.8. *If $f(x) = \sum_{k=1}^{N'} B_k \sin(k\theta)$, and $F(x) = \int_{-\infty}^x f(\theta) d\theta$, then Equation (1.14) converges to $F(x)$.*

Proof. It is known that the sine series of $f(\theta)$ converges to $f(\theta)$, which means the limit of the tails, i.e., the sum of the residual terms after the N -th term in the summation, is zero. In Equation (1.14), the new coefficients of $F(x)$ are $\frac{B_k}{k}$. Thus, the sum of the new tails is smaller than that of $f(\theta)$ by a factor better than N , since $N+1$ is the start term of the residual tail. Therefore, the new series converges faster than the previous one, i.e., the new series expansion of $F(x)$ based on the sine expansion of $f(x)$ converges faster than the sine series expansion of $f(\theta)$. ■

1.3.2 Numerical Comparison

Fang and Oosterlee [24] gave a truncation range of the distribution of log return i.e., $\log(S_t/S_0)$, using the COS method.

$$[a, b] = [c_1 - L\sqrt{c_2 + \sqrt{c_4}}, c_1 + L\sqrt{c_2 + \sqrt{c_4}}]$$

with $L = 10$ and c_n denotes the n -th cumulant of the distribution of the log return. Figure 1.1 shows the recovering PDF and CDF of a VG model using these two methods with inputs $\theta = -0.14$, $\nu = 0.2$, and $\sigma = 0.12$. Figure 1.2 presents the maximum error over the whole domain on \log_{10} base of the two methods when recovering PDF of the VG distribution. The faster convergence rate of the COS method was shown in Fang and Oosterlee [24]. Similar as the FFT, the COS method has the complexity of $O(N\log N)$. Given the same N , they share similar computational speed. With the faster error convergence, the COS method could spend less time than the FFT to reach the same accuracy.

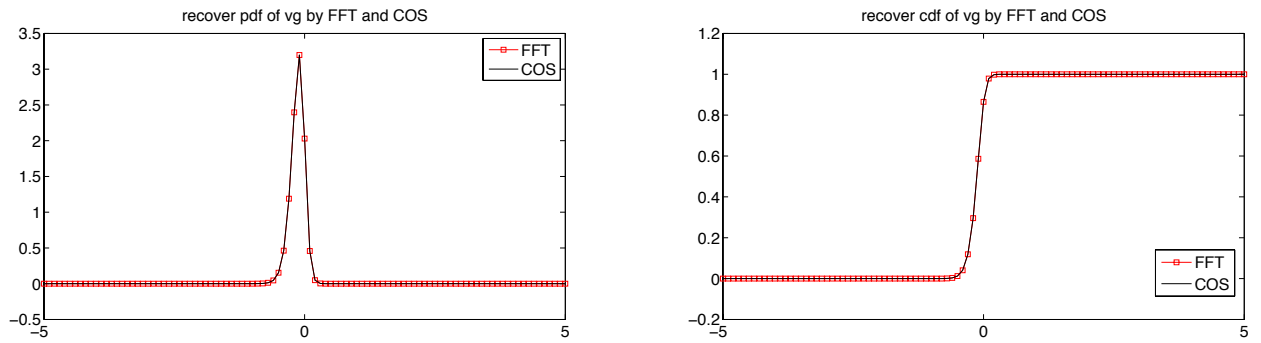


Figure 1.1: Recovered density function of the VG model by FFT and COS

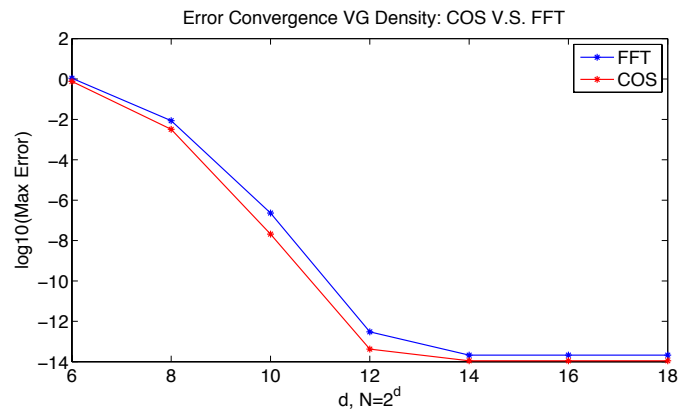


Figure 1.2: Error convergence for recovering the VG density function by FFT and COS

1.3.3 Statistical Fit

Seneta [49] presented a study on fitting the variance-gamma model to log returns. Here, two methods - FFT and COS - are used to calibrate models. Six stocks (Amazon, Apple, Dell, Cisco, IBM and Intel) were selected from the technology and industry sector. The study examined the period between January 1, 2001 and December 31, 2004. The length of the data is 1004 for each stock. For each stock, the log returns need to subtract their respective mean value. The Maximum likelihood Estimation (MLE) is used for statistical model calibration. The following is a brief of MLE. Let N denote the number of observations, $X_t(\sigma, \theta, \nu)$. $f(x; \sigma, \theta, \nu)$ denotes the PDF of $X_t(\sigma, \theta, \nu)$, the log likelihood function can be expressed as:

$$L(\sigma, \theta, \nu) = \sum_{i=1}^N \log (f(x; \sigma, \theta, \nu)). \quad (1.15)$$

Then, the value of parameters σ , θ and ν can be obtained by maximizing the log likelihood function L . Table 1.2 gives the estimation results for the three parameters of Variance Gamma (VG) distribution. Madan [33] mentioned that θ is insignificant when using a daily log return to calibrate VG. The reason is that θ is the parameter for the drift of the Brownian motion, and the daily log return has a very small drift close to zero. Thus, the other two parameters are much more important to determine the VG process for the distribution of daily log return data. Figure 1.3 presents the empirical distribution of the market data with the calibrated VG and normal distribution. The VG fit obviously gives a better statistical description on the tails and peakness of the empirical distribution on all of the six stocks. The statistics test also reveals the same information.

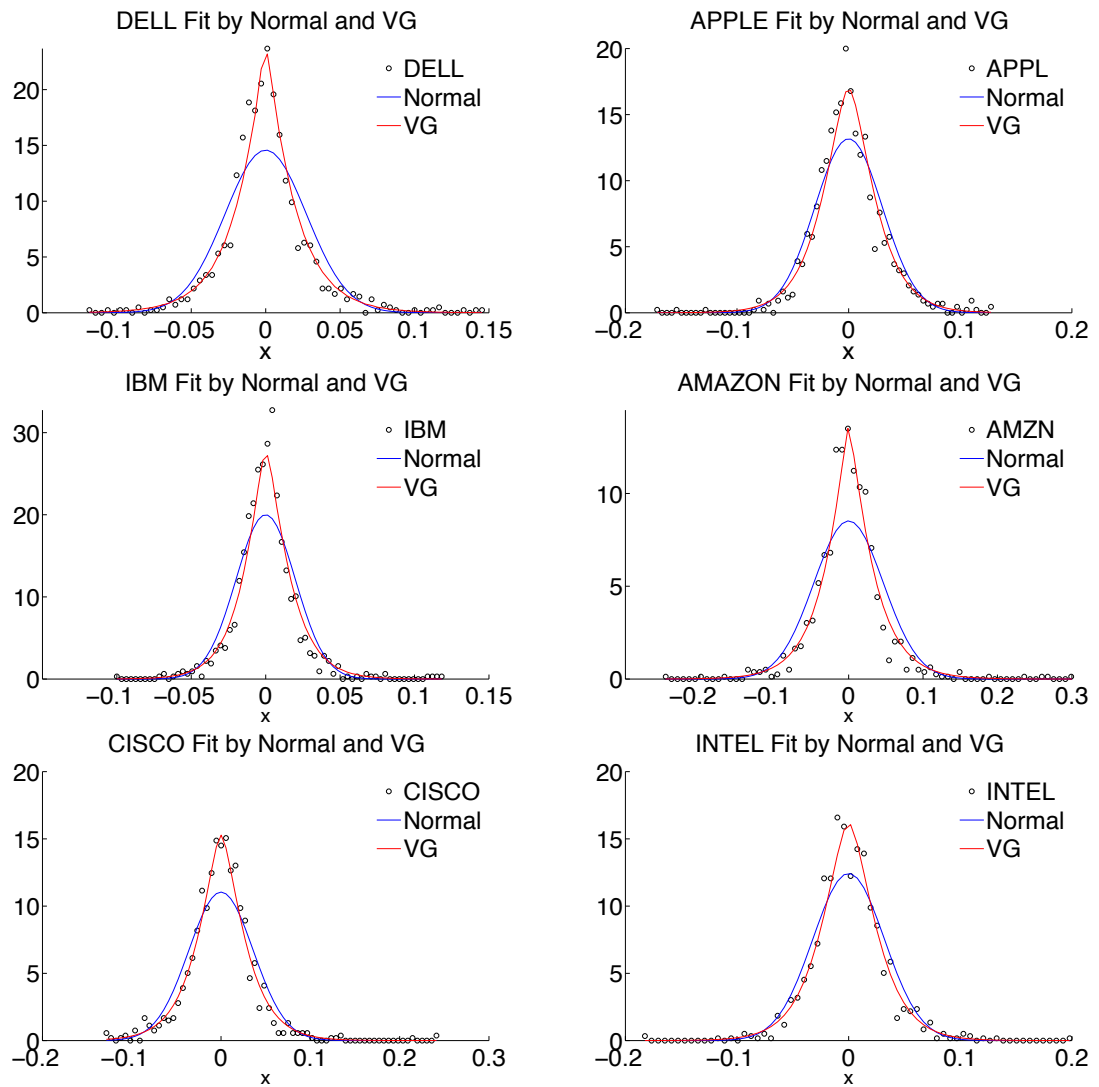


Figure 1.3: Data Fit by Normal and VG

Table 1.3: Estimated VG Parameters by MLE

NAME	θ	ν	σ
DELL	0.00008	0.9095	0.0271
APPL	-0.00004	0.5508	0.0303
IBM	0.0009	0.7094	0.0204
AMZN	0.0010	0.8292	0.0450
CISCO	0.0002	0.6392	0.0354
INTEL	0.0000	0.5335	0.0315

In statistics, the Kolmogorov-Smirnov test (KS-test) is widely used as a tool to test these estimated parameters. The KS-test quantifies the distance between the empirical distribution function of the samples and the cumulative distribution function of the reference distribution. The KS-test used here has a significance level of 5%, used to determine whether the data is from the distribution of the VG process with the estimated parameters. The results are positive for the 6 stocks.

Chapter 2

The Conic Two-Price Markets

2.1 Introduction

The evaluation of trading strategies or investment is always a major concern in financial markets. A simple and powerful tool for measuring cash flows is the Sharpe ratio [50], which describes the valuation as the ratio of the excess return or the expectation of the asset return less the risk-free rate of return, to the standard deviation of the excess return. For investors, the Sharpe ratio of a good trade would have high positive value, i.e., high excess return with low risk (standard deviation). However, in some situations, the Sharpe ratio would not recognize a good trade when asset returns are not normally distributed.

Like the Sharpe ratio, most performance measures are defined as ratios of reward to risk. For example, the Treynor ratio is defined as the excess return over the portfolio's beta, while Jensen's alpha evaluates the difference between the abnormal return of the portfolio and its expected value. In order to develop a non-arbitrage compatible performance measure, Bernardo and Ledoit [8] proposed the Gain-Loss ratio, which recognizes an arbitrage if and only if the Gain-Loss ratio is infinity. Although the Gain-Loss ratio improves the economical quality of the Sharpe ratio, the symmetric treatment of small losses and large losses leaves some room for improvement. Artzner, Delbaen, Eber and Heath [3] developed a new measurement

of risk called the coherent risk measure with the following properties: monotonicity, sub-additivity, positive homogeneity, and translation invariance. They pointed out that the popular risk measure Value at Risk (VAR), which estimates the amount of portfolio losses at a given confidence level based on the statistical distribution of historical prices, lacks sub-additivity. Therefore, VAR violates the general idea that diversification can reduce risk. Following these works [3] [14], Cherny and Madan [18] proposed a new performance evaluation, acceptability indices. This nonnegative real number is defined as the acceptability level of a set of random variables which are the terminal cash flows of a trading strategy or an investment. Each acceptable level is associated with a convex cone and a set of pricing kernels. If a cash flow is said to be acceptable at level α , the expectation of the cash flow is positive under every pricing kernel associated with the acceptability level α . When the acceptable level is high, the associated convex cone is smaller and the set of the related pricing kernels is large. An arbitrage is defined as the acceptability level reaches infinity, which makes an agreement with the Gain-Loss ratio. Properties and examples of the acceptability indices will be discussed later in this chapter. Both the acceptability indices and the coherent risk measures are associated with the acceptability set [18] [3]. Hence, on the same acceptability set, we can build up the associated coherent risk measure and the associated acceptability indices [18].

Derivative pricing is mostly based on non-arbitrage argument. As discussed in Chapter 1, in incomplete markets, non-arbitrage pricing is not plausible since there is no perfect hedge to replicate the payoff of derivatives. Moreover, the prices of derivatives are determined as the two directions of trading: buy or sell. Investors

buy a security at ask prices and sell it at bid prices. Ask prices are always higher than bid prices. The Gain-Loss ratio is used to price derivatives in incomplete markets [8]. Treating the illiquid market as a counterparty, Cherny and Madan [19] extended the new performance measure to the conic finance theory and proposed a way to price derivatives based on the evaluation of residual cash flows using the acceptability indices. They also developed closed-form formulas of ask and bid prices of European options.

Here are some studies based on the conic finance theory and its associated two-price market. Pricing and hedging of exotic derivatives such as cliquets, structured products, tensor specific in the two-price market is studied [37] [40] [36] [38]. [39] elaborated the connection between this conic financial market and corporate finance. Credit and liquidity risk modeling are discussed in [23] [34]. [17] studied profits, capital, leverage and return of markets. Hedging by adjusting gamma with existence of skewness is discussed in [30], the equilibria model of structured products is proposed in [41], and an application of a new portfolio selection method is presented in [29] .

The rest of this chapter presents the definition and properties of acceptability indices, illustrates the way to price derivatives using the two-price market model and last, discusses the hedging methods in the two-price markets.

2.2 Acceptability Index

2.2.1 Definition

Definition 2.1. *An index of acceptability α is said to be the acceptability index of bounded random cash flows X , if for each $\gamma \geq 0$, there exists a set of probability measures D_γ that the expectation of X under each probability measure $Q \in D_\gamma$ is nonnegative, then the acceptability index α is defined as :*

$$\alpha(X) = \sup\{\gamma \geq 0 : E^Q[X] \geq 0, \forall Q \in D_\gamma\}. \quad (2.1)$$

Since the acceptability index is based on the coherent risk measures, the link between the acceptability index and the coherent risk measure is elaborated in [18].

A coherent risk measure of random variable X is defined as:

$$\rho_\gamma(X) = -\inf E^Q[X], \forall Q \in D_\gamma, \gamma \geq 0, \quad (2.2)$$

then we have the corresponding acceptability index α defined as:

$$\alpha(X) = \sup\{\gamma \geq 0 : \rho_\gamma(X) \leq 0\}. \quad (2.3)$$

The four properties of acceptability index are :

1 Monotonicity: if $\alpha(X) \geq \gamma$ and $Y \geq X$, then $\alpha(Y) \geq \gamma$;

2 Quasi-concavity: if $\alpha(X) \geq \gamma$ and $\alpha(Y) \geq \gamma$, then $\alpha(X + Y) \geq \gamma$;

3 Scale Invariance: if $\alpha(X) \geq \gamma$ and a constant $c > 0$, then $\alpha(cX) \geq \gamma$;

4 Fatou property: For a sequence of random variables $\{Y_i\}$, if $|Y_i| \leq 1$, $\alpha(Y_i) \geq$

γ and converges to a random variable X in probability, then $\alpha(X) \geq \gamma$.

2.2.2 Weighted Value at Risk (WVAR) Acceptability Indices

The *Weighted Value at Risk* (WVAR) [18], a coherent risk measure, is defined as:

$$WVAR_\gamma = - \int_{\mathbb{R}} y d\Psi_\gamma(F_X(y)), \quad (2.4)$$

where $\Psi^\gamma(x)$ has a one-to-one relationship with the original probability measure $F_X(x)$. Moreover, $\Psi^\gamma(x)$ is an increasing concave continuous function on the interval $[0, 1]$ with $\Psi^\gamma(0) = 0$ and $\Psi^\gamma(1) = 1$. Thus, $\Psi^\gamma(x)$ is also called a concave distortion.

Then, the corresponding WVAR acceptability index $\alpha(X)$ is defined as

$$\alpha(X) = \sup\{\gamma \geq 0 : \int_{\mathbb{R}} x d\Psi^\gamma(F_X(x)) \geq 0\}, \quad (2.5)$$

where $\Psi^\gamma(x)$ is an increasing function of γ . The distorted expectation $\int_{-\infty}^{\infty} x d\Psi^\gamma(F_X(x))$ is the expected value of random variable X under a new probability measure Q , with a new distribution function $\Psi^\gamma(F_X(x))$, where $F_X(x)$ is the original distribution function of X . When γ increases, the new probability measure Q distort the original distribution $F_X(x)$ increasingly to the left. When $\gamma = 0$, there is no distortion for $F_X(x)$, i.e., $\Psi^{\gamma=0}(F_X(x)) = F_X(x)$. Hence, we can think of $\alpha(X)$ as the maximum distortion level γ that the distorted expectation of X keeps nonnegative. The distortion level γ can be treated as a measure of bad scenarios. We are looking for the worst scenario level where the cash flow X can keep the expectation nonnegative. It is obvious that a high $\alpha(X)$ indicates a good trade. In this sense, γ is also called the stress level of the cash flow X .

If samples of the cash flow X are known, the distorted expectation can be

computed as the following discrete form based on its empirical distribution:

$$\int_{-\infty}^{\infty} x d\Psi^{\gamma}(F_X(x)) = \sum_{i=1}^N x_i \left(\Psi^{\gamma} \left(\frac{i}{N} \right) - \Psi^{\gamma} \left(\frac{i-1}{N} \right) \right), \quad (2.6)$$

where $x_i, i = 1 \dots N$ are the samples of X sorted increasingly. This equation clearly states that the distorted expectation is a weighted sum of the original distribution.

This computational form is very useful when using Monte Carlo simulation.

A list of WVAR acceptability indices are presented in [18]. Four popular ones are MINVAR, MAXVAR, MAXMINVAR and MINMAXVAR.

Definition 2.2. *MINVAR*

The concave distortion of a MINVAR acceptability index is given by the function:

$$\Psi^{\gamma}(u) = 1 - (1 - u)^{\gamma+1}, \gamma \geq 0, u \in [0, 1]. \quad (2.7)$$

Let $u = F_X(x)$, the derivative of Equation (2.7) is

$$\frac{d\Psi^{\gamma}(F_X(x))}{dx} = (\gamma + 1)(1 - F_X(x))^{\gamma} f_X(x),$$

where $f_X(x)$ is the PDF of X . The stress level γ is the largest number of independent draws from the distribution of X such that the expected value of the minimum of $\gamma + 1$ draws is still positive. The derivative shows that MINVAR puts more weight on losses and less weight on gains than the original distribution. However, for large losses, when x goes to negative infinity, $F_X(x)$ is close to 0 and the new weight on large losses can not reach positive infinite levels.

Definition 2.3. *MAXVAR*

The concave distortion of a MAXVAR acceptability index is given by the function:

$$\Psi^\gamma(u) = u^{\frac{1}{\gamma+1}}, \gamma \geq 0, u \in [0, 1]. \quad (2.8)$$

Similar to MINVAR, we have the derivative of Equation (2.8)

$$\frac{d\Psi^\gamma(F_X(x))}{dx} = \frac{1}{\gamma+1} (F_X(x))^{\frac{-\gamma}{\gamma+1}} f_X(x).$$

The stress level γ is the largest number of independent draws from the distribution of X such that the expected value of the maximum of $\gamma + 1$ draws is still positive. When x goes to negative infinity, unlike MINVAR, the new weights by MAXVAR can go to infinity. For large gains, $F_X(x)$ is close to 1 and the new weights are always positive. It is the drawback of MAXVAR.

Definition 2.4. *MAXMINVAR*

The concave distortion of a MAXMINVAR acceptability index is given by the function:

$$\Psi^\gamma(u) = (1 - (1 - u)^{\gamma+1})^{\frac{1}{\gamma+1}}, \gamma \geq 0, u \in [0, 1]. \quad (2.9)$$

MAXMINVAR constructs the worst case by MINVAR followed by MAXVAR.

The derivative of Equation (2.9) is

$$\frac{d\Psi^\gamma(F_X(x))}{dx} = (1 - F_X(x))^\gamma (1 - (1 - F_X(x))^{\gamma+1})^{\frac{-\gamma}{\gamma+1}} f_X(x).$$

This derivative illustrates that MAXMINVAR could reweight large losses to infinity and large gains to zero.

Definition 2.5. *MINMAXVAR*

The concave distortion of a MINVAR acceptability index is given by the function:

$$\Psi^\gamma(u) = 1 - (1 - u^{\frac{1}{\gamma+1}})^{\gamma+1}, \gamma \geq 0, u \in [0, 1]. \quad (2.10)$$

MINMAXVAR constructs the worst case by MAXVAR first then by MINVAR.

The derivative of equation (2.10) is

$$\frac{d\Psi^\gamma(F_X(x))}{dx} = (1 - F_X(x)^{\frac{1}{\gamma+1}})^\gamma F_X(x)^{\frac{-\gamma}{\gamma+1}} f_X(x).$$

Same as MAXMINVAR, MINMAXVAR could reweight large losses to infinity and large gains to zero.

2.3 Option Pricing in Two-Price Markets

WVAR acceptability indices can be used to build up a model for bid and ask prices of random cash flows [19]. We now consider the trade direction from the view of market makers because bid and ask prices are determined by their competition. They sell securities at competitive ask or offer prices and buy them back at competitive bid prices.

If the terminal cash flow of a contingent claim is X , a seller sells it at the ask price a and at the same time owns the obligation to pay X back to her or his counterparty at the maturity. The residual cash flow of the seller is $a - X$ with the performance measure, $\alpha(a - X)$. Given a stress level γ , we have:

$$\alpha(a - X) \geq \gamma,$$

or apply Equation (2.5),

$$\int_{-\infty}^{\infty} x d\Psi^\gamma(F_{a-X}(x)) \geq 0, \quad (2.11)$$

which gives

$$a_\gamma(X) = - \int_{-\infty}^{\infty} x d\Psi^\gamma(F_{-X}(x)). \quad (2.12)$$

Equation (2.12) states that the ask price of a random cash flow X at the stress level γ is the negative value of the distorted expectation of the random cash flow $-X$ based on the concave distorted function Ψ^γ .

If a buyer purchases this derivative X at the bid price b from investors, the buyer pays out b and earns cash flow X at the maturity. The residual cash flow of the buyer is $X - b$ with the performance measure $\alpha(X - b)$. Given a stress level γ , we have:

$$\alpha(X - b) \geq \gamma,$$

apply Equation (2.5),

$$\int_{-\infty}^{\infty} x d\Psi^\gamma(F_{X-b}(x)) \geq 0, \quad (2.13)$$

which gives

$$b_\gamma(X) = \int_{-\infty}^{\infty} x d\Psi^\gamma(F_X(x)). \quad (2.14)$$

Equation (2.14) states that the bid price of a random cash flow X given the stress level γ is the distorted expectation of X based on the concave distorted function Ψ^γ .

Application of Equation (2.14) and Equation (2.12) onto European options leads to closed-form formulas for bid and ask prices. A European call option C written on the underlying asset S with strike price K and maturity T has a terminal

payoff $(S - K)^+$. A European put option P written on S with strike price K and maturity T has a terminal payoff $(K - S)^+$. The closed-form bid and ask prices derived by [19] are

$$a_\gamma(C) = \int_K^\infty \Psi^\gamma(1 - F_S(s))ds, \quad (2.15)$$

$$a_\gamma(P) = \int_0^K \Psi^\gamma(F_S(s))ds, \quad (2.16)$$

$$b_\gamma(C) = \int_K^\infty (1 - \Psi^\gamma(F_S(s)))ds, \quad (2.17)$$

$$b_\gamma(P) = \int_0^K (1 - \Psi^\gamma(1 - F_S(s)))ds. \quad (2.18)$$

2.4 Hedging in Two-Price Markets

Hedging is the problem of deciding the optimal strategy to allocate the initial capital in order to protect investors from the embedded risk of their positions in derivatives. As discussed in Chapter 1, Black-Scholes delta hedging is a popular choice for option hedging and it states that investors need to hold δ shares of stock with price S to make their portfolio including an option with price V riskless. As we know,

$$\delta = \frac{\partial V}{\partial S}.$$

When jumps jeopardize market completeness, a perfect hedge of contingent claims is not guaranteed. However, the way to hedge in complete markets provides ideas for hedging in incomplete markets. As Föllmer and Schied discussed in [26], there are some ways to hedge contingent claims in incomplete markets. Superhedging tries to figure out the cheapest trading strategy, which has the minimal capital with the obligation of the terminal cash flow of contingent claims. There is no risk-preference

in this method, i.e., no need to determine the risk-aversion parameter. However, it leads to wide price bounds of contingent claims. The way to maximize expected utility functions is to minimize hedging errors. One popular way is local quadratic hedging, which minimizes the quadratic hedging errors of contingent claims. For a one-period problem, we can write the minimization of local quadratic hedging errors as follows:

$$(v_0^*, \delta_0^*) = \operatorname{argmin} E[(H - v_0 - \delta_0(S_T - S_0))^2],$$

where H is the terminal payoff of the contingent claim, v_0 is the initial position in money market account, v_0^* and δ_0^* are the optimized values of v_0 and δ_0 , δ_0 is the number of shares of the underlying asset, S_T is the stock price at the maturity, S_0 is the initial stock price,

In [37], the one-period hedging problem is minimizing the capital, i.e., the ask price less the bid price of a hedged cash flow over a time horizon. Using Equation (2.12) and (2.14), we can write the one-period problem of capital minimization as,

$$\delta_0^* = \operatorname{argmin} \left(- \int_{-\infty}^{\infty} x d\Psi^\lambda(F_{-X}(x)) - \int_{-\infty}^{\infty} x d\Psi^\lambda(F_X(x)) \right),$$

where $X = H - \delta_0(S_T - S_0)$, $F_X(x)$ is the distribution function of X , $\Psi^\lambda(x)$ is the distorted function and λ is the stress level.

We compare the two hedging methods, local quadratic hedging error minimization and capital minimization, with a numerical test. In order to hedge a European call option with strike price 105 and one-year maturity, we assume the underlying asset S follows a Variance Gamma process with $\sigma = 0.2$, $\theta = -0.3$ and $\nu = 0.5$. The initial prices are from 50 to 250. The strike price of the European call option is

105. Monte Carlo simulation with 50,000 simulation paths is used. The position in the stock at the initial time is presented in Figure 2.1. The observation shows that for out-of-the-money call options, option writers need to hold more stocks if using the quadratic hedging error minimization method. For in-the-money call options, option writers need to hold more stocks if using the capital minimization method. As the stress level λ increases, more stocks are needed for out-of-the-money options and fewer stocks are needed for in-the-money options.

Observation in [37] shows that the gamma-adjusted delta of a target cash flow is less than the Black-Scholes delta since the downside risk exposure is more expensive when markets are skewed downwards. Hence, the adjusting gamma part exists in the presence of skewness. A multi-period dynamic hedging model is developed from the nonlinear expectation theory by Cohen and Elliott [20], which provides a consistent time series of bid and ask prices. A non-uniform grid of 100 stock price levels is constructed for each time period based on the algorithm described by Mijatović and Pistorius [46]. The gamma-adjusted deltas for each period are then chosen to minimize the capital of each period, successively. The processes of the bid and ask prices at time t , i.e., Y_t^u for a time step of h are presented as:

$$Y_t^u = E_t[Y_{t+1}^u] + h \int_{-\infty}^{\infty} x d\Psi(F_t^u(x), \lambda, \gamma)$$

$$F_t^u(x) = Pr(Y_{t+1}^u - E_t[Y_{t+1}^u] \leq x)$$

where $u = a, b$ denotes ask prices or bid prices, $E_t[Z]$ denotes the expectation of the random variable Z at time t and Pr denotes the probability. More interesting hedging problems can also be addressed using this dynamic hedging system.

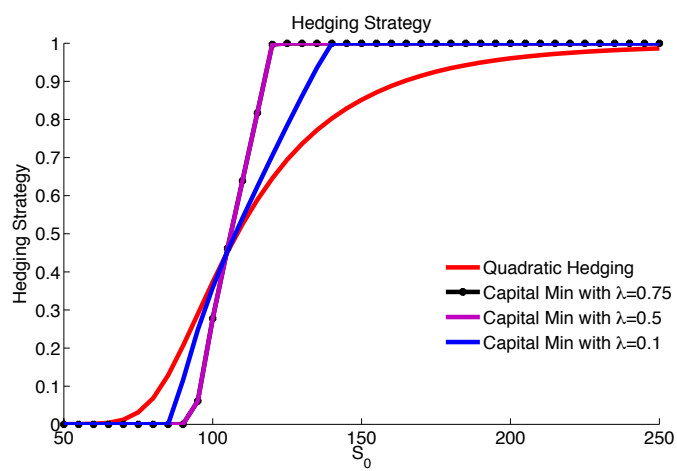


Figure 2.1: Hedging strategy comparison of local quadratic error minimization and capital minimization with input variables $S_0 = [50 : 5 : 200]$, $K = 105$, $\sigma = 0.2$, $\theta = -0.3$ and $\nu = 0.5$. The underlying asset follows a Variance Gamma model.

Chapter 3

The Trading Advantages of Structured Products

3.1 Introduction

Equity structured products, which are combinations of fundamental instruments from the spot and derivative markets, have been popular in the United States since the 1980s. Since their introduction, this type of investment tools has grown very rapidly. Structured products are designed and tailored to meet customers' specific needs. The major advantage of these products is that they provide various positions in derivatives without the need for actual transactions. In addition, the bid-ask spreads of structured products are always lower than those of the corresponding components. Generally, structured products can be separated into two types: those with plain vanilla option components and those with exotic option components.

Structured products usually combine several fundamental instruments, resulting in a variety of payoff patterns with maturities ranging from months to years. The complexity of these products makes pricing them unclear. A series of studies have been conducted to discuss the pricing fairness and embedded risk of these structured products. The study by Stoimenov and Wilkens [52] revealed the discrepancies between market prices and theoretical values of these products in German primary and secondary markets. Burth, Kraus and Wohlwend [12] investigated the differ-

ence in the pricing behavior of different issuers of structured products. From the perspective of classical finance theory, Bernard and Boyle [7] explained the reasons why consumers might prefer more complex contracts when they believe there is a good chance to get the maximum return. The two-price market theory by Cherny and Madan [18] [19] is used to demonstrate the trading advantages of structured products from the investors' point of view. The theory is constructed by describing the market as a counterparty. There have also been applications of this theory using structured products. Madan and Schoutens [38] investigated the implied stress levels from the bid and ask prices of exotic options and observed negative stress levels for capped cash flows as well as positive stress levels for uncapped cash flows. Madan, Pistorius and Schoutens [36] obtained dynamically consistent bid and ask prices by applying the two-price market theory and a Markov chain.

In this study, in order to investigate the trading advantages, the bid and ask prices are derived under the two-price market framework. Mathematical proofs and numerical modeling illustrate the trading advantages from the investors' perspective. It is observed that for investors, it is always cheaper to buy these products than to trade their component instruments separately, and it is always more expensive to sell these products than to trade their component instruments separately.

The outline of the rest of the section is as follows. Section 3.2 briefly describes the two-price market theory. Section 3.3 presents the closed-form formulas for the bid and ask prices of option spreads: bull spreads, bear spreads, strangles, straddles and butterfly spreads with numerical illustrations based on a geometric Brownian motion (GBM) and VGSSD. Section 3.4 discusses the advantages of trading exotic

options: cliquet options, reverse cliquet options and spread options. The bid and ask prices are computed using Monte Carlo Simulation for the Geometric Brownian Motion and Variance Gamma Process (VG).

3.2 The Two-Price Markets

The two-price market theory developed by Cherny and Madan [18] [19] starts from a market as a counterparty and states that the bid and ask prices of contingent claims are determined by the acceptability or quality of the cash flows. The following is a brief introduction to the two-price market theory. In two-price market theory, the quality of the cash flows given a certain acceptability level is determined by the nonlinear expectation of the cash flows. For a contingent claim with the terminal payoff X , at the maturity T , the seller pays the cash flow X and the buyer receives the cash flow X . Then the bid and ask prices in terms of distortions are defined as

$$b(X) = \int_{-\infty}^{\infty} x d\Psi(F(x), \lambda), \quad (3.1)$$

$$a(X) = - \int_{-\infty}^{\infty} x d\Psi(1 - F(-x), \lambda). \quad (3.2)$$

where x is a random variable of the cash flow, $F(x)$ is the distribution function of x , $\Psi(x, \lambda)$ is called the distorted function, and λ is the stress level. There is a list of choices for the distorted functions. We use the MINMAXVAR defined as $\Psi(u, \lambda, \gamma) = 1 - (1 - u^{\frac{1}{1+\lambda}})^{1+\lambda}$, which reweights large losses up to infinity and large gains down to zero. The distorted expectation used for bid and ask prices can also be computed numerically using the empirical distribution of the cash flows as described

in Cherny and Madan [19]:

$$\int_{-\infty}^{\infty} x d\Psi(F(x), \lambda, \gamma) = \sum_{n=1}^N x_n \left(\Psi\left(\frac{n}{N}, \lambda, \gamma\right) - \Psi\left(\frac{n-1}{N}, \lambda, \gamma\right) \right), \quad (3.3)$$

where x_i are samples from the distribution of X and are sorted in increasing order.

3.3 Option Spreads

Option spreads are linear combinations of plain vanilla options which are often used as strategies. Investigation of option spreads could lead to interesting discoveries regarding packaging benefits in two-price markets. Bull call spreads, bear put spreads, straddles, and butterfly spreads all have plain vanilla options as a component. The trading advantages are illustrated by comparing the cost of trading these spreads and the cost of trading their components separately using the GBM and VGSSD process introduced in Section 1.2.

3.3.1 Bull Spread

A bull spread longs a call option at the strike price K_1 and shorts a call option at the strike price K_2 with the same maturity T , where $K_2 > K_1$. The cash flow is

$$C = (S - K_1)^+ - (S - K_2)^+.$$

Bull spreads could be used to replicate digital options. For the bid price, the cash flow is $C = (S - K_1)^+ - (S - K_2)^+$. The terminal payoff shows that the cash flow $C \in [0, K_2 - K_1]$. The distribution function of C in terms of S has three parts:

$$C < 0, F_C(c) = 0;$$

$$C \in [0, K_2 - K_1), F_C(c) = F_S(s);$$

$$C \geq K_2 - K_1, F_C(c) = 1.$$

Thus, the bid price of a bull spread is

$$\begin{aligned} \int_{-\infty}^{\infty} cd\Psi(F_C(c)) &= \int_{-\infty}^0 cd\Psi(F_C(c)) + \int_0^{K_2-K_1} cd\Psi(F_C(c)) + \int_{K_2-K_1}^{\infty} cd\Psi(F_C(c)) \\ &= \int_0^{K_2-K_1} cd\Psi(F_C(c)) \\ &= c\Psi(F_C(c))\Big|_0^{K_2-K_1} - \int_{K_1}^{K_2} \Psi(F_S(s))ds \\ &= K_2 - K_1 - \int_{K_1}^{K_2} \Psi(F_S(s))ds \end{aligned}$$

For the ask price, the cash flow is $C = -(S - K_1)^+ + (S - K_2)^+$. The range of the cash flow is $C \in [K_1 - K_2, 0]$. The distribution function of C in terms of S also has three parts:

$$C \geq 0, F_C(c) = 1;$$

$$C \in [K_1 - K_2, 0), F_C(c) = 1 - F_S(s);$$

$$C < K_1 - K_2, F_C(c) = 0.$$

We define a new random variable $\tilde{C} = C + K_2 - K_1$ with the same distribution as C . Thus, the ask price of a bull spread is

$$\begin{aligned} - \int_{-\infty}^{\infty} cd\Psi(F_C(c)) &= - \int_{-\infty}^{\infty} (\tilde{c} - K_2 + K_1)d\Psi(F_C(\tilde{c})) \\ &= - \int_{-\infty}^{\infty} \tilde{c}d\Psi(F_C(\tilde{c})) + (K_2 - K_1) \int_{-\infty}^{\infty} d\Psi(F_C(\tilde{c})) \\ &= - \int_0^{K_2-K_1} \tilde{c}d\Psi(F_C(\tilde{c})) + (K_2 - K_1) \\ &= -(K_2 - K_1) + \int_{K_1}^{K_2} \Psi(1 - F_S(s))ds + (K_2 - K_1) \\ &= \int_{K_1}^{K_2} \Psi(1 - F_S(s))ds \end{aligned}$$

In short, the bid and ask prices for a bull spread are:

$$Bull_Spread_{Bid} = K_2 - K_1 - \int_{K_1}^{K_2} \Psi(F_S(s))ds, \quad (3.4)$$

$$Bull_Spread_{Ask} = \int_{K_1}^{K_2} \Psi(1 - F_S(s))ds. \quad (3.5)$$

For investors, buying a bull spread at the ask price is equivalent to buying a call option with the strike price K_1 at the ask price and selling a call option with the strike price K_2 at the bid price. Hence, the buying advantage is defined as:

$$\begin{aligned} buying_advantage_bull &= \frac{(Call_{Ask}^{K_1} - Call_{Bid}^{K_2}) - Bull_Spread_{Ask}}{Call_{Ask}^{K_1} - Call_{Bid}^{K_2}} \\ &= \frac{\int_{K_2}^{\infty} (\Psi(F_S(s)) + \Psi(1 - F_S(s)) - 1)ds}{\int_{K_1}^{\infty} \Psi(1 - F_S(s))ds - \int_{K_2}^{\infty} (1 - \Psi(F_S(s)))ds}. \end{aligned}$$

Selling a bull spread at the bid price is equivalent to selling a call option with the strike price K_1 at the bid price and buying a call option with the strike price K_2 at the ask price. Hence, the selling advantage is defined as:

$$\begin{aligned} selling_advantage_bull &= \frac{Bull_Spread_{Bid} - (Call_{Bid}^{K_1} - Call_{Ask}^{K_2})}{Call_{Bid}^{K_1} - Call_{Ask}^{K_2}} \\ &= \frac{\int_{K_2}^{\infty} (\Psi(F_S(s)) + \Psi(1 - F_S(s)) - 1)ds}{\int_{K_1}^{\infty} (1 - \Psi(F_S(s)))ds - \int_{K_2}^{\infty} \Psi(1 - F_S(s))ds}. \end{aligned}$$

Bid and ask prices of call options with strike prices K_1 and K_2 could be computed using Equation (2.15) and Equation (2.17). We proved that selling a call option with the strike price K_1 and buying a call option with the strike price K_2 at the same time is always cheaper than selling the bull spread. On the other hand, the cost of buying a call option with the strike price K_1 and selling a call option with the strike price K_2 at the same time is always more expensive than buying the bull spread. The proof is presented in the Appendix. For the buying

advantages of bull spread, the numerator is always positive. When $K_2 - K_1$ goes to 0, the denominator decreases to 0 first and then reaches the minimum value $\int_{K_2}^{\infty} (1 - \Psi(1 - F_S(s)) - \Psi(1 - F_S(s))) ds$. Thus, as K_1 increases to K_2 , the sell benefits of bull spread increases to infinity before decreasing to -1. For the selling advantages of bull spread, the numerator is always positive. When $K_2 - K_1$ goes to 0, the denominator decreases to the minimum value $\int_{K_2}^{\infty} (\Psi(F_S(s)) + \Psi(1 - F_S(s)) - 1) ds$. Thus, as K_1 increases to K_2 , the buy benefit of bull spread increases and reaches the maximum value 1.

A numerical test was performed on a Geometric Brownian motion (GBM) for better illustration. The input variables are:

$$S_0 = 100; K_1 = 80; K_2 = 120; r = 0.02; \sigma = 0.2; \lambda = 0.25,$$

where r is the risk free rate, σ is the volatility and λ is the stress level in the distorted function MINMAXVAR $\Psi(x)$ in Equation (2.10). Figure 3.1 depicts the packaging benefits of trading a bull call spread rather than trading its components, with two separate call options having a constant high strike price K_2 . Figure 3.2 presents the packaging benefits of trading a bull call spread rather than trading its components, with the two separate call options having a constant low strike price K_1 . The observation from both figures demonstrates that the trading advantage of bull spreads increases as maturity increases, and the maximum benefit exists when the two strike prices are close to the spot price. Hence, for investors who buy a bull call spread, longing a deep in-the-money option and shorting a deep out-of-the-money option leads to few benefits; for investors who sell a bull call spread,

shorting deep in-the-money option and longing deep out-of-the-money option also leads to few benefits. The smaller the difference between the two strike prices, the more benefits the investors gain. More tests show that the benefits of trading bull spreads increase when the volatility of the underlying asset and the stress level increase. Thus, trading a bull spread in illiquid and volatile markets has more benefits than trading it in liquid and less volatile markets.

The VGSSD is used to investigate the benefits of trading a bull spread in skewed markets. The input variables of VGSSD are:

$$S_0 = 100; K_2 = 120; r = 0.02; \sigma = 0.2; \nu = 0.5; \gamma = 0.5; \lambda = 0.25.$$

Figures 3.3 and 3.4 depict how the packaging benefits vary when the market changes from left-skewed with $\theta = -0.1$ to right-skewed with $\theta = 0.1$. As presented in Table 1.2, θ in VGSSD controls the skewness of the distribution. Empirical work [5] discovered that the distribution of financial returns after the 1987 crash were left-skewed with a typical value of $\theta = -0.3$. We observed that the packaging benefits increase as the market skewness changed from negative to positive. Significant selling advantages of bull spreads with maturity at one year and $K_1 = 90$ were observed in the right-skewed market. This is due to a large increase in the ask price of the call option with strike price K_2 in the right-skewed market. Thus, the cash flow of selling a call option with strike price K_1 and buying a call option with strike price K_2 reduces dramatically in the right-skewed market. Take $T = 1$ and $K_1 = 90$ as an example. In the right-skewed market with $\theta = 0.1$, the ask price of the out-of-the-money (OTM) call option with strike price K_2 increases much more

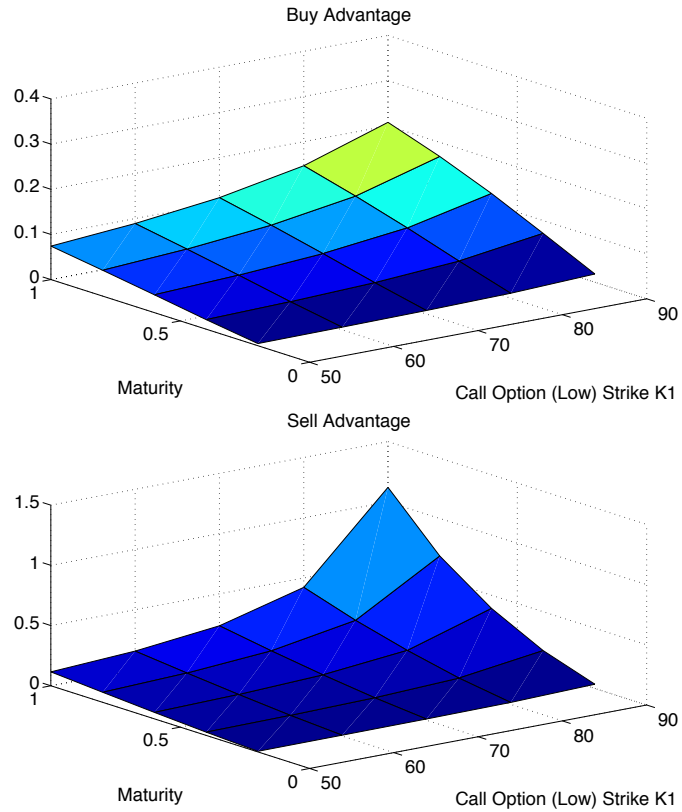


Figure 3.1: Buy and sell advantages of trading a bull spread using GBM with input variables $S_0 = 100$, $K_2 = 120$, $\sigma = 0.2$ and $\lambda = 0.25$.

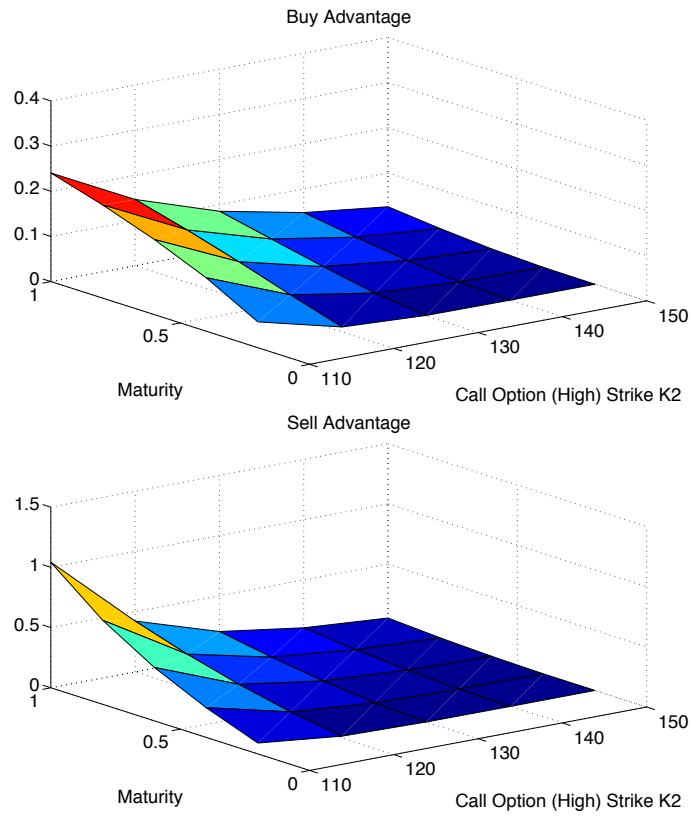


Figure 3.2: Buy and sell advantages of trading a bull spread using GBM with input variables $S_0 = 100$, $K_2 = 120$, $\sigma = 0.2$ and $\lambda = 0.25$.

than the bid price. This enlarges the bid-ask spread of this OTM call option. For the in-the-money (ITM) call option, the price variations in both the ask price and the bid price of the ITM call option are trivial. As we can see in Figure 3.5, the probability of stock price being at the maturity larger than K_2 in the right-skewed market is higher than that in the left-skewed market, which makes the ask price of call option with strike price K_2 in the right-skewed market much higher than in the left-skewed market. It is not hard to imagine that in a right-skewed market with unlimited upside gains and limited downside losses, investors favor longing OTM call options rather than shorting them. If the positive skewness continues to increase, the probability of unlimited upside gains increases and ask prices of OTM call options continue to increase. In terms of a buying advantage, both the ask prices of the call option with strike price K_1 and bid prices of the call option with strike price K_2 increase in the right-skewed market; however, the ask prices of the call option with strike price K_1 increase more, which makes a slight increase in buying advantages in the right-skewed market.

When negative skewness continues to decrease, the probability of stock price at the maturity larger than K_2 increases as described in Figure 3.5. This increases the ask price of the OTM call option and increases the selling advantage in a more left-skewed market. As negative θ continues to decrease, the variance of VGSSD increases, which in turn increases the trading benefits. More tests show that when the market skewness changes from positive to negative, the benefits (especially the selling benefits) decrease before increasing. It is observed that the minimum value occurs at $\theta = -0.25$. Thus, for investors, there are more benefits to trading bull

spreads in right-skewed or more left-skewed markets.

3.3.2 Bear Spread

A bear spread sells a put option at the strike price K_1 and longs a put option at the strike price K_2 with the same maturity T , where $K_2 > K_1$. The cash flow is

$$C = (K_2 - S)^+ - (K_1 - S)^+.$$

For the bid price, the cash flow is $C = (K_2 - S)^+ - (K_1 - S)^+$. The distribution function of C in terms of S has three parts:

$$C < 0, F_C(c) = 0;$$

$$C \in [0, K_2 - K_1), F_C(c) = 1 - F_S(s);$$

$$C \geq K_2 - K_1, F_C(c) = 1.$$

Thus, the bid price of a bear spread is

$$\begin{aligned} \int_{-\infty}^{\infty} cd\Psi(F_C(c)) &= \int_{-\infty}^0 cd\Psi(F_C(c)) + \int_0^{K_2-K_1} cd\Psi(F_C(c)) + \int_{K_2-K_1}^{\infty} cd\Psi(F_C(c)) \\ &= \int_0^{K_2-K_1} cd\Psi(F_C(c)) \\ &= c\Psi(F_C(c))\Big|_0^{K_2-K_1} - \int_{K_1}^{K_2} \Psi(1 - F_S(s))ds \\ &= K_2 - K_1 - \int_{K_1}^{K_2} \Psi(1 - F_S(s))ds \end{aligned}$$

For the ask price, the cash flow is $C = -(K_2 - S)^+ + (K_1 - S)^+$. The range of the cash flow is $C \in [K_1 - K_2, 0]$. The distribution function of C in terms of S also has three parts:

$$C \geq 0, F_C(c) = 1;$$

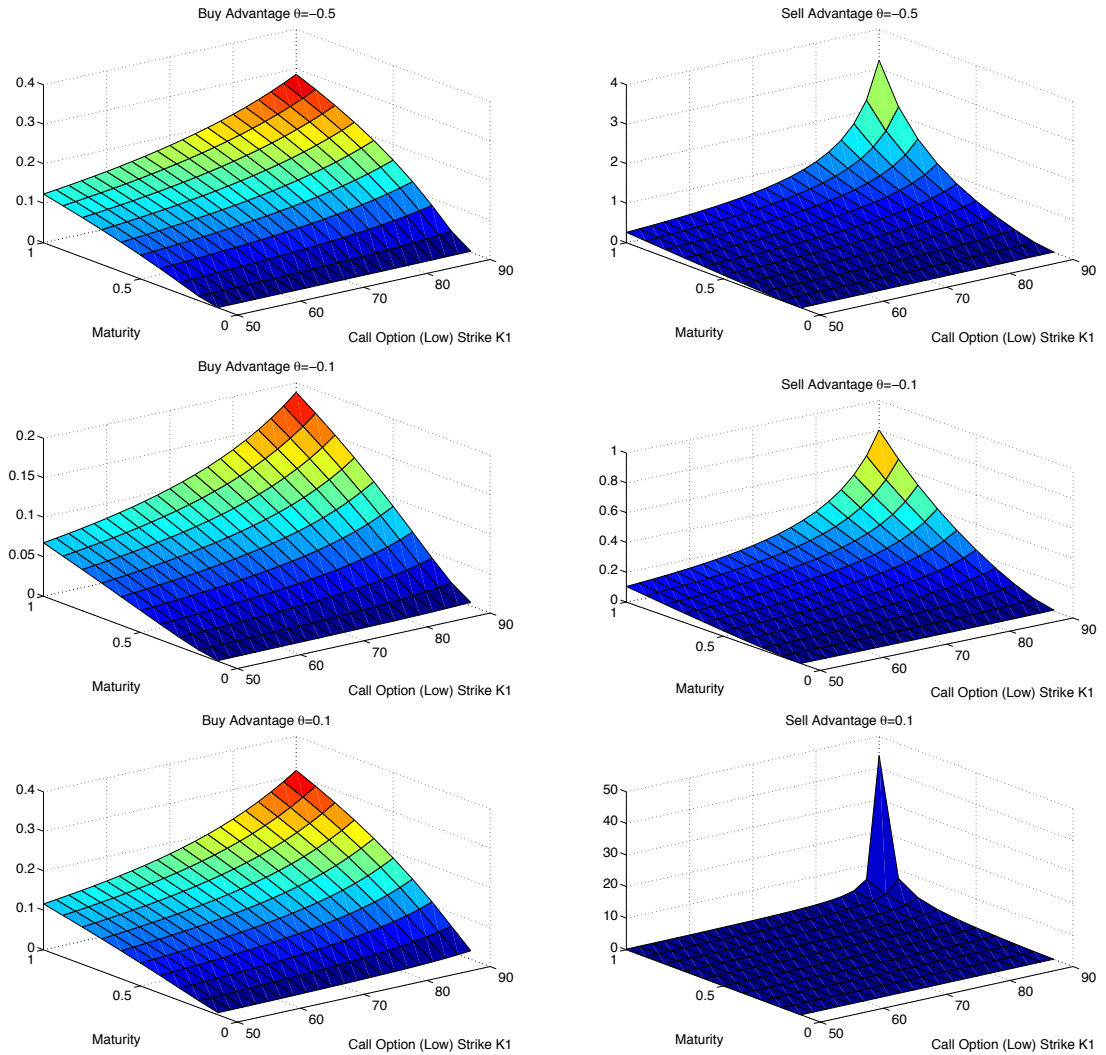


Figure 3.3: Buy and sell advantages of trading a bull spread using VGSSD with input variables $S_0 = 100$, $K_2 = 120$, $\sigma = 0.2$, $\nu = 0.5$, $\gamma = 0.5$ and $\lambda = 0.25$.

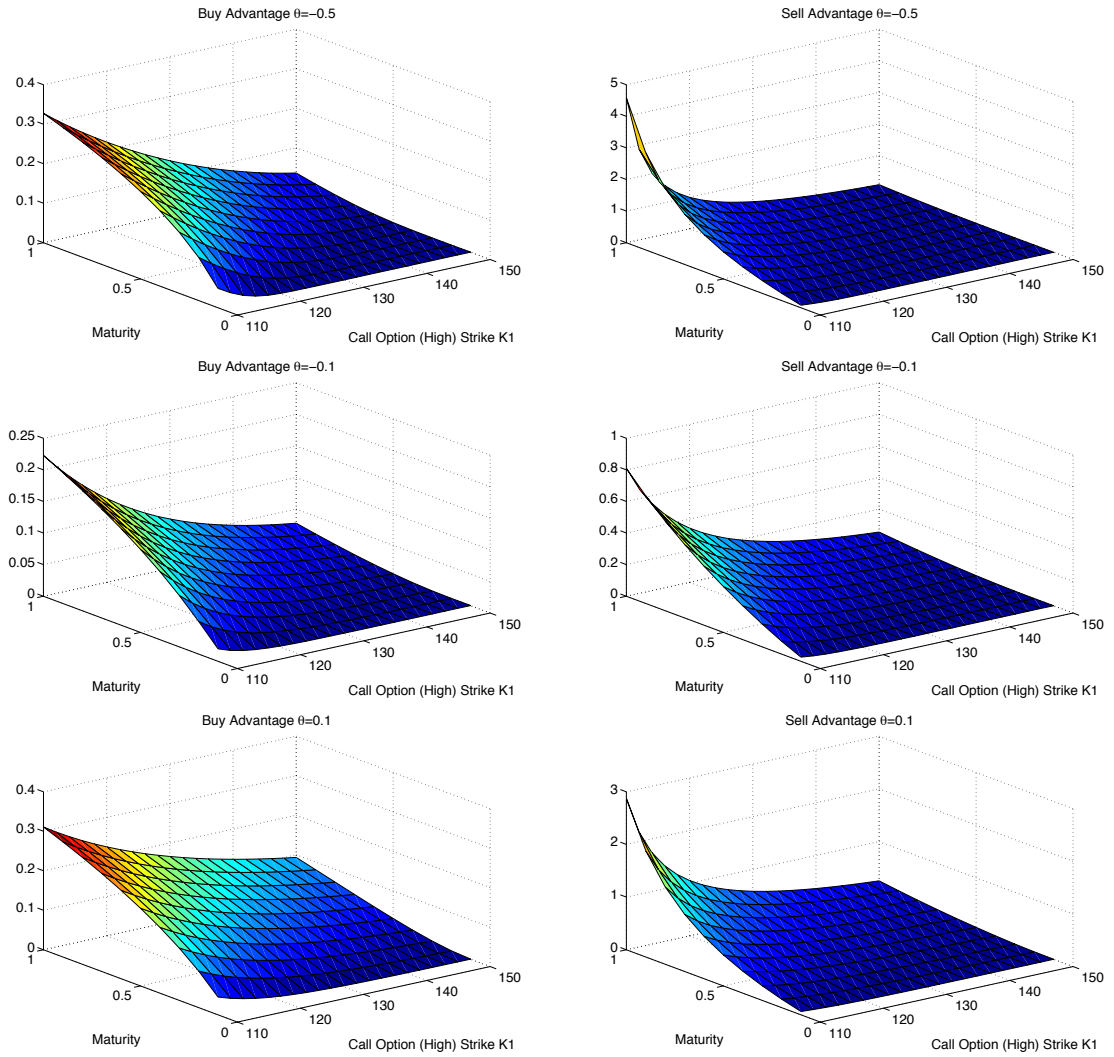


Figure 3.4: Buy and sell advantages of trading a bull spread using VGSSD with input variables $S_0 = 100$, $K_1 = 80$, $\sigma = 0.2$, $\nu = 0.5$, $\gamma = 0.5$ and $\lambda = 0.25$.

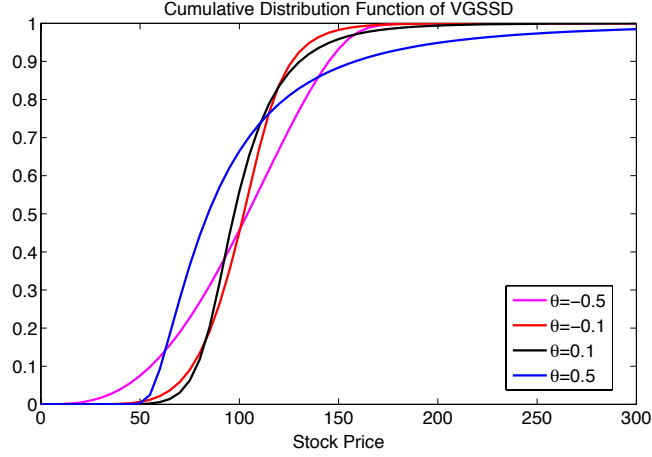


Figure 3.5: Cumulative distribution function of VGSSD with $T=1$.

$$C \in [K_1 - K_2, 0), F_C(c) = F_S(s);$$

$$C < K_1 - K_2, F_C(c) = 0.$$

A new random variable is defined as $\tilde{C} = C + K_2 - K_1$ with the same distribution as C . Thus, the ask price of a bear spread is

$$\begin{aligned} - \int_{-\infty}^{\infty} cd\Psi(F_C(c)) &= - \int_{-\infty}^{\infty} (\tilde{c} - K_2 + K_1)d\Psi(F_C(\tilde{c})) \\ &= - \int_{-\infty}^{\infty} \tilde{c}d\Psi(F_C(\tilde{c})) + (K_2 - K_1) \int_{-\infty}^{\infty} d\Psi(F_C(\tilde{c})) \\ &= - \int_0^{K_2 - K_1} \tilde{c}d\Psi(F_C(\tilde{c})) + (K_2 - K_1) \\ &= -(K_2 - K_1) + \int_{K_1}^{K_2} \Psi(F_S(s))ds + (K_2 - K_1) \\ &= \int_{K_1}^{K_2} \Psi(F_S(s))ds \end{aligned}$$

In short, the bid and ask prices for a bear spread are:

$$Bear_Spread_{Bid} = K_2 - K_1 - \int_{K_1}^{K_2} \Psi(1 - F_S(s))ds, \quad (3.6)$$

$$Bear_Spread_{Ask} = \int_{K_1}^{K_2} \Psi(F_S(s))ds. \quad (3.7)$$

Buying a bear spread is equivalent to buying a put option with the strike price K_2 at the ask price and selling a put option with the strike price K_1 at the bid price. Hence, the buying advantage is defined as:

$$\begin{aligned} \text{buying_advantage_bear} &= \frac{(Put_{Ask}^{K_2} - Put_{Bid}^{K_1}) - \text{Bear_Spread}_{Ask}}{Put_{Ask}^{K_2} - Put_{Bid}^{K_1}} \\ &= \frac{\int_0^{K_1} (\Psi(F_S(s)) + \Psi(1 - F_S(s)) - 1) ds}{\int_0^{K_2} \Psi(F_S(s)) - \int_0^{K_1} (1 - \Psi(1 - F_S(s))) ds}. \end{aligned}$$

Selling a bear spread is equivalent to selling a put option with the strike price K_2 at the bid price and buying a put option with the strike price K_1 at the ask price. Hence, the selling advantage is defined as:

$$\begin{aligned} \text{selling_advantage_bear} &= \frac{\text{Bear_Spread}_{Bid} - (Put_{Bid}^{K_2} - Put_{Ask}^{K_1})}{Put_{Bid}^{K_2} - Put_{Ask}^{K_1}} \\ &= \frac{\int_0^{K_1} (\Psi(F_S(s)) + \Psi(1 - F_S(s)) - 1) ds}{\int_0^{K_2} (1 - \Psi(1 - F_S(s))) ds - \int_0^{K_1} \Psi(F_S(s))}. \end{aligned}$$

We proved that buying a bear spread is always cheaper, which indicates that the cost of buying a put option with the strike price K_2 and selling a put option with the strike price K_1 at the same time will always be more expensive than the cost of buying the bear spread. On the other hand, selling a bear spread is always more expensive, which indicates that the price of selling a put option with the strike price K_2 and buying a put option with the strike price K_1 at the same time is always cheaper than the price of selling the bear spread. For buying advantages of bear spread, the numerator is always positive. When $K_2 - K_1$ goes to 0, the denominator decreases to the minimum value $\int_0^{K_2} (\Psi(F_S(s)) + \Psi(1 - F_S(s)) - 1) ds$. Thus, as K_1 increases to K_2 , the buy benefit of bear spread increases and reaches the maximum value 1. For selling advantages of bear spread, the numerator is always

positive. When $K_2 - K_1$ goes to 0, the denominator decreases to the minimum value $\int_0^{K_2} (1 - \Psi(F_S(s)) - \Psi(1 - F_S(s))) ds$. Thus, as K_1 increases to K_2 , the sell benefit of bear spread increases to infinity first as long as the denominator keeps positive and then drops to limits -1, since the denominator reaches the minimum negative value.

Figure 3.6 presents the trading advantages of a bear spread when the model of the underlying asset is GBM and the high strike K_2 is a constant. Figure 3.7 presents the buying and selling benefits of trading a bear spread when the model of the underlying asset is GBM and the low strike K_1 is a constant. The input variables are the same as those used for the bull spread. These two figures demonstrate that trading bear spreads with deep OTM put options and deep ITM put options leads to few benefits. More tests show that as the stress level and the volatility of the underlying assets increase, the packaging benefits increase.

Additionally, VGSSD is used to investigate the impact of market skewness in trading bear spreads. Input variables are the same as those used in the bull spread. Unlike bull spreads, when market skewness changes from negative to positive, the packaging benefits reduce first and then increase after a critical point. We also found that negative-skewed and more positive-skewed markets enlarge bid-ask spreads of put options and bear spreads. When θ increases from -0.1 to a positive value, the ask and bid prices for the bear spread and the put option with high strike price K_2 increase; however, the bid and ask prices for the put option with low strike price K_1 reduce first and then increase. When θ increases from -0.1 to 0.1, the relatively large increase in the ask price of the bear spread dominates the variation in buying

benefits and reduces the benefits. On the other hand, the relatively large decrease in the ask price of the put option with strike price K_1 dominates the variation in selling benefits while reducing the selling benefits. When θ continues to increase to 0.5, the relatively large increase in the ask prices of the put option with strike price K_2 and K_1 dominates the variation in buying and selling benefits respectively, resulting in an increase in the benefits. The significant increase in the variance of VGSSD increases the trading benefits when θ increases to 0.5. When the market skewness changes from positive to negative with limited upside gain and unlimited downside risk, investors tend to favor longing deep OTM put options and shorting deep ITM put options. Thus, trading bear spreads in left-skewed or more right-skewed markets brings investors more packaging benefits.

3.3.3 Strangle

A strangle longs a put option at strike price K_1 and a call option at strike price K_2 with the same maturity. K_2 is higher than the put strike price K_1 . The cash flow of the strangle is

$$C = (K_1 - S)^+ + (S - K_2)^+.$$

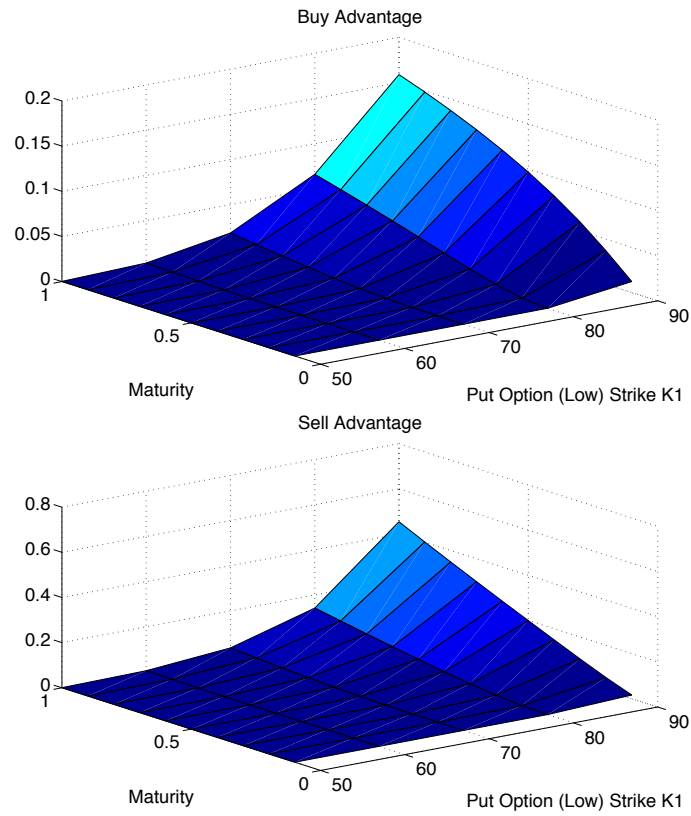


Figure 3.6: Buy and sell advantages of trading a bear spread using GBM with input variables $S_0 = 100$, $K_2 = 120$, $\sigma = 0.2$ and $\lambda = 0.25$.

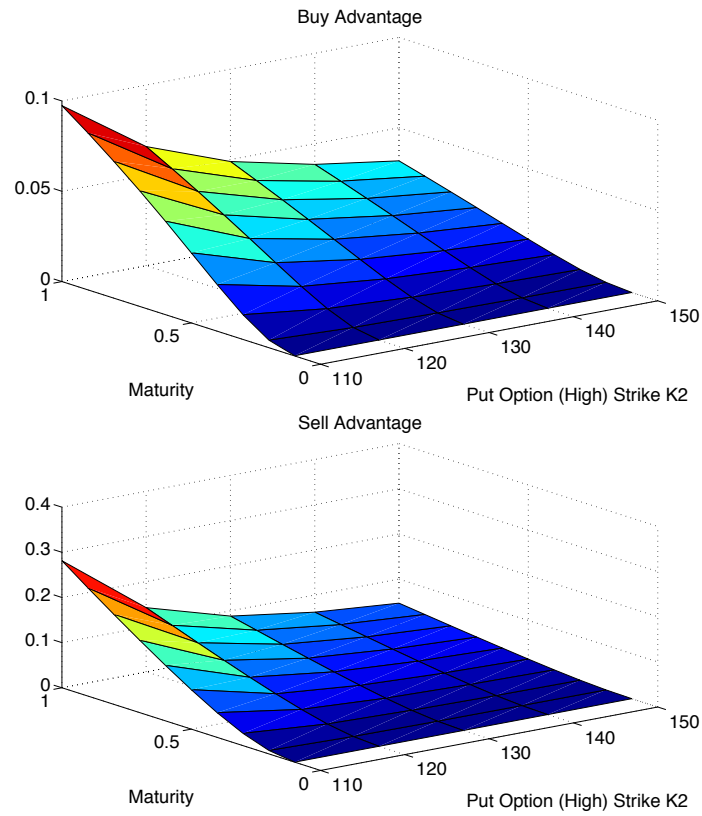


Figure 3.7: Buy and sell advantages of trading a bear spread using GBM with input variables $S_0 = 100$, $K_1 = 80$, $\sigma = 0.2$ and $\lambda = 0.25$.

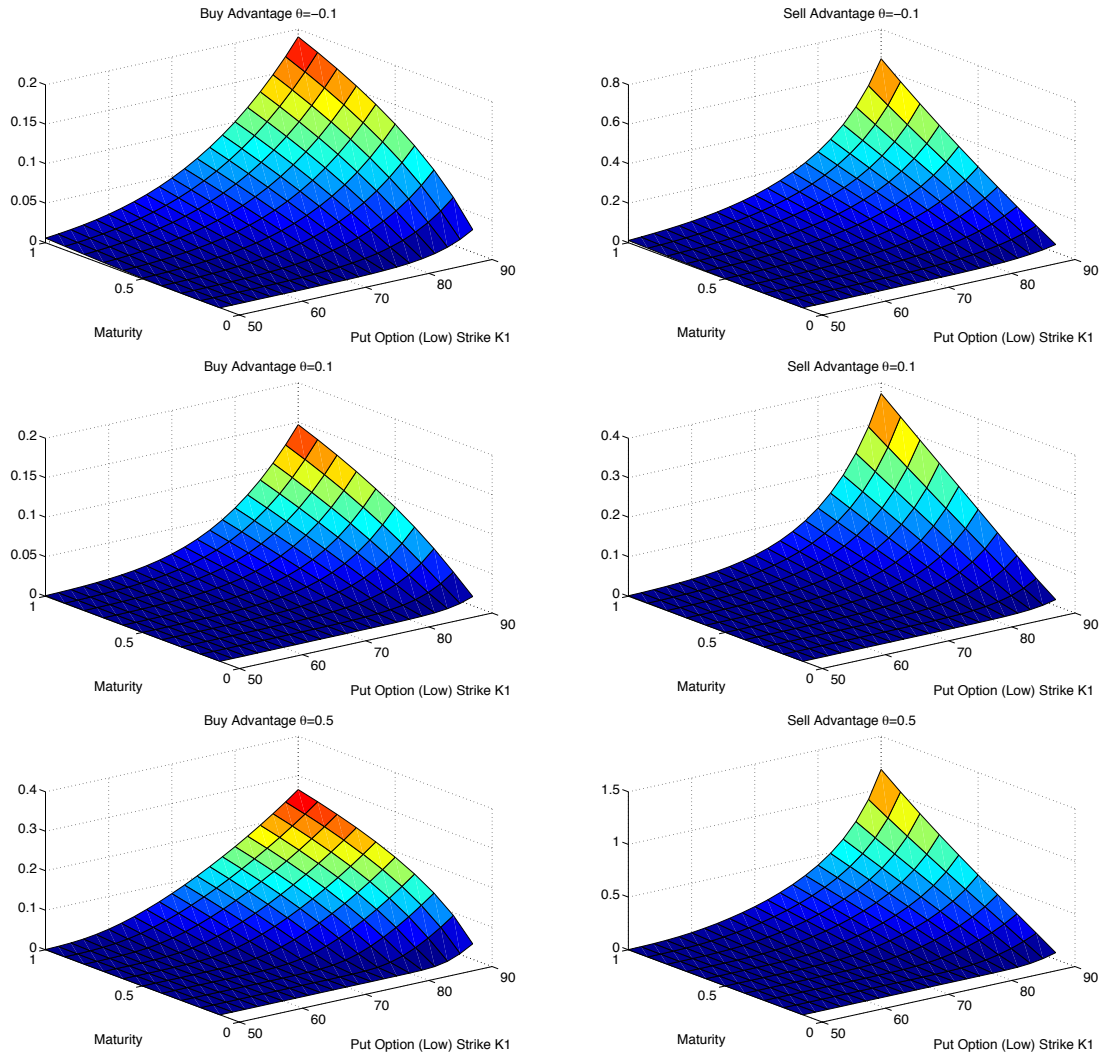


Figure 3.8: Buy and sell advantages of trading a bear spread using VGSSD with input variables $S_0 = 100$, $K_2 = 120$, $\sigma = 0.2$, $\nu = 0.5$, $\gamma = 0.5$ and $\lambda = 0.25$.

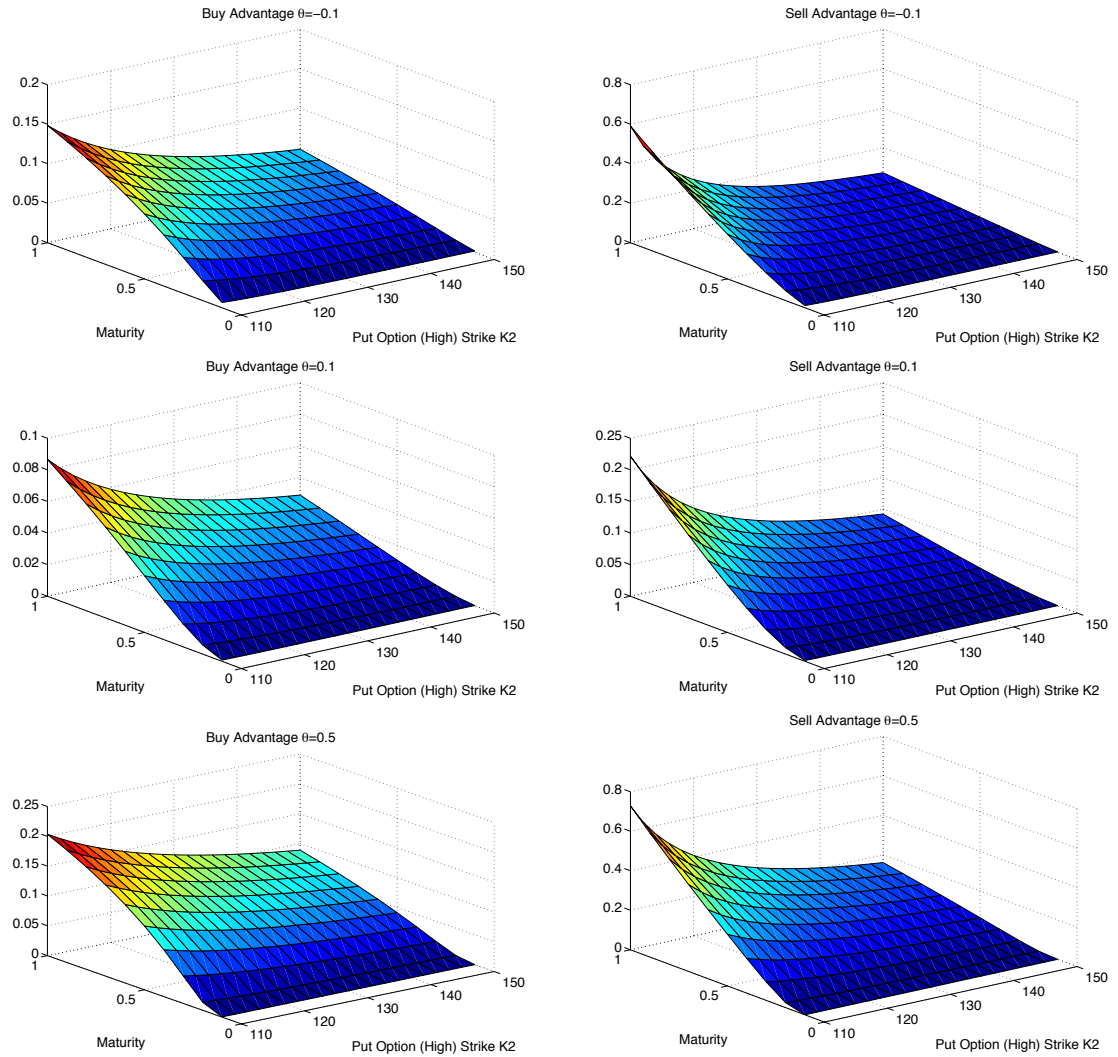


Figure 3.9: Buy and sell advantages of trading a bear spread using VGSSD with input variables $S_0 = 100$, $K_1 = 80$, $\sigma = 0.2$, $\nu = 0.5$, $\gamma = 0.5$ and $\lambda = 0.25$.

The bid price of the strangle is

$$\begin{aligned}
\int_{-\infty}^{\infty} cd\Psi(F_C(c)) &= \int_{-\infty}^{K_1} cd\Psi(F_C(c)) + \int_{K_1}^{\infty} cd\Psi(F_C(c)) \\
&= \int_{K_2}^{K_1+K_2} (S - K_2)d\Psi(F_S(s) - F_S(K_2 + K_1 - s)) + \\
&\quad \int_{K_1+K_2}^{\infty} (S - K_2)d\Psi(F_S(s)) \\
&= K_1 + \int_{K_1+K_2}^{\infty} (1 - \Psi(F_S(s)))ds - \int_{K_2}^{K_1+K_2} \Psi(F_S(s) - F_S(K_2 + K_1 - s))ds.
\end{aligned}$$

For the ask price, the cash flow is $C = -(K_1 - S)^+ - (S - K_2)^+$. The ask price of the strangle is the negative of the following:

$$\begin{aligned}
\int_{-\infty}^{\infty} cd\Psi(F_C(c)) &= \int_{-\infty}^{-K_1} cd\Psi(F_C(c)) + \int_{-K_1}^0 cd\Psi(F_C(c)) \\
&= \int_{\infty}^{K_1+K_2} (K_2 - S)d\Psi(1 - F_S(S)) + \\
&\quad \int_{-K_1}^0 cd\Psi(F_S(c + K_1) + F_S(K_1 + K_2) - F_S(K_2 - c)) \\
&= - \int_{K_1+K_2}^{\infty} \Psi(1 - F_S(s))ds - \int_0^{K_1} \Psi(F_S(s) + 1 - F_S(K_1 + K_2 - s))ds.
\end{aligned}$$

In summary, the bid and ask prices for a strangle are:

$$Strangle_{Bid} = K_1 + \int_{K_1+K_2}^{\infty} (1 - \Psi(F_S(s)))ds - \int_{K_2}^{K_1+K_2} \Psi(F_S(s) - F_S(K_2 + K_1 - s))ds,$$

$$Strangle_{Ask} = \int_{K_1+K_2}^{\infty} \Psi(1 - F_S(S))ds + \int_0^{K_1} \Psi(F_S(s) + 1 - F_S(K_1 + K_2 - s))ds.$$

Buying a strangle is equivalent to buying a put option with strike price K_1 and a call option with strike price K_2 . Hence, the buying advantage is defined as:

$$buying_advantage_strangle = \frac{(Put_{Ask}^{K_1} + Call_{Ask}^{K_2}) - Strangle_{Ask}}{Put_{Ask}^{K_1} + Call_{Ask}^{K_2}}.$$

Selling a strangle is equivalent to selling a put option with strike price K_1 and a call option with strike price K_2 . Hence, the selling advantage is defined as:

$$selling_advantage_strangle = \frac{Strangle_{Bid} - (Put_{Bid}^{K_1} + Call_{Bid}^{K_2})}{Put_{Bid}^{K_1} + Call_{Bid}^{K_2}}.$$

Figures 3.10 and 3.11 depict the benefits of trading a strangle using a Geometric Brownian motion. The input variables are the same as those used in the bull spread test. As previously discussed, when the maturity, volatility, and stress levels increase, the trading benefits increase. Generally, when the maturity is close to zero and the strike price of the put option is close to the spot price, the bid and ask prices of the strangle, put option, and call option are all very small. This results in a serious decrease near the spot price as shown in Figure 3.10. Trading a short-maturity strangle with a deep OTM call option and a deep OTM put option may only lead to a few benefits.

Figures 3.12 and 3.13 present the benefits of trading a strangle using VGSSD. As θ increases from negative to positive, buying and selling advantages decrease. As the market skewness increases, the ask prices of the OTM call option and the strangle increase dramatically. The difference between the ask price of the strangle and the sum of the ask prices of the two options does not change much. The increase in the sum of the ask prices of the two options reduces the buying benefits.

3.3.4 Straddle

A straddle longs a put option and a call option at the same strike price K with the same maturity. When it reaches the expiration date, a large movement in either

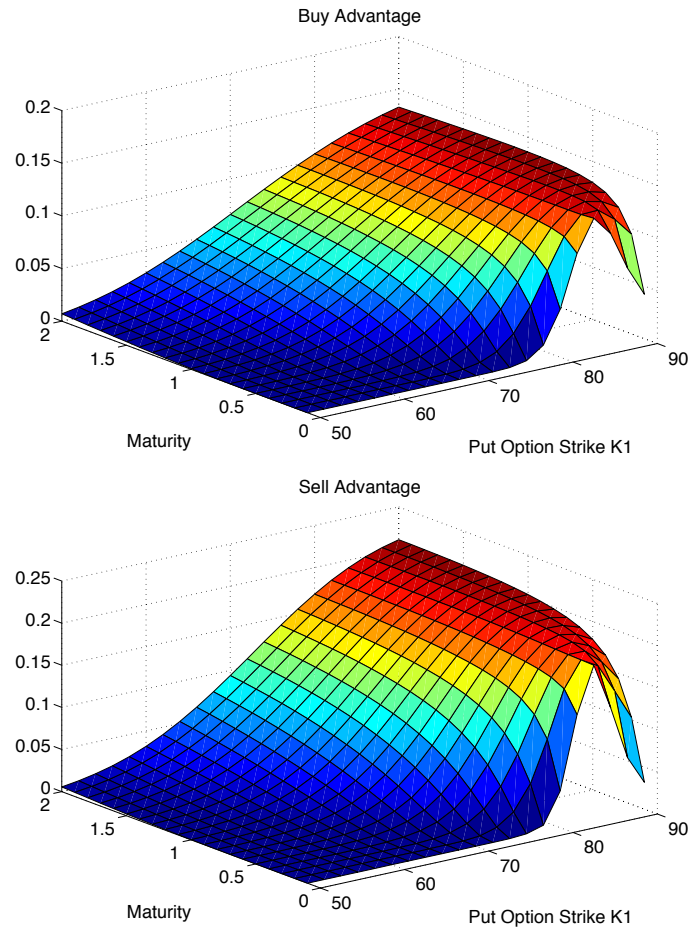


Figure 3.10: Buy and sell advantages of trading a strangle using GBM with input variables $S_0 = 100$, $K_2 = 120$, $\sigma = 0.2$ and $\lambda = 0.25$.

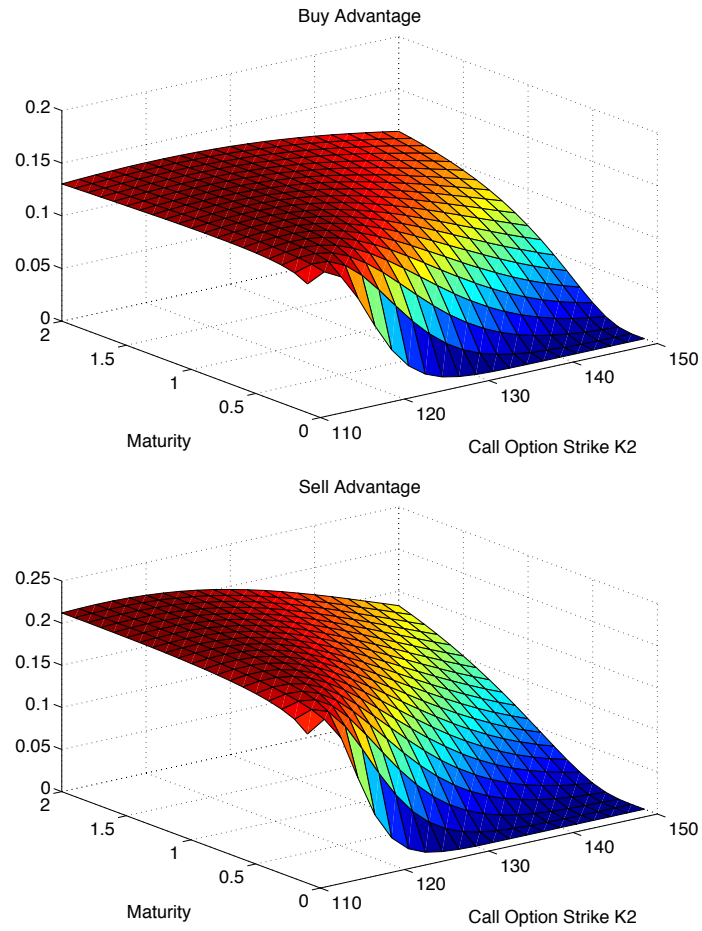


Figure 3.11: Buy and sell advantages of trading a strangle using GBM with input variables $S_0 = 100$, $K_1 = 80$, $\sigma = 0.2$ and $\lambda = 0.25$.

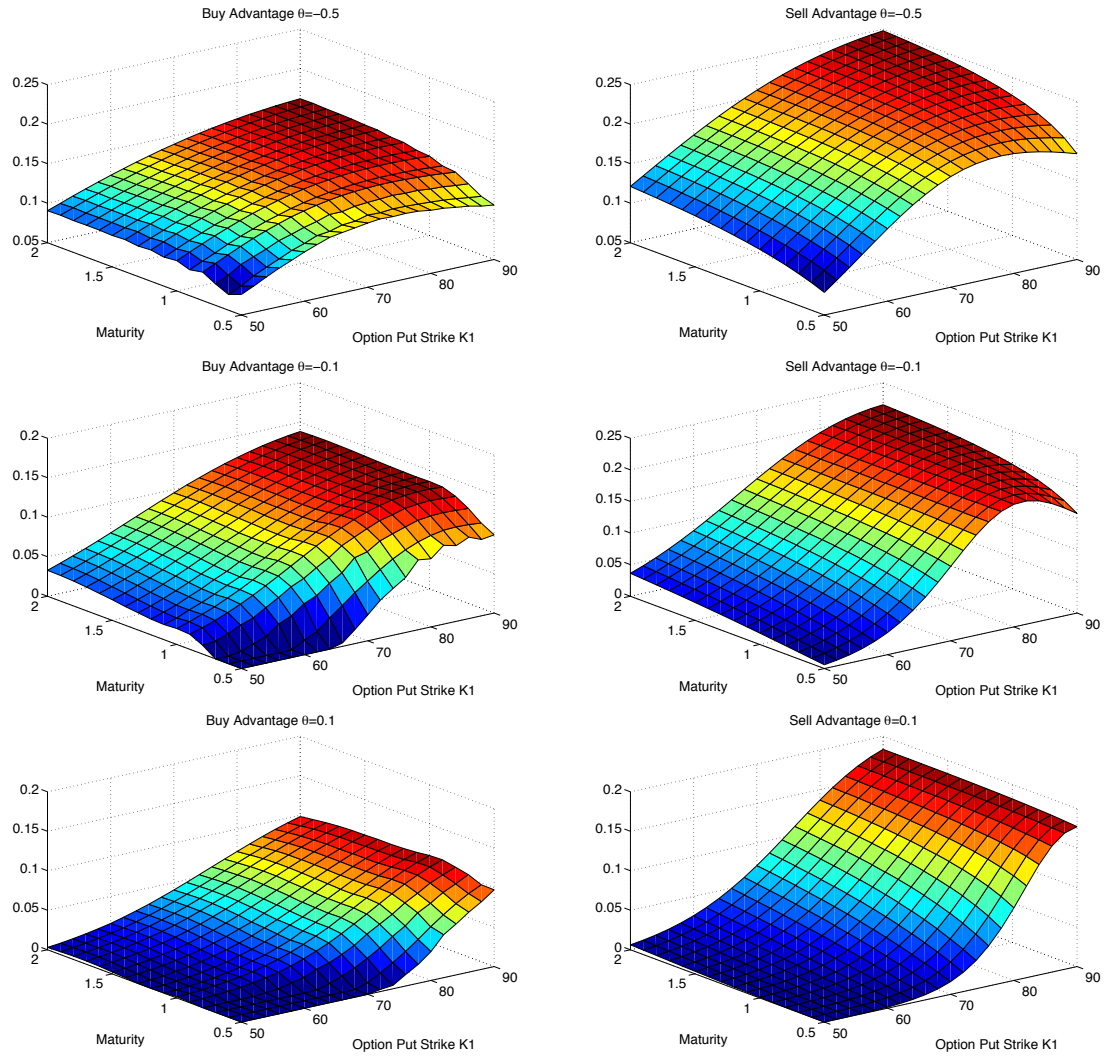


Figure 3.12: Buy and sell advantages of trading a strangle using VGSSD with input variables $S_0 = 100$, $K_2 = 120$, $\sigma = 0.2$, $\nu = 0.5$, $\gamma = 0.5$ and $\lambda = 0.25$.

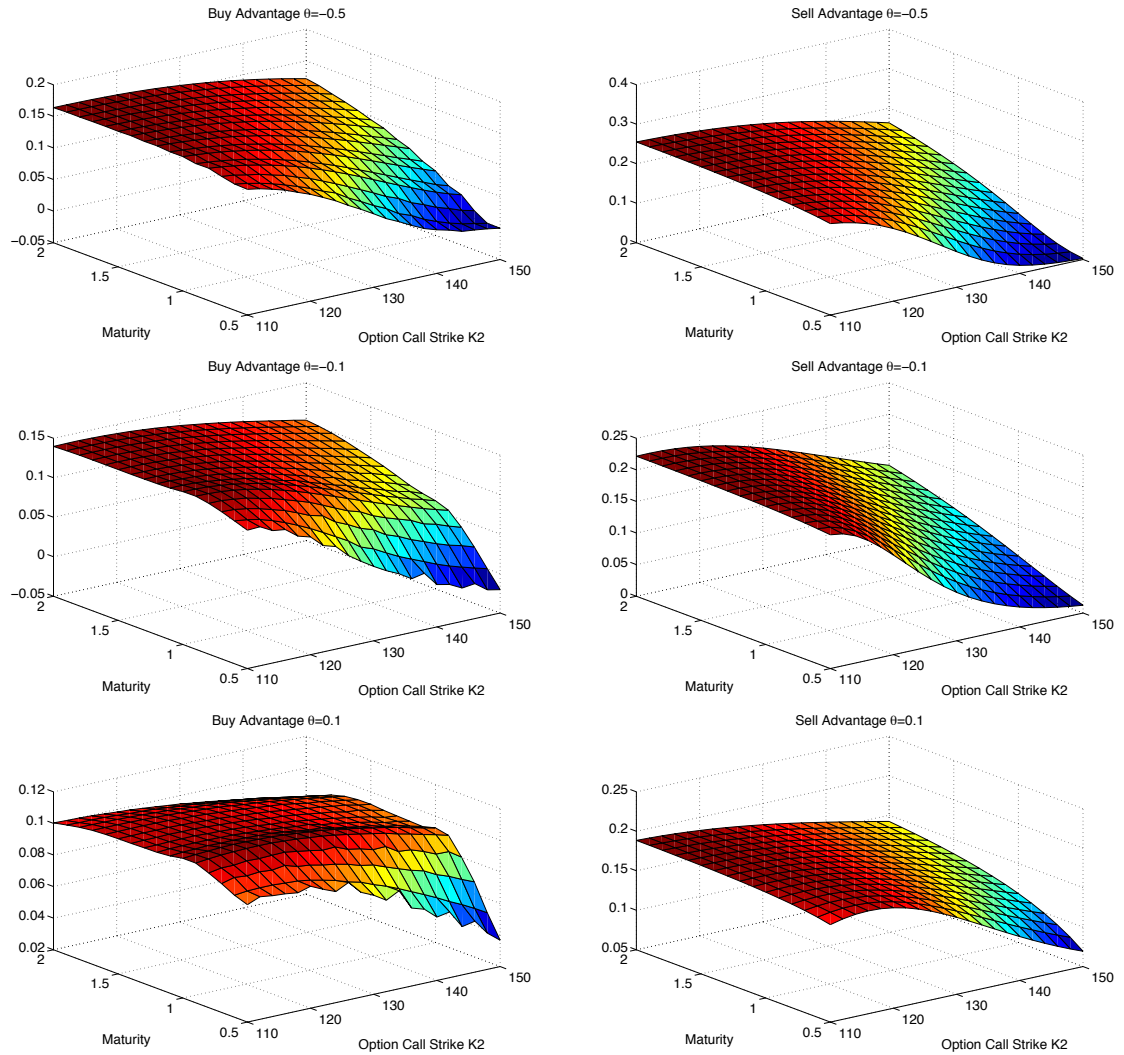


Figure 3.13: Buy and sell advantages of trading a strangle using VGSSD with input variables $S_0 = 100$, $K_1 = 90$, $\sigma = 0.2$, $\nu = 0.5$, $\gamma = 0.5$ and $\lambda = 0.25$.

direction leads to profit for a long position. On the other hand, if the stock price at maturity is close to the strike price K , the payoff is close to zero. Straddles are used as trading instruments for volatility. If the volatility is expected to be high in the future, a long position in straddle is desired. Moreover, straddles could be used to replicate the payoff of variance swaps with weights inversely proportional to K^2 [27]. The cash flow of a straddle is

$$C = (K - S)^+ + (S - K)^+.$$

According to the bid and ask prices of strangles, for straddles, $K_1 = K_2 = K$, the bid and ask prices for a straddle are:

$$\begin{aligned} Straddle_{Bid} &= K + \int_{2K}^{\infty} (1 - \Psi(F_S(s)))ds - \int_K^{2K} \Psi(F_S(s) - F_S(2K - s))ds, \\ Straddle_{Ask} &= \int_{2K}^{\infty} \Psi(1 - F_S(S))ds + \int_0^K \Psi(F_S(s) + 1 - F_S(2K - s))ds. \end{aligned}$$

Buying a straddle is equivalent to buying a put option and a call option at the the strike price K . Hence, the buying advantage is defined as:

$$buying_advantage_straddle = \frac{(Put_{Ask}^K + Call_{Ask}^K) - Straddle_{Ask}}{Put_{Ask}^K + Call_{Ask}^K}.$$

Selling a straddle is equivalent to selling a put option and a call option at the the strike price K . Hence, the selling advantage is defined as:

$$selling_advantage_straddle = \frac{Straddle_{Bid} - (Put_{Bid}^K + Call_{Bid}^K)}{Put_{Bid}^K + Call_{Bid}^K}.$$

Figure 3.14 presents the numerical results performed on a Geometric Brownian motion. The input variables are the same as the bull spread test except only one

strike price is used and the range of the strike price is $[50, 150]$. The maximum benefit for trading straddles is found near the spot price. Thus, longing straddles with an ATM call and put options would provide the maximum benefits.

3.3.5 Butterfly Spread

A butterfly spread longs one call option at the strike price K_1 and one call option at the strike price K_3 at the same time, shorts two call options at the strike price K_2 with the same maturity T , where $K_3 > K_2 > K_1$ and $K_3 - K_2 = K_2 - K_1 = a$, a is a constant. The cash flow is

$$C = (K_1 - S)^+ - 2(K_2 - S)^+ + (K_3 - S)^+.$$

For the bid price, the cash flow is $C = (K_1 - S)^+ - 2(K_2 - S)^+ + (K_3 - S)^+$ which can be separated into the following parts:

$$S \in [0, K_1) \cup (K_3, \infty), C(S) = 0;$$

$$S \in [K_1, K_2], C(S) = S - K_1;$$

$$S \in [K_2, K_3], C(S) = K_3 - S.$$

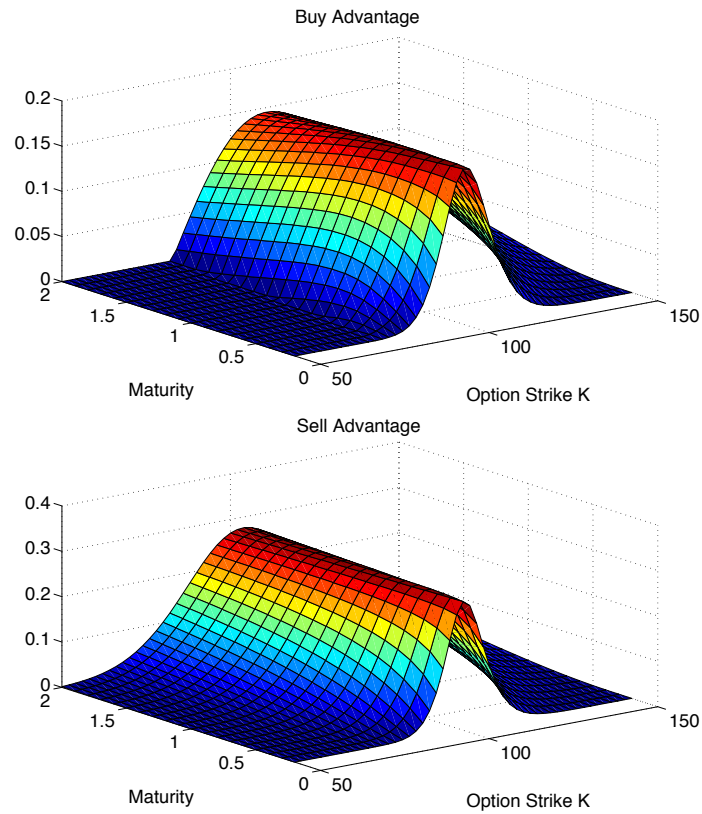


Figure 3.14: Buy and sell advantages of trading a straddle using GBM with input variables $S_0 = 100$, $\sigma = 0.2$ and $\lambda = 0.25$.

Thus, the bid price of a butterfly spread is

$$\begin{aligned}
\int_{-\infty}^{\infty} cd\Psi(F_C(c)) &= \int_{-\infty}^0 cd\Psi(F_C(c)) + \int_0^a cd\Psi(F_C(c)) + \int_a^{\infty} cd\Psi(F_C(c)) \\
&= \int_0^a cd\Psi(F_C(c)) \\
&= \int_0^a cd\Psi(F_C(S - K_1 \leq c)1_{K_1 \leq s \leq K_2} + F_C(K_3 - S \leq c)1_{K_2 \leq S \leq K_3}) \\
&= \int_{K_1}^{K_2} (s - K_1)d\Psi(F_S(s) + 1 - F_S(2K_2 - s)) \\
&= K_2 - K_1 - \int_{K_1}^{K_2} \Psi(F_S(s) + 1 - F_S(2K_2 - s))ds \\
&= a - \int_{K_1}^{K_2} \Psi(F_S(s) + 1 - F_S(2K_2 - s))ds.
\end{aligned}$$

For the ask price, the cash flow is $C = -(K_1 - S)^+ + 2(K_2 - S)^+ - (K_3 - S)^+$.

The range of the cash flow is $C \in [-a, 0]$. Random variable C is a function of S which also has the following parts:

$$S \in [0, K_1) \cup (K_3, \infty), C(S) = 0;$$

$$S \in [K_1, K_2], C(S) = K_1 - S;$$

$$S \in [K_2, K_3], C(S) = S - K_3.$$

Thus, the ask price of a butterfly spread is

$$\begin{aligned}
-\int_{-\infty}^{\infty} cd\Psi(F_C(c)) &= -\left(\int_{-\infty}^0 cd\Psi(F_C(c)) + \int_0^a cd\Psi(F_C(c)) + \int_a^{\infty} cd\Psi(F_C(c))\right) \\
&= -\int_{-a}^0 cd\Psi(F_C(c)) \\
&= -\int_{-a}^0 cd\Psi(F_C(K_1 - s \leq c)1_{K_1 \leq s \leq K_2} + F_C(s - K_3 \leq c)1_{K_2 \leq s \leq K_3}) \\
&= -\int_{K_2}^{K_3} (s - K_3)d\Psi(F_S(s) - F_S(2K_2 - s)) \\
&= \int_{K_2}^{K_3} \Psi(F_S(s) - F_S(2K_2 - s))ds.
\end{aligned}$$

In summary, the bid and ask prices for a butterfly spread are:

$$Butterfly_{Bid} = a - \int_{K_1}^{K_2} \Psi(F_S(s) + 1 - F_S(2K_2 - s)) ds, \quad (3.8)$$

$$Butterfly_{Ask} = \int_{K_2}^{K_3} \Psi(F_S(s) - F_S(2K_2 - S)) ds. \quad (3.9)$$

Buying a butterfly is equivalent to buying one put option with the strike price K_1 and one with K_3 the same time selling two put options with the strike price K_2 . Hence, the buying advantage of a butterfly spread is defined as:

$$buying_advantage_butterfly = \frac{(Put_{Ask}^{K_1} + Put_{Ask}^{K_3} - 2 \times Put_{Bid}^{K_2}) - Butterfly_{Ask}}{Put_{Ask}^{K_1} + Put_{Ask}^{K_3} - 2 \times Put_{Bid}^{K_2}}.$$

Selling a butterfly is equivalent to selling one put option with the strike price at K_1 and one with K_3 at the same time buying two put options with the strike price at K_2 . Hence, the selling advantage of a butterfly is defined as:

$$selling_advantage_butterfly = \frac{Butterfly_{Bid} - (Put_{Bid}^{K_1} + Put_{Bid}^{K_3} - 2 \times Put_{Ask}^{K_2})}{Put_{Bid}^{K_1} + Put_{Bid}^{K_3} - 2 \times Put_{Ask}^{K_2}}.$$

We proved that buying a butterfly spread is always cheaper, which indicates that the price of buying one put option with the strike price K_1 together with K_3 and selling two put options with the strike price K_2 is always more expensive than the price of buying the butterfly spread. On the other hand, the selling advantage of a butterfly spread is always positive, which indicates that the price of selling one put option with the strike price K_1 as well as one with K_3 and buying two put options with the strike price K_2 is always lower than the price of selling the butterfly. The numerical test for the trading advantages of butterfly spreads with constant K_2 under GBM is shown in Figure 3.15. The input variables are:

$$S_0 = 100; K_2 = 100; a = [15 : 5 : 30]; r = 0.01; \sigma = 0.2; \lambda = 0.05.$$

Relatively low stress levels are used to study butterfly spreads. It is observed that butterfly spreads, a combination of two bear put spreads, are more sensitive to stress levels than a single bear spread. Hence, in the same market, a butterfly spread has more trading benefits than its components, a single bear spread, or a single bull spread. This suggests that the more options there are in the combination, the greater the packaging benefits of trading it.

Figure 3.16 depicts the benefits of trading a butterfly spread in skewed markets. Similar to bull spreads, trading butterfly spreads in more left-skewed and right-skewed markets brings more benefits to investors. As the difference of the two strike prices decreases and the maturity increases, the trading benefits also increase.

3.3.6 Risk Reversal

A risk reversal longs a call option at the strike price K_2 and shorts a put option at the strike price K_1 with the same maturity T , where $K_2 > K_1$. The cash flow is

$$C = (S - K_2)^+ - (K_1 - S)^+.$$

For the bid price, the cash flow is $C = (S - K_2)^+ - (K_1 - S)^+$. The range of the terminal payoff is $C \in [-K_1, \infty]$. The distribution function of C in terms of S is:

$$F_C(c) = F_S(s).$$

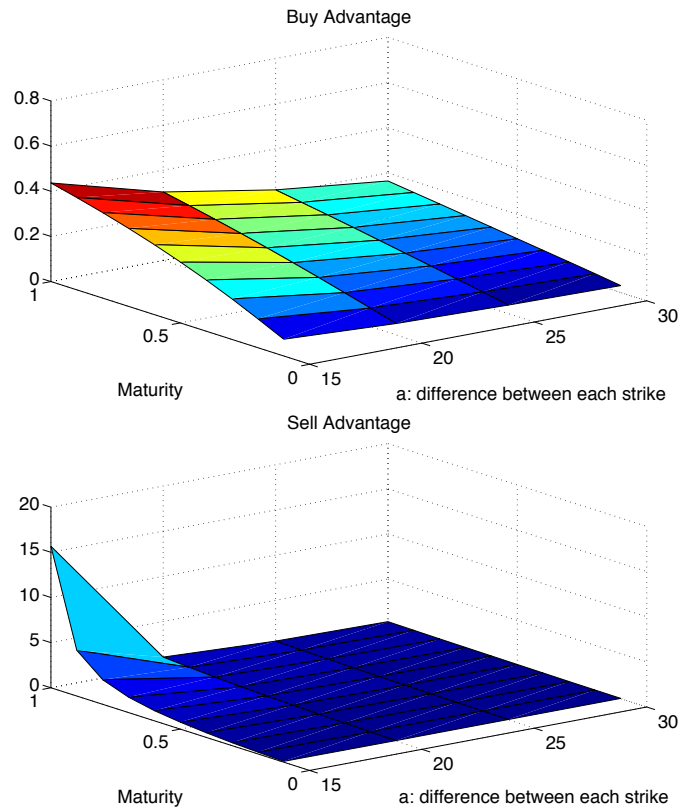


Figure 3.15: Buy and sell advantages of trading a butterfly spread using GBM with input variables $S_0 = 100$, $K_2 = 120$, $\sigma = 0.2$ and $\lambda = 0.05$.

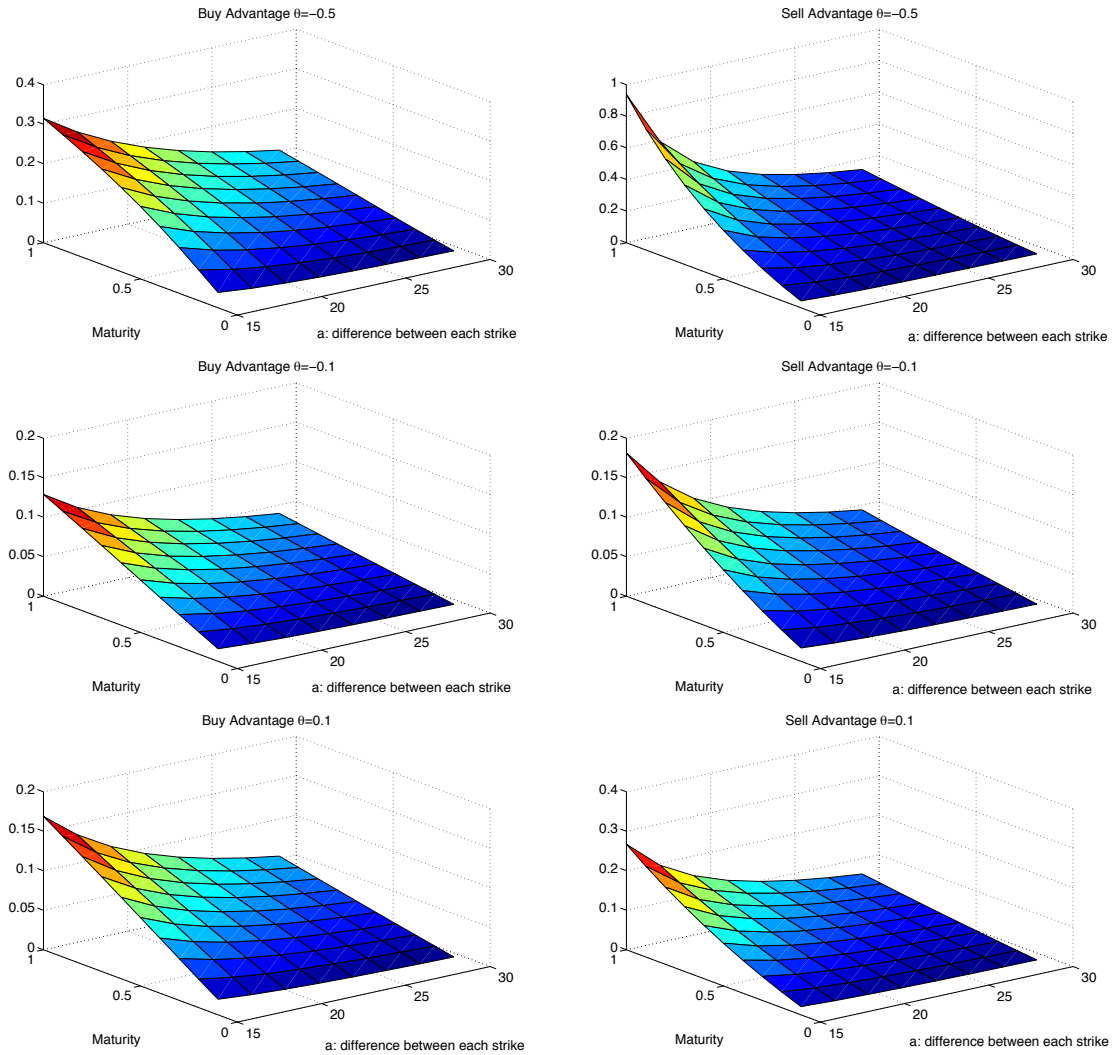


Figure 3.16: Buy and sell advantages of trading a butterfly spread using VGSSD with input variables $S_0 = 100$, $K_2 = 120$, $\sigma = 0.2$, $\nu = 0.5$, $\gamma = 0.5$ and $\lambda = 0.05$.

Thus, the bid price of a risk reversal is

$$\begin{aligned}
\int_{-\infty}^{\infty} cd\Psi(F_C(c)) &= \int_{-K_1}^0 cd\Psi(F_C(c)) + \int_0^{\infty} cd\Psi(F_C(c)) \\
&= \int_0^{K_1} (S - K_1)d\Psi(F_S(s)) + \int_{K_2}^{\infty} (S - K_2)d\Psi(F_S(s)) \\
&= (S - K_1)\Psi(F_S(s))\Big|_0^{K_1} - \int_0^{K_1} \Psi(F_S(s))ds + \\
&\quad (S - K_2)\Psi(F_S(s))\Big|_{K_2}^{\infty} - \int_{K_2}^{\infty} \Psi(F_S(s))ds \\
&= \int_{K_2}^{\infty} (1 - \Psi(F_S(s)))ds - \int_0^{K_1} \Psi(F_S(s))ds \\
&= Call_{Bid}^{K_2} - Put_{Ask}^{K_1}.
\end{aligned}$$

For the ask price, the cash flow is $C = -(S - K_2)^+ + (K_1 - S)^+$. The range of the cash flow is $C \in [-\infty, K_1]$. The distribution function of C in terms of S is:

$$F_C(c) = 1 - F_S(s).$$

Thus, the ask price of a risk reversal is

$$\begin{aligned}
-\int_{-\infty}^{\infty} cd\Psi(F_C(c)) &= -\int_{-\infty}^0 cd\Psi(F_C(c)) - \int_0^{K_1} d\Psi(F_C(c)) \\
&= \int_{K_2}^{\infty} \Psi(1 - F_S(s))ds - \int_0^{K_1} (1 - \Psi(1 - F_S(s)))ds \\
&= Call_{Ask}^{K_2} - Put_{Bid}^{K_1}.
\end{aligned}$$

Recall Equation (2.15)-(2.18) which described bid and ask prices of European call and put options. We discovered that the bid price of a risk reversal is the bid price of a call option with strike price K_2 , less the ask price of a put option with strike price K_1 , and the ask price of a risk reversal is the ask price of a call option with strike price K_2 , less the bid price of a put option with strike price K_1 . Thus, there is no packaging benefit in trading risk reversal aside from trading the two

component options separately. For the part with nonzero terminal cash flows, there is no overlap payoff in the two options. This is the reason why trading a risk reversal is not different from trading its component options.

3.4 Exotic Options

Cliquet type options are essentially a series of consecutive forward-start at-the-money options with a single premium determined in advance. Their payoffs are dependent on relative returns of the underlying assets after a series of predetermined dates. Caps and floors are used to fix the maximum and minimum of returns. As a result, investors are protected from downside risk and limited in upside gains.

3.4.1 Cliquet Options

An N -month cliquet is defined with the end of every month as the predetermined date. These returns, which are protected capital and limited gain, are first floored with zero and then capped with a positive value. A comparison of pricing cliquet options using different models by simulation could be found in [51]. The final payoff for this cliquet is the sum of these modified relative returns, and defined as:

$$CL = \sum_{i=1}^N \min \left(\max \left(\frac{S_i - S_{i-1}}{S_i}, 0 \right), cap \right).$$

Holding a cliquet is equivalent to holding a series of call spreads. Hence, the buying advantage is defined as:

$$buying_advantage_cliquet = \frac{Call_Spread_{Ask} - Cliquet_{Ask}}{Call_Spread_{Ask}}.$$

Selling a cliquet is equivalent to selling a series of call spreads. Hence, the selling advantage is defined as:

$$selling_advantage_cliquet = \frac{Call_Spread_{Bid} - Cliquet_{Bid}}{Call_Spread_{Bid}}.$$

Since closed-form pricing formulas for cliquets are hard to obtain, the Monte Carlo approach is popular in pricing these instruments. The number of the simulation path is 50,000. Equation 3.3 is used for computing the distorted expectation numerically. The range of caps is $[0.05, 0.15]$. Table 3.1 presents the bid and ask prices of cliquets and their corresponding series of call spreads under GBM with the following input variables:

$$S_0 = 100; floor = 0; T = [0.5, 1, 2]; r = 0.01; \sigma = 0.2; \lambda = 0.1.$$

The pricing comparison is also illustrated under the Variance Gamma (VG) process described in Madan and Seneta [42] and Madan, Carr and Chang [33], a time changed Brownian motion by a gamma process. If $X(t; \sigma, \nu, \theta)$ follows VG, the process can be described as:

$$X(t; \sigma, \nu, \theta) = \theta g(t; \nu) + \sigma W(g(t; \nu)),$$

where σ is the volatility, ν is the variance rate of the gamma time change, θ is the drift and W is a Brownian motion. Table 3.2 presents the computed bid and ask prices under the VG process with the same variables for GBM and the others are:

$$\theta = -0.3;$$

$$\nu = 0.5;$$

It is observed that the bid-ask spreads of cliquets are lower than the corresponding series of call spreads under both models. The positive selling advantages and buying advantages indicate the package advantages of trading structured products for investors. Moreover, when N increases, i.e., more call spreads are added into the series, the results suggest that greater trading advantages to cliquets exist.

3.4.2 Reverse Cliquet Options

An N -month reverse cliquet can also be defined using the end of every month as the predetermined monthly date. These returns are first capped with zero and floored with a negative value. These contracts give holders a nominal return R^* for bearing the downside risk. The range of floors is $[-0.15, -0.05]$. The final payoff is the sum of the modified relative returns, and defined as:

$$RECL = R^* + \sum_{i=1}^N \max \left(\min \left(\frac{S_i - S_{i-1}}{S_i}, 0 \right), floor \right).$$

Holding a reverse cliquet is equivalent to holding a series of put spreads and bonds. Hence, the buying advantage is defined as:

$$buying_advantage_reverse_cliquet = \frac{Put_Spread_{Ask} - Reverse_Cliquet_{Ask}}{Call_Spread_{Ask}}.$$

Selling a reverse cliquet is equivalent to selling a series of put spreads. Hence, the selling advantage is defined as:

$$selling_advantage_reverse_cliquet = \frac{Put_Spread_{Bid} - Reverse_Cliquet_{Bid}}{Put_Spread_{Bid}}.$$

The same parameters for cliquet options are used with $R^* = [0.25, 0.5, 1.0]$ for 6-month, 12-month, and 24-month reverse cliquets respectively. Tables 3.3 and 3.4

Table 3.1: Advantages of Trading a Cliquet (GBM) for 6, 12 and 24 Months

Maturity	Cap	Spread Ask	Cliquet Ask	Spread Bid	Cliquet Bid	Buy	Sell
6 months	0.05	0.1188	0.1089	0.0830	0.0914	0.0827	0.1015
	0.10	0.1621	0.1460	0.1069	0.1199	0.0993	0.1210
	0.15	0.1720	0.1537	0.1107	0.1249	0.1064	0.1283
12 months	0.05	0.2364	0.2112	0.1651	0.1863	0.1066	0.1283
	0.10	0.3220	0.2814	0.2122	0.2447	0.1261	0.1530
	0.15	0.3419	0.2964	0.2201	0.2555	0.1332	0.1604
24 months	0.05	0.4704	0.4107	0.3286	0.3762	0.1269	0.1450
	0.10	0.6425	0.5483	0.4237	0.4960	0.1467	0.1708
	0.15	0.6833	0.5772	0.4403	0.5199	0.1553	0.1809

Table 3.2: Advantages of Trading a Cliquet (VG) for 6, 12 and 24 Months

Maturity	Cap	Spread Ask	Cliquet Ask	Spread Bid	Cliquet Bid	Buy	Sell
6 months	0.05	0.1296	0.1223	0.1014	0.1075	0.0567	0.0602
	0.10	0.1458	0.1349	0.1089	0.1175	0.0749	0.0792
	0.15	0.1495	0.1375	0.1097	0.1188	0.0801	0.0837
12 months	0.05	0.2580	0.2404	0.2020	0.2157	0.0681	0.0679
	0.10	0.2883	0.2619	0.2153	0.2355	0.0918	0.0939
	0.15	0.2978	0.2686	0.2188	0.2407	0.0983	0.1001
24 months	0.05	0.5138	0.4732	0.4017	0.4299	0.0791	0.0701
	0.10	0.5753	0.5141	0.4291	0.4724	0.1065	0.1010
	0.15	0.5943	0.5263	0.4368	0.4845	0.1145	0.1092

present a comparison of the bid and ask prices of the reverse cliquets, and their corresponding series of put spreads along with bonds under GBM and VG processes with the same inputs as Tables 3.1 and 3.2. Positive selling advantages and buying advantages are observed. It is also observed that when N increases, i.e., more put spreads are added into the series, greater trading advantages of reverse cliquets. Similar as butterfly spreads, this observation suggests that the more options in the combination, the more trading benefits there are.

3.4.3 Spread Option

A spread option is written on two underlying assets S_1 and S_2 with correlation ρ , $|\rho| \leq 1$. The terminal payoff of a spread option with the strike price K is

$$SO = (S_1 - S_2 - K)^+.$$

We define a new contingent claim based on this spread option as a sum of a series of spread options at time t_i , $i = 1, \dots, n$.

$$SSO = \sum_{i=1}^n (S_1 - S_2 - K)_i^+. \quad (3.10)$$

We can model these two assets as two correlated Geometric Brownian motions:

$$dS_1 = S_1\mu_1 dt + S_1\sigma_1 dW_1, \quad (3.11)$$

$$dS_2 = S_2\mu_2 dt + S_2\sigma_2 dW_2, \quad (3.12)$$

with $dW_1 dW_2 = \rho dt$.

Table 3.3: Advantages of Trading a Reverse Cliquet (GBM) for 6, 12 and 24 Months

Maturity	Floor	Spread Ask	Cliquet Ask	Spread Bid	Cliquet Bid	Buy	Sell
6 months	-0.15	0.1402	0.1267	0.0825	0.0997	0.0966	0.2089
	-0.10	0.1435	0.1308	0.0898	0.1056	0.0884	0.1755
	-0.05	0.1643	0.1557	0.1284	0.1384	0.0522	0.0775
12 months	-0.15	0.2779	0.2441	0.1620	0.2053	0.1219	0.2677
	-0.10	0.2842	0.2524	0.1771	0.2168	0.1119	0.2244
	-0.05	0.3269	0.3054	0.2554	0.2808	0.0657	0.0996
24 months	-0.15	0.5506	0.4750	0.3211	0.4216	0.1374	0.3128
	-0.10	0.5595	0.4886	0.3460	0.4383	0.1268	0.2670
	-0.05	0.6441	0.5962	0.5016	0.5615	0.0743	0.1195

Table 3.4: Advantages of Trading a Reverse Cliquet (VG) for 6, 12 and 24 Months

Maturity	Floor	Spread Ask	Cliquet Ask	Spread Bid	Cliquet Bid	Buy	Sell
6 months	-0.15	0.1775	0.1752	0.1204	0.1242	0.0133	0.0320
	-0.10	0.1891	0.1873	0.1447	0.1476	0.0096	0.0200
	-0.05	0.2101	0.2090	0.1841	0.1858	0.0053	0.0093
12 months	-0.15	0.3543	0.3493	0.2410	0.2502	0.0140	0.0384
	-0.10	0.3754	0.3715	0.2866	0.2937	0.0105	0.0250
	-0.05	0.4177	0.4152	0.3656	0.3700	0.0060	0.0120
24 months	-0.15	0.6993	0.6901	0.4734	0.4954	0.0131	0.0464
	-0.10	0.7438	0.7365	0.5676	0.5849	0.0098	0.0304
	-0.05	0.8278	0.8232	0.7247	0.7352	0.0055	0.0144

Monte Carlo simulation is used to estimate the trading advantages of this product with 50000 paths. The input variables are:

$$S_1^0 = S_2^0 = 100; K = 5; dt = 1/12; r = 0; \sigma_{S_1} = 0.2; \sigma_{S_2} = 0.3; \lambda = 0.25,$$

where σ_1 and σ_2 are the volatility of the assets S_1 and S_2 respectively. ρ is the correlation of S_1 and S_2 . Tables 3.5 to 3.11 present the packaging benefits of spread options with the different values of correlation of the two underlying assets. It is observed that trading benefits increase as maturity increases, and more trading benefits exist for high positive correlations. These tables suggest that trading a spread option with zero correlation of the two underlying assets always has more packaging benefits than trading a spread option with negatively correlated underlying assets, and fewer packaging benefits than trading a spread option with positive correlated underlying assets. We also observed that both bid and ask prices of spread options increase as the correlation decreases. Thus, spread options with negative correlation have higher bid and ask prices than those with positive correlation. If the correlation of the two underlying assets is negative, the price difference of the two assets increases due to the opposing directions of price movements. Hence, the bid and ask prices increase. The larger bid and ask prices of spread options with negatively correlated assets lead to fewer trading benefits.

Table 3.5: Advantages of Trading a Spread Option with Noncorrelated Assets (Bivariate Normal): Correlation=0

Month	Single Ask (total)	SSO Ask	Single Bid (total)	SSO Bid	Buy	Sell
12	142.5178	134.1395	44.7080	48.8576	0.0588	0.0928
18	240.9112	225.8787	73.3895	80.6015	0.0624	0.0983
24	338.0898	315.4484	99.5793	110.0911	0.0670	0.1056
30	445.1717	414.8676	126.9418	140.7310	0.0681	0.1086
36	554.2107	515.2695	154.6618	172.0905	0.0703	0.1127
42	671.9222	623.7329	182.3374	203.4292	0.0717	0.1157
48	788.7780	729.8538	209.2120	234.4510	0.0747	0.1206

Table 3.6: Advantages of Trading a Spread Option with Correlated Assets (Bivariate Normal): Correlation=0.25

Month	Single Ask (total)	SSO Ask	Single Bid (total)	SSO Bid	Buy	Sell
12	119.8049	112.6716	37.0259	40.4892	0.0595	0.0935
18	200.0891	187.2567	59.6595	65.7123	0.0641	0.1015
24	280.0613	261.2442	80.3394	88.9611	0.0672	0.1073
30	363.2141	337.4860	100.9580	112.4162	0.0708	0.1135
36	444.1037	411.0764	119.7758	134.1526	0.0744	0.1200
42	537.0000	495.9116	141.0950	158.4099	0.0765	0.1227
48	616.8355	568.9686	157.2352	177.0667	0.0776	0.1261

Table 3.7: Advantages of Trading a Spread Option with Correlated Assets (Bivariate Normal): Correlation=0.5

Month	Single Ask (total)	SSO Ask	Single Bid (total)	SSO Bid	Buy	Sell
12	91.6796	85.9647	27.6183	30.3449	0.0623	0.0987
18	150.3519	140.2693	43.4716	48.0700	0.0671	0.1058
24	209.8583	195.1046	58.0112	64.5516	0.0703	0.1127
30	266.0811	246.2673	70.6313	79.1337	0.0745	0.1204
36	321.4271	296.2481	81.7520	92.1343	0.0783	0.1270
42	377.7897	347.4772	92.5071	104.6503	0.0802	0.1313
48	431.9216	395.6475	102.4219	116.4940	0.0840	0.1374

Table 3.8: Advantages of Trading a Spread Option with Correlated Assets (Bivariate Normal): Correlation=0.75

Month	Single Ask (total)	SSO Ask	Single Bid (total)	SSO Bid	Buy	Sell
12	58.6739	54.8134	16.9472	18.7200	0.0658	0.1046
18	90.7384	84.2287	24.6520	27.5013	0.0717	0.1156
24	118.8682	109.6483	30.3452	34.2015	0.0776	0.1271
30	146.6139	134.5385	35.7869	40.5911	0.0824	0.1342
36	169.1055	154.3117	38.9596	44.5563	0.0875	0.1437
42	191.0698	173.3989	42.2058	48.6210	0.0925	0.1520
48	211.9959	191.5644	45.1373	52.3158	0.0964	0.1590

Table 3.9: Advantages of Trading a Spread Option with Correlated Assets (Bivariate Normal): Correlation=-0.25

Month	Single Ask (total)	SSO Ask	Single Bid (total)	SSO Bid	Buy	Sell
12	164.8799	155.4877	52.5434	57.2241	0.0570	0.0891
18	276.6713	259.6211	85.6166	93.8790	0.0616	0.0965
24	401.0235	375.5856	120.9701	133.1596	0.0634	0.1008
30	531.1714	496.7154	155.9655	172.1217	0.0649	0.1036
36	661.4954	617.1012	189.7731	210.2832	0.0671	0.1081
42	792.7057	737.7024	222.6291	247.2371	0.0694	0.1105
48	928.5326	861.8479	255.0222	284.4667	0.0718	0.1155

Table 3.10: Advantages of Trading a Spread Option with Correlated Assets (Bivariate Normal): Correlation=-0.5

Month	Single Ask (total)	SSO Ask	Single Bid (total)	SSO Bid	Buy	Sell
12	182.2616	171.9338	58.4074	63.5708	0.0567	0.0884
18	311.9491	293.1819	97.9628	107.1739	0.0602	0.0940
24	448.1054	420.3243	136.5484	150.0317	0.0620	0.0987
30	597.9071	560.0548	179.1627	197.1597	0.0633	0.1005
36	759.7603	710.4188	223.6783	246.9020	0.0649	0.1038
42	906.6096	845.1462	261.7655	289.9662	0.0678	0.1077
48	1056.2	983.3750	297.0474	329.9895	0.0690	0.1109

Table 3.11: Advantages of Trading a Spread Option with Correlated Assets (Bivariate Normal): Correlation=-0.75

Month	Single Ask (total)	SSO Ask	Single Bid (total)	SSO Bid	Buy	Sell
12	201.0389	189.6973	65.3216	71.0573	0.0564	0.0878
18	340.5055	320.2519	107.9157	118.0108	0.0595	0.0935
24	497.3702	466.8745	154.5985	169.5686	0.0613	0.0968
30	668.3898	626.8636	204.1623	224.1170	0.0621	0.0977
36	828.6765	775.7913	247.3565	272.6291	0.0638	0.1022
42	1002.1	936.7430	292.5809	323.1550	0.0652	0.1045
48	1176.5	1098.2	337.9832	374.2433	0.0666	0.1073

3.5 Summary

We investigated the trading advantages of structured products based on the two-price market theory. Numerical tests of bull spreads, bear spreads, butterfly spreads, and straddles used along with mathematical proofs clearly illustrate the package advantages of structured products. Buying these spreads is always cheaper than trading their components separately, and selling these spreads is always more expensive than trading their components separately. We also studied the impact of market skewness in trading bull and bear spreads. Numerical tests on the VGSSD model suggest that for bull spreads more trading benefits exist in right-skewed markets and more left-skewed markets. When the market skewness changes from negative to positive, the trading benefits increase. On the other hand, for bear spreads, more trading benefits exist in left-skewed markets and extreme right-skewed markets. When the market skewness changes from negative to positive, trading benefits reduce first and then increase after a critical point. At the same stress level, a butterfly spread has more trading advantages than a bull call spread or a bear put spread. This suggests that more packaging benefits exist if there are more options are in the combination.

Numerical results obtained for cliquet and reverse cliquet options reach the same conclusion as option spreads; trading these products rather than their components could bring more benefits to investors. These trading advantages indicate the bid-ask spreads of these structured products are less than their corresponding components or lower transaction costs. Asymmetry is observed for selling and buy-

ing advantages from numerical results. Moreover, the longer the maturities of the cliquets and reverse cliquets, the greater the trading advantages for investors. These discoveries suggest that the level of trading advantages increases with the combination complexity of structured products. If more components with non-zero terminal cash flow are added into structured products, more benefits exist for trading these products. It was also observed that if the interval of the terminal cash flow of a single component in the structured product is larger, more trading benefits exist. If the terminal cash flow of the structured product is monotonic, like a risk reversal, there is no benefit to trading it in the conic two-price markets.

We observed that the correlation of underlying assets plays a crucial role in terms of packaging benefits in trading spread options. As correlation increases from negative to positive, bid and ask prices of spread options reduce, but trading benefits increase. If the prices of the two underlying assets move in the same direction, the spread option prices decrease. If the prices of the two underlying assets move in the opposite directions, the spread option prices increase. Greater spread option prices with negatively correlated assets leads to fewer trading benefits. As the total number of spread options increases, the trading benefits of a series of spread options also increase.

Chapter 4

Option Implied Liquidity

4.1 Introduction

”In business, economics or investment, market liquidity is an asset’s ability to be sold without causing a significant movement in the price and with minimum loss of value. Money, or cash in hand, is the most liquid asset, and can be used immediately to perform economic actions like buying, selling, or paying debt, meeting immediate wants and needs,” as defined in [53]. Thus, liquidity risk arises from situations when a party wants to trade an asset but can not find a counterparty to trade with. On the other hand, if an asset is easily bought or sold on the market, the asset is said to be liquid. As we know, bid and ask prices are defined by the market makers’ perspective. Like grocers [43], bid-ask spreads reflect investors’ demand rather than market makers’. Usually, bid-ask spreads can be used as an indicator of liquidity. Highly liquid assets have small spreads, whereas illiquid assets have large spreads. As discussed in [28], two important assumptions in classical option pricing theory are that markets are frictionless and competitive. Frictionless markets have no transaction costs, no taxes, and no bid-ask spreads. In competitive markets, the trading size of securities has no impact on price. It is believed that the violation of the two assumptions in real markets leads to the existence of liquidity risk. Some works that investigated liquidity risk using option pricing theory are discussed in

[28]. Observations show that bid-ask spreads evolve in a market with no variation in liquidity, but change nonlinearly with maturity and volatility. Hence, bid-ask spreads are not a perfect measure for liquidity. Corcuera J. M., et.al [23] introduced the concept of the implied liquidity parameter by using the two-price market model based on the conic finance theory. A nonlinear distorted expectation with one parameter, called the 'implied liquidity parameter,' is involved for pricing. The smaller the implied liquidity parameter, the more liquid the security and the lower the bid-ask spread. The Geometric Brownian motion was used to model the risk-neutral process of log returns. Their observation on the implied liquidity parameters of the at-the-money options of the S&P500 and Dow Jones Index demonstrates that vanilla options with high strike prices always have high implied liquidity parameters; in other words, low liquidity. Their historical study showed a significant drying up of liquidity in the weeks following the bankruptcy of Lehman Brothers. Derivatives on liquidity was also proposed as a hedging instrument in the future.

Here, we follow their work and continue to model the liquidity parameter implied by market option prices as a nonlinear function of strike prices and maturities with sophisticated risk-neutral price models. This could be a way to investigate the detailed structure of the liquidity parameter over the option surface. Moreover, the liquidity parameters are not just estimated for the at-the-money options, but over the option surface across different maturities and strike prices.

4.2 Nonlinear Least Square

In order to investigate the implied liquidity parameter, option calibration is an obvious choice and the first step. We assume the market is not a hedged one. In incomplete markets, options are not redundant. Thus, the available option prices could be an important source for model parameters and market information. The calibrated model parameters can be used for pricing exotic options and hedging. Option model calibration is defined as seeking the optimized risk-neutral model \mathbb{Q} with parameters θ , which could best approximate the market option prices across different strike prices and maturities.

The most popular approach to calibrate option models is to minimize the sum of the quadratic pricing error [1] [6], i.e.,:

$$J(\theta) = \sum_{i=1}^N \left(C(T_i, K_i) - \hat{C}(T_i, K_i) \right)^2, \quad (4.1)$$

where $C(T_i, K_i)$ is the market option price at maturity T_i and strike price K_i , \hat{C} is the modeled option price with model parameters θ at T_i and strike price K_i . For the case in this section, the objective function is the sum of the quadratic error of ask and bid prices of call and put options. Hence, the estimated parameters θ^* which are the best approximation of market option prices are given by:

$$\theta^* = \operatorname{argmin} \sum_{i=1}^N \left(C(T_i, K_i) - \hat{C}(T_i, K_i) \right)^2.$$

As we know, all the call and put options could be separated into three groups: the in-the-money (ITM) option where the strike price is less than the spot price, the at-the-money (ATM) option where the strike price is equal to the spot price, and

the out-of-the-money (OTM) option where the strike price is larger than the spot price. First, we use the OTM call and put options to study the implied liquidity parameters and model the implied liquidity parameters as quadratic functions of moneyness and linear functions of maturity as described in the following.

Let $x = \ln(S/K)$ be moneyness, and t be maturity. We first assume,

$$\lambda = \lambda_0 + ax + bx^2 + ct. \quad (4.2)$$

In order to investigate the relationship between moneyness and maturities, we assume,

$$\lambda = \lambda_0 + ax + bx^2 + ct + dxt. \quad (4.3)$$

The stress level λ is used in the distorted function MINMAXVAR which is described in Chapter 2,

$$\Psi_\lambda(u) = 1 - (1 - u^{\frac{1}{1+\lambda}})^{1+\lambda}.$$

VGSSD, introduced in Chapter 1 with characteristic function Equation 1.3, is used as the risk-neutral process of log stock prices. Along with the distorted function, the two equations model the bid and ask option prices under a specified risk-neutral process of VGSSD and a specified stress level λ . Hence, we have eight parameters to be estimated using nonlinear least squares: four parameters in VGSSD, θ , ν , σ, γ , and four parameters in stress levels, λ_0 , a , b and c . Tables 4.1 to 4.3 present the numerical results for S&P500 index options (SPX) every quarter from 2007 to 2010. Standard errors are measured by the square root of the inverse Hessian matrix of the objective function. Tables 4.5 to 4.7 present the results for NASDAQ

100 index options (NDX) and Tables 4.9 to 4.11 present the results for Dow Jones index options (DJX). Tables 4.13 to 4.21 present the estimated and analysis results for index options using Equation (4.3) for modeling λ . Three terms used in the fit statistics are defined as follows.

Let N be the total number of option prices used in the calibration. APE which denotes the average absolute error as a percentage of the mean price is defined as:

$$APE = \frac{1}{Prices_{Mean}} \sum_{i=1}^N \frac{|Price_{Market} - Price_{Model}|}{N}.$$

AAE which denotes the average absolute error is defined as :

$$AAE = \sum_{i=1}^N \frac{|Price_{Market} - Price_{Model}|}{N}.$$

RMSE which denotes the root mean square error is defined as:

$$RMSE = \sqrt{\sum_{i=1}^N \frac{(Price_{Market} - Price_{Model})^2}{N}}.$$

Usually, one with APE lower than 5% is considered a good calibration.

When the moneyness x in Equation (4.2) is zero, the stress level λ which is the stress level for the ATM options is the value of λ_0 . The results from Tables 4.1, 4.5, and 4.9 suggest that, significant high stress levels of SPX, NDX and DJX are estimated on September 30, 2008 and December 31, 2008. This observation reaches the same agreement as [23] that a serious liquidity risk exists in the credit crisis in 2008. When the moneyness x is equal to $-\frac{a}{2b}$, the stress level λ reaches its minimum. From the three tables, we found that the values of a are mostly negative and the values of b are mostly positive, hence, OTM put options always have the minimum value of stress levels across the option surface. The strike prices

with minimum value of λ and the spot prices are presented in Tables 4.1, 4.5, and 4.9. It indicates that put options with minimum stress levels are most liquid on the option surface, and investors use these options to protect themselves if market is going down. It is observed that the value of c is always close to zero. Given parameter identification results, there is no linear relationship between stress levels and maturities. However, nonlinear relationship between these two might exist. Figure 4.1 presents the VGSSD modeled ask and bid option prices as well as the market option prices of SPX on December 31, 2008. Figure 4.2 depicts the variation of stress level λ on the option surface. The relatively steeper slope for the OTM put options suggests that the market for OTM put options is more illiquid than that for OTM call options. The limited downside gain for put options discourages investors to trade these options.

4.3 Model Estimation Analysis

The process of model calibration is an inverse problem of option pricing. Unfortunately, this inverse problem is ill-posed. In the Black-Scholes-Merton model, the only estimated parameter is volatility σ . In more complex models, like jump-diffusion models, stochastic volatility models are developed, the problem of parameter identification becomes more difficult. Different ways to calibrate models have been developed, such as the Hermite approximation of likelihood [2] and weighted non-parametric approximation [22]. Due to the non-convex objective function in Equation 4.1, the global minimum may not be reached. Problems then arise to

question the quality of the calibration results. The most serious concerning is the parameter identification problem. It is possible that many other sets of parameters in this model could experience the same minimized pricing error. In this case, the minimum has a flat region which causes the objective function to have a low sensitivity with respect to the model parameters. This problem is not just due to the lack of option prices data; rather, the amount of option price data is less than the number of model parameters that needs to be estimated. Cont and Tankov [22] presented examples of this situation. Besides the uniqueness problem, another issue is that since the objective function is non-convex, the local minimum could always be reached; however, are these local minimums are the true solution we are looking for? Which model parameters dominate the minimization results? To answer these questions, a sensitivity analysis of estimated model parameters is crucial in order to examine the quality of the estimation results and recognize the significance of these parameters in the minimization.

The approach to identify estimated parameters in [32] is to compute the average value of the first order derivative of the absolute pricing error with respect to each model parameter,

$$\left| \frac{\partial \frac{1}{2}(w_i - w_i^m)^2}{\partial \theta_k} \right|,$$

w_i is market price, w_i^m is model price and then take the average value across all options. The higher the value, the more the parameter is identified.

Tables 4.4, 4.8 and 4.12 present the eight parameter identification results for SPX, NDX and DJX respectively. σ , θ , λ_0 and c are more identified than the rest

of eight parameters. Figure 4.3 depicts the identification for each parameter on different strike prices and four maturities 0.4712, 0.9699, 1.4685 and 1.9671. As we observe, θ and c are mostly identified by the longest put options, σ , ν , λ_0 , a and b are mostly identified by the longest OTM call and put options, γ is mostly identified by the longest OTM options and the shortest ATM options. Tables 4.13 to 4.21 present the estimated night parameters for SPX, NDX and DJX. The observation on parameter identification suggests that parameter d is not well identified.

Table 4.1: SPX OTM Calibrated Parameters : λ has four parameters.

Date	σ	ν	θ	γ	λ_0	a	b	c	min (x)	min (K)	Spot
20070328	0.1188	0.9666	-0.1039	0.5609	0.0163	-0.0015	0.3278	-0.0038	0.0023	1413.99	1417.23
20070627	0.1303	0.9212	-0.1146	0.5583	0.0089	-0.0015	0.1044	-0.0013	0.0072	1495.56	1506.34
20070927	0.1433	0.8376	-0.1500	0.5701	0.0110	-0.0104	0.2203	0.0006	0.0236	1495.65	1531.38
20071226	0.1798	1.0336	-0.1624	0.5547	0.0069	-0.0039	0.0772	-0.0003	0.0253	1460.30	1497.66
20080327	0.2044	1.1125	-0.2084	0.5403	0.0054	-0.0109	0.0701	0.0008	0.0777	1226.59	1325.76
20080627	0.1824	0.6914	-0.2225	0.5322	0.0092	-0.0132	0.1342	-0.0012	0.0492	1217.03	1278.38
20080930	0.2042	0.4489	-0.3314	0.4390	0.0208	-0.0138	0.1803	-0.0070	0.0383	1121.01	1164.74
20081231	0.2967	0.8677	-0.3751	0.5234	0.0295	-0.0082	0.0139	-0.0088	0.2950	672.52	903.25
20090331	0.3111	0.6339	-0.3950	0.4683	0.0155	-0.0060	0.0785	-0.0038	0.0382	767.95	797.87
20090630	0.2213	0.8144	-0.2596	0.5695	0.0131	-0.0226	0.1117	0.0021	0.1012	830.87	919.32
20090930	0.2173	0.8495	-0.2270	0.5890	0.0090	-0.0077	0.0471	0.0011	0.0817	974.11	1057.08
20091229	0.1969	0.9642	-0.1908	0.5938	0.0110	-0.0082	0.0449	-0.0006	0.0913	1027.92	1126.20
20100331	0.1760	1.1091	-0.1549	0.6175	0.0150	-0.0008	0.0017	-0.0031	0.2353	924.24	1169.43
20100630	0.2480	1.4532	-0.2669	0.5705	0.0083	-0.0189	0.0719	0.0033	0.1314	903.77	1030.71

Table 4.2: SPX OTM Calibration Fit Statistics : λ has four parameters.

Date	APE	AAE	RMSE
20070328	0.0231	0.7580	0.8942
20070627	0.0186	0.5962	0.8589
20070927	0.0199	0.8930	1.1487
20071226	0.0198	1.0462	1.4261
20080327	0.0445	2.4665	3.1536
20080627	0.0168	0.7037	0.8990
20080930	0.0275	1.2777	1.7318
20081231	0.0350	1.4999	1.9483
20090331	0.0193	0.8191	1.0577
20090630	0.0281	0.9188	1.1293
20090930	0.0236	0.8082	0.9677
20091229	0.0237	0.8595	1.1343
20100331	0.0335	0.9443	1.1709
20100630	0.0313	1.3839	1.7867

Table 4.3: Standard Error: SPX OTM Calibrated Parameters (basis point)

Date	σ	ν	θ	γ	λ_0	a	b	c
20070328	5	28	6	10	37	49	235	27
20070627	2	18	5	6	10	36	173	7
20070927	6	55	10	14	8	33	138	6
20071226	14	53	21	8	10	19	62	7
20080327	5	7	6	7	5	17	21	4
20080627	9	69	18	10	7	24	96	6
20080930	13	53	33	9	6	17	62	5
20081231	4	21	4	9	6	10	24	4
20090331	8	48	19	9	5	12	32	4
20090630	10	122	23	16	7	17	38	5
20090930	6	81	12	18	11	27	65	8
20100331	1	37	5	3	9	9	69	6
20100630	3	30	3	2	7	17	31	4

Table 4.4: Parameter Identification: SPX OTM Calibrated Parameters

Date	σ	ν	θ	γ	λ_0	a	b	c
20070328	186	5	147	14	73	5	1	94
20070627	178	4	118	16	70	6	1	99
20070927	242	12	197	25	128	10	2	162
20071226	307	10	240	48	198	18	4	312
20080327	583	22	539	87	492	41	8	646
20080627	156	10	106	18	96	9	2	108
20080930	3854	106	2487	371	2001	196	35	2279
20081231	226	14	162	61	249	37	11	362
20090331	113	10	59	24	107	16	6	118
20090630	143	8	87	25	96	17	6	141
20090930	140	7	81	18	87	14	5	114
20091229	581	19	404	87	373	38	8	493
20100331	167	6	114	17	86	13	4	110
20100630	4120	137	2925	600	2380	297	74	3432

Table 4.5: NDX OTM Calibrated Parameters : λ has four parameters.

Date	σ	ν	θ	γ	λ_0	a	b	c	min (x)	min (K)	Spot
20070328	0.1583	0.6667	-0.1564	0.5394	0.0047	-0.0072	0.0023	0.0003	1.5652	370.12	1770.54
20070627	0.1695	0.7334	-0.1410	0.5936	0.0055	-0.0117	0.0935	-0.0025	0.0626	1815.82	1933.06
20070927	0.1992	1.0007	-0.1325	0.5885	0.0060	-0.0025	0.0947	-0.0025	0.0132	2068.90	2096.39
20071226	0.2264	0.7529	-0.2020	0.5902	0.0195	-0.0089	0.0597	-0.0138	0.0745	1983.45	2136.94
20080327	0.2502	0.8110	-0.2546	0.5557	0.0063	-0.0008	0.0263	0.0015	0.0152	1751.05	1777.89
20080627	0.2360	0.5392	-0.2757	0.5484	0.0043	-0.0025	0.0290	0.0002	0.0431	1777.43	1855.72
20080930	0.2512	0.4736	-0.3389	0.4660	0.0168	-0.0075	0.0598	-0.0015	0.0627	1497.70	1594.63
20081231	0.3363	0.8045	-0.4165	0.5372	0.0083	-0.0005	0.0289	-0.0025	0.0087	1201.21	1211.65
20090331	0.3231	0.5643	-0.4045	0.4866	0.0049	-0.0008	0.0541	0.0054	0.0074	1227.90	1237.01
20090630	0.2533	0.9510	-0.2265	0.5743	0.0072	-0.0090	0.0425	0.0002	0.1059	1328.83	1477.25
20090930	0.2320	0.8624	-0.2314	0.5881	0.0028	-0.0070	0.0378	0.0020	0.0926	1566.97	1718.99
20091229	0.2203	0.9496	-0.1784	0.6140	0.0044	-0.0128	0.0521	0.0001	0.1228	1655.62	1872.02
20100331	0.1950	1.0608	-0.1551	0.6297	0.0052	-0.0075	0.0134	-0.0004	0.2796	1480.30	1958.34
20100630	0.2718	1.1849	-0.2778	0.5468	0.0137	-0.0096	0.0435	-0.0070	0.1103	1557.44	1739.14

Table 4.6: NDX OTM Calibration Fit Statistics : λ has four parameters.

Date	APE	AAE	RMSE
20070328	0.0136	0.6510	0.7826
20070627	0.0086	0.4288	0.5508
20070927	0.0155	1.0032	1.1600
20071226	0.0275	2.5309	4.0160
20080327	0.0325	2.8418	3.9571
20080627	0.0083	0.7509	0.9709
20080930	0.0119	0.8158	1.0019
20081231	0.0173	1.1005	1.4489
20090331	0.0163	0.9179	1.1568
20090630	0.0191	0.9790	1.2334
20090930	0.0241	1.1683	1.3863
20091229	0.0165	0.9924	1.2715
20100331	0.0177	0.8368	1.1123
20100630	0.0171	1.3479	1.7834

Table 4.7: Standard Error: NDX OTM Calibrated Parameters (basis point)

Date	σ	ν	θ	γ	λ_0	a	b	c
20070328	8	83	17	11	7	53	340	5
20070627	8	7	13	45	4	35	175	3
20070927	4	20	6	11	6	20	81	6
20071226	9	54	19	4	3	10	37	2
20080327	4	23	9	5	3	8	33	2
20080627	4	24	10	5	3	9	40	3
20080930	7	39	20	8	5	10	48	5
20081231	5	32	10	5	4	7	26	2
20090331	7	44	20	6	4	8	29	3
20090630	2	131	1	21	2	17	37	1
20090930	4	8	6	13	8	21	58	8
20091229	49	651	99	9	4	21	54	3
20100331	3	21	6	4	6	28	83	5
20100630	9	14	11	3	6	16	44	6

Table 4.8: Parameter Identification: NDX OTM Calibrated Parameters

Date	σ	ν	θ	γ	λ_0	a	b	c
20070328	135	8	83	18	64	5	1	47
20070627	3462	176	3299	248	2465	198	31	2519
20070927	355	10	239	23	222	18	3	224
20071226	9646	348	8114	1546	6444	614	100	10292
20080327	584	23	539	87	492	41	9	647
20080627	157	10	107	18	97	9	2	109
20080930	9941	268	6059	618	4828	507	83	4703
20081231	217	14	126	62	246	42	12	364
20090331	180	17	79	39	157	31	10	187
20090630	223	9	117	23	153	23	8	165
20090930	247	13	146	23	157	26	9	141
20091229	310	12	185	51	197	28	9	246
20100331	235	7	150	29	131	16	5	142
20100630	11840	411	8748	976	6720	728	153	6995

Table 4.9: DJX OTM Calibrated Parameters : λ has four parameters.

Date	σ	ν	θ	γ	λ_0	a	b	c	min (x)	min (K)	Spot
20070328	0.1236	1.1695	-0.0855	0.5687	0.0151	0.0063	0.0594	-0.0025	-0.0530	129.70	123.00
20070627	0.1416	1.1745	-0.0855	0.5682	0.0090	0.0100	0.0049	-0.0001	-1.0204	372.53	134.28
20070927	0.1553	0.9774	-0.1125	0.5801	0.0110	-0.0033	0.1553	-0.0018	0.0106	137.66	139.13
20071226	0.1694	0.9907	-0.1540	0.5562	0.0132	-0.0184	0.1658	-0.0035	0.0555	128.21	135.52
20080327	0.2008	1.1130	-0.1845	0.5370	0.0064	-0.0104	0.0059	0.0011	0.8814	50.96	123.02
20080627	0.1821	0.9178	-0.1809	0.5262	0.0066	-0.0135	0.1297	0.0002	0.0520	107.72	113.47
20080930	0.2148	0.7809	-0.2358	0.4578	0.0136	-0.0378	0.2576	-0.0004	0.0734	100.83	108.51
20081231	0.2827	0.7512	-0.3557	0.5124	0.0104	-0.0181	0.0706	0.0005	0.1282	77.20	87.76
20090331	0.3000	0.6458	-0.3421	0.4555	0.0120	-0.0281	0.0605	-0.0013	0.2322	60.32	76.09
20090630	0.2203	1.0249	-0.2130	0.5771	0.0089	-0.0231	0.0561	0.0001	0.2059	68.75	84.47
20090930	0.2079	0.9110	-0.1961	0.5897	0.0073	-0.0199	0.0539	0.0008	0.1846	80.75	97.12
20091229	0.1843	0.9145	-0.1665	0.6004	0.0077	-0.0220	0.0773	-0.0003	0.1423	91.46	105.45
20100331	0.1670	1.1635	-0.1321	0.6268	0.0089	-0.0356	0.1106	0.0006	0.1609	92.43	108.57
20100630	0.2428	1.4282	-0.2199	0.5522	0.0169	-0.0533	0.1408	0.0033	0.1892	80.89	97.74

Table 4.10: DJX OTM Calibration Fit Statistics : λ has four parameters.

Date	APE	AAE	RMSE
20070328	0.0299	0.0971	0.1246
20070627	0.0149	0.0628	0.0885
20070927	0.0258	0.1138	0.1449
20071226	0.0124	0.0567	0.0729
20080327	0.0366	0.1969	0.2527
20080627	0.0164	0.0682	0.0853
20080930	0.0347	0.5917	1.1328
20081231	0.0175	0.0934	0.1192
20090331	0.0166	0.0721	0.0941
20090630	0.0163	0.0552	0.0779
20090930	0.0238	0.0879	0.1042
20091229	0.0281	0.0892	0.1099
20100331	0.0229	0.0693	0.0865
20100630	0.0295	0.1198	0.1569

Table 4.11: Standard Error: DJX OTM Calibrated Parameters (basis point)

Date	σ	ν	θ	γ	λ_0	a	b	c
20070328	55	110	21	49	79	519	1199	61
20070627	49	125	57	133	34	231	1294	22
20070927	20	195	23	104	59	200	1003	42
20071226	28	242	36	89	64	183	885	51
20080327	67	275	84	23	44	15	325	32
20080627	45	246	62	88	59	253	926	50
20080930	27	150	32	67	46	136	979	36
20081231	173	1588	393	117	40	108	322	25
20090331	14	50	21	14	46	89	280	34
20090630	1	118	23	112	87	227	619	70
20090930	29	297	30	127	85	224	589	61
20091229	52	1	74	1	29	8	962	25
20100331	38	109	47	6	125	394	701	104
20100630	36	117	32	16	75	298	719	57

Table 4.12: Parameter Identification: DJX OTM Calibrated Parameters

Date	σ	ν	θ	γ	λ_0	a	b	c
20070328	0.0591	0.2901	2.9102	0.1760	0.8742	0.0635	0.0083	1.1912
20070627	2.2661	0.0329	1.4927	0.2316	0.9947	0.0720	0.0109	1.6287
20070927	3.7582	0.0809	2.3995	0.3207	1.7768	0.1285	0.0188	2.4597
20071226	1.5345	0.0513	1.0744	0.1306	0.8078	0.0803	0.0149	0.9986
20080327	4.9919	0.1500	4.0165	0.6727	3.6679	0.3198	0.0580	5.1023
20080627	1.5004	0.0551	1.0242	0.1501	0.8587	0.0723	0.0113	0.9166
20080930	2.1635	0.1143	1.4198	0.3207	1.5059	0.1661	0.0314	1.9645
20081231	1.6489	0.1187	0.9978	0.4323	1.5567	0.2617	0.0812	2.4894
20090331	1.1832	0.0752	0.5408	0.2031	1.0091	0.1590	0.0475	1.3453
20090630	0.9032	0.0299	0.5662	0.1102	0.5840	0.0668	0.0157	0.6964
20090930	1.6737	0.0674	0.9701	0.1988	1.0305	0.1475	0.0454	1.3770
20091229	1.6991	0.0638	1.0394	0.1907	0.9283	0.1132	0.0300	1.1063
20100331	1.3560	0.0369	0.8577	0.0951	0.6341	0.0796	0.0207	0.7294
20100630	1.8487	0.0719	1.5349	0.2915	1.6122	0.2547	0.0801	2.0017

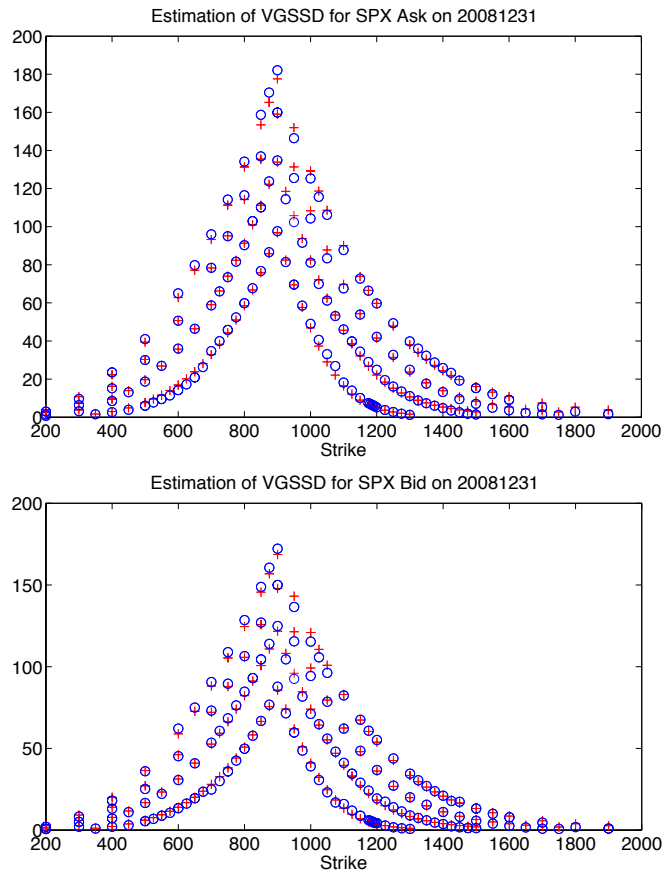


Figure 4.1: Market ask and bid option prices are blue circles and model ask and bid option prices are denoted by red dots. The risk-neutral model is VGSSD and data are OTM option prices on the SPX on December 31, 2008.

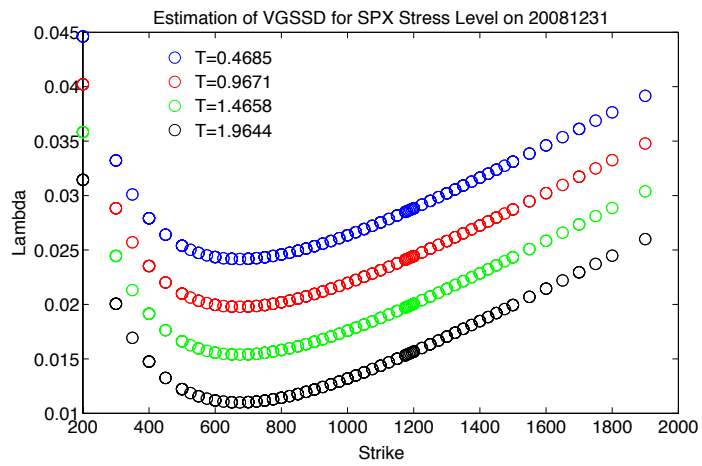


Figure 4.2: Estimated stress level λ is denoted by blue circles. The risk-neutral model is VGSSD and data are OTM option prices on the SPX on December 31, 2008.

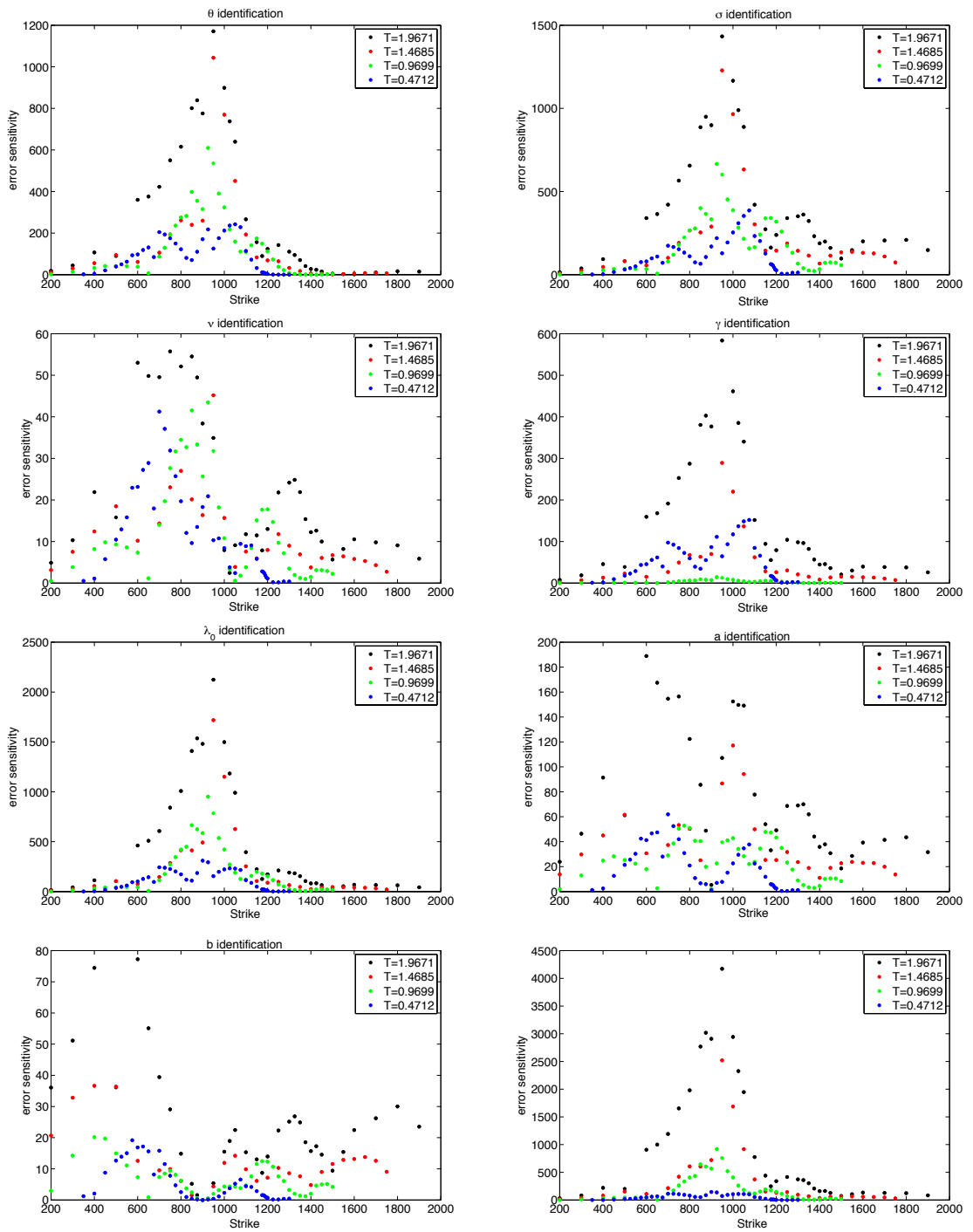


Figure 4.3: Parameter identifications are across different maturities and strike price. The risk-neutral model is VGSSD and data are OTM option prices on the SPX on December 31, 2008.

Table 4.13: SPX OTM Calibrated Parameters : λ has five parameters.

Date	σ	ν	θ	γ	λ_0	a	b	c	d
20070328	0.1189	0.9648	-0.1040	0.5614	0.0162	0.0402	0.0235	-0.0027	-0.0004
20070627	0.1303	0.9212	-0.1146	0.5583	0.0089	0.0015	0.1044	-0.0013	0.0000
20070927	0.1449	0.8520	-0.1478	0.5648	0.0097	-0.0177	0.1550	0.0018	-0.0136
20071226	0.1798	1.0336	-0.1624	0.5547	0.0069	-0.0039	0.0772	-0.0003	0.0000
20080327	0.2062	1.1143	-0.2060	0.5420	0.0056	-0.0034	0.0324	0.0010	-0.0027
20080627	0.1823	0.6912	-0.2226	0.5322	0.0091	-0.0101	0.1346	-0.0011	-0.0027
20080930	0.2043	0.4491	-0.3313	0.4390	0.0209	-0.0245	0.1809	-0.0070	0.0083
20081231	0.2967	0.8681	-0.3751	0.5235	0.0299	-0.0208	0.0153	-0.0090	0.0080
20090331	0.3110	0.6335	-0.3952	0.4683	0.0151	0.0007	0.0776	-0.0035	-0.0050
20090630	0.2214	0.8145	-0.2595	0.5696	0.0131	-0.0234	0.1107	0.0021	0.0007
20090930	0.2173	0.8489	-0.2271	0.5890	0.0090	-0.0078	0.0472	0.0011	0.0001
20091229	0.1961	2.0073	-0.1671	0.6279	0.0232	-0.0272	0.0209	-0.0185	0.0166
20100331	0.1756	1.1031	-0.1555	0.6177	0.0160	-0.0291	0.0693	-0.0039	0.0072
20100630	0.2480	1.4532	-0.2669	0.5705	0.0083	-0.0189	0.0719	0.0033	0.0001

Table 4.14: NDX OTM Calibrated Parameters : λ has five parameters.

Date	σ	ν	θ	γ	λ_0	a	b	c	d
20070328	0.1583	0.6667	-0.1563	0.5394	0.0046	-0.0072	0.0024	0.0003	0.0001
20070627	0.1695	0.7324	-0.1412	0.5935	0.0056	-0.0123	0.0935	-0.0026	0.0016
20070927	0.1989	0.9976	-0.1331	0.5890	0.0060	0.0055	0.0953	-0.0025	-0.0028
20071226	0.2264	0.7513	-0.2021	0.5901	0.0194	0.0182	0.0019	-0.0134	-0.0156
20080327	0.2501	0.8100	-0.2548	0.5557	0.0064	-0.0096	0.0294	0.0015	0.0075
20080627	0.2360	0.5391	-0.2757	0.5484	0.0043	-0.0070	0.0311	0.0002	0.0082
20080930	0.2512	0.4738	-0.3388	0.4661	0.0164	-0.0392	0.0636	-0.0010	0.0309
20081231	0.3352	0.7967	-0.4187	0.5368	0.0085	-0.0103	0.0320	-0.0026	0.0063
20090331	0.3231	0.5644	-0.4045	0.4867	0.0050	-0.0141	0.0567	0.0054	0.0111
20090630	0.2531	0.9492	-0.2267	0.5743	0.0073	-0.0107	0.0427	0.0002	0.0015
20090930	0.2320	0.8624	-0.2314	0.5881	0.0029	-0.0075	0.0375	0.0018	0.0006
20091229	0.2204	0.9508	-0.1782	0.6140	0.0044	-0.0119	0.0519	0.0002	-0.0006
20100331	0.1953	1.0617	-0.1547	0.6280	0.0040	-0.0002	0.0385	0.0003	-0.0080
20100630	0.2717	1.1840	-0.2780	0.5468	0.0141	-0.0191	0.0412	-0.0073	0.0096

Table 4.15: DJX OTM Calibrated Parameters : λ has five parameters.

Date	σ	ν	θ	γ	λ_0	a	b	c	d
20070328	0.1236	1.1701	-0.0855	0.5687	0.0151	0.0006	0.0573	-0.0026	0.0040
20070627	0.1416	1.1745	-0.0855	0.5682	0.0090	0.0100	0.0049	-0.0001	0.0001
20070927	0.1532	0.9400	-0.1168	0.5797	0.0107	0.0173	0.2081	-0.0018	-0.0143
20071226	-0.1693	0.9904	-0.1541	0.5562	0.0129	-0.0110	0.1663	-0.0034	-0.0058
20080627	0.1819	0.9148	-0.1813	0.5260	0.0068	-0.0224	0.1345	-0.0001	0.0074
20080930	0.2148	0.7808	-0.2358	0.4577	0.0132	-0.0218	0.2510	-0.0001	-0.0116
20081231	0.2827	0.7510	-0.3557	0.5123	0.0101	-0.0125	0.0695	0.0007	-0.0032
20090331	0.2996	0.6435	-0.3429	0.4558	0.0108	-0.0668	0.0036	-0.0002	0.0151
20090630	0.2203	1.0248	-0.2130	0.5771	0.0087	-0.0202	0.0564	0.0002	-0.0023
20090930	0.2078	0.9091	-0.1963	0.5896	0.0073	-0.0194	0.0540	0.0009	-0.0004
20091229	0.1844	0.9160	-0.1663	0.6001	0.0068	-0.0064	0.0760	0.0003	-0.0100
20100331	0.1669	1.1633	-0.1322	0.6267	0.0068	-0.0025	0.1122	0.0023	-0.0269
20100630	0.2425	1.4244	-0.2203	0.5522	0.0155	-0.0360	0.1403	0.0045	-0.0131

Table 4.16: Standard Error: SPX OTM Calibrated Parameters (basis point)

Date	σ	ν	θ	γ	λ_0	a	b	c	d
20070328	8	19	11	6	5	163	264	3	117
20070627	3	16	2	12	12	131	175	8	81
20070927	4	27	5	12	7	35	144	6	20
20071226	4	4	5	7	2	57	61	1	34
20080327	2	47	3	4	6	55	56	4	38
20080627	5	34	10	11	5	48	77	5	14
20080930	5	20	8	9	8	184	61	6	142
20081231	5	21	7	8	6	33	25	4	20
20090331	7	41	16	9	6	41	32	5	29
20090630	6	31	9	11	10	74	37	6	42
20090930	4	36	6	16	10	6	45	8	21
20091229	3	8	2	3	16	28	42	10	16
20100331	4	24	3	11	14	111	101	10	77
20100630	3	24	2	17	7	51	33	4	29

Table 4.17: Parameter Identification: SPX OTM Calibrated Parameters

Date	σ	ν	θ	γ	λ_0	a	b	c	d
20070328	205.2418	6.3250	159.4075	15.5778	79.9765	6.2101	1.0777	101.7701	8.3513
20070627	178.9675	4.8110	118.4678	16.2145	70.6964	6.0387	1.0422	99.2049	7.2053
20070927	256.5644	12.2894	203.3730	26.4682	134.4839	10.4442	1.8376	170.9368	13.7571
20071226	307.4613	10.3934	240.4606	48.7591	198.6031	18.2799	4.1495	312.0927	20.6385
20080327	594.4583	22.1259	536.5133	88.0090	498.3922	41.5933	8.5932	655.1632	54.7240
20080627	156.9170	10.0130	106.8282	18.3243	96.7777	9.1847	1.9651	108.8061	10.5723
20090930	270.0099	43.5666	172.8430	40.6260	213.8523	20.6489	4.7864	252.7778	26.2194
20081231	222.1386	14.3352	159.7915	60.2297	246.0308	36.6491	11.2974	356.2985	53.3169
20090331	113.3332	9.9936	58.8509	24.3624	107.4579	16.6339	5.5750	118.7161	20.8895
20090630	141.0717	8.9625	88.5600	25.8318	96.3435	17.9628	6.9282	141.3400	28.3679
20090930	140.1713	6.8779	81.0895	18.2767	87.7269	13.9333	4.7308	113.9669	18.7508
20091229	704.4512	13.9006	950.2111	141.7342	694.5050	67.0872	20.4121	1099.6371	103.0503
20100331	165.0154	5.5206	113.7844	17.0480	85.9354	12.7232	4.2600	109.4973	17.3059
20100630	200.4355	8.9703	180.2153	46.9937	184.0464	35.3432	15.1417	268.9116	55.1771

Table 4.18: Standard Error: NDX OTM Calibrated Parameters (basis point)

Date	σ	ν	θ	γ	λ_0	a	b	c	d
20070328	5	2	9	15	7	15	321	6	57
20070627	11	94	24	14	9	7	178	8	37
20070927	3	9	5	29	6	65	78	6	59
20071226	3	51	10	4	3	31	37	2	18
20080327	3	27	5	5	3	26	35	2	18
20080627	7	42	18	5	3	30	40	3	25
20080930	7	37	19	8	5	48	48	6	46
20081231	6	52	13	4	2	21	25	1	13
20090331	7	43	19	6	4	25	29	3	18
20090630	3	24	4	10	7	48	38	6	39
20090930	13	65	26	23	10	75	56	10	72
20091229	1	20	4	8	6	52	65	4	31
20100331	3	44	4	5	7	62	78	5	44
20100630	3	10	3	6	8	47	39	7	40

Table 4.19: Parameter Identification: NDX OTM Calibrated Parameters

Date	σ	ν	θ	γ	λ_0	a	b	c	d
20070328	135.8371	8.0888	83.4436	17.9536	63.6553	5.4906	0.9185	47.4890	3.7061
20070627	118.4098	4.7666	66.6023	6.7086	56.6663	4.8312	0.8314	51.9956	4.1613
20070927	347.0096	9.5023	234.1619	22.6391	217.1890	17.0151	3.3047	218.1626	16.6810
20071226	493.5818	22.1182	293.6767	87.5029	365.9505	35.3962	6.5957	532.8003	51.9430
20080327	1053.5131	47.5076	697.0162	192.2943	965.6037	75.7089	14.0473	1367.9085	98.7027
20080627	255.5974	19.1518	132.4113	34.2705	185.6956	18.1804	3.5096	173.8705	18.5563
20080930	215.2058	20.2482	96.3880	22.3528	145.2425	21.4351	5.1208	132.8863	21.1282
20081231	214.6623	14.0130	126.7379	62.0832	246.1059	42.1926	12.1898	367.1068	63.7246
20090331	179.6940	16.4410	78.8970	38.4454	157.3025	30.6512	10.2641	186.4368	37.9522
20090630	223.3704	9.1507	116.9367	23.2849	152.7600	23.1322	7.8372	165.1577	25.3953
20090930	246.8284	13.3988	146.3080	22.7392	157.6664	26.0867	9.2285	141.4172	25.2006
20091229	310.8207	12.0884	184.5728	51.1397	197.1272	28.6737	8.8124	245.8163	41.1506
20100331	240.0719	7.4541	153.5234	29.8674	134.1906	16.3250	4.5555	148.0186	19.0502
20100630	325.4474	17.2160	263.5969	53.3128	313.8789	44.7941	13.3603	285.7503	45.2782

Table 4.20: Standard Error: DJX OTM Calibrated Parameters (basis point)

Date	σ	ν	θ	γ	λ_0	a	b	c	d
20070328	25	154	31	89	29	644	2387	2	642
20070627	47	92	73	93	68	596	1369	42	360
20070927	49	273	81	74	62	122	1390	42	59
20071226	19	277	8	86	60	454	874	48	375
20080627	33	74	46	97	60	90	1048	52	64
20080930	21	241	55	67	50	464	644	37	323
20081231	19	184	16	58	42	281	279	26	156
20090331	59	418	147	76	16	130	281	5	62
20090630	36	370	51	0	103	852	663	82	590
20090930	34	62	48	104	98	715	580	69	471
20091229	34	175	92	175	113	945	1339	82	579
20100331	44	127	56	63	140	1130	1337	119	942
20100630	8	95	25	76	69	309	151	59	311

Table 4.21: Parameter Identification: DJX OTM Calibrated Parameters

Date	σ	ν	θ	γ	λ_0	a	b	c	d
20070328	1.6881	0.0264	1.1778	0.1197	0.6341	0.0405	0.0045	0.8770	0.0557
20070627	2.1909	0.0290	1.3994	0.2210	0.9618	0.0626	0.0083	1.5693	0.1023
20070927	3.6475	0.0896	2.4106	0.3181	1.7405	0.1273	0.0191	2.4069	0.1746
20071226	1.5387	0.0512	1.0769	0.1312	0.8079	0.0806	0.0150	0.9989	0.1007
20080627	1.4971	0.0556	1.0268	0.1499	0.8592	0.0723	0.0113	0.9182	0.0813
20080930	2.1511	0.1145	1.4181	0.3199	1.5035	0.1657	0.0313	1.9622	0.2213
20081231	1.6487	0.1191	0.9969	0.4327	1.5548	0.2625	0.0816	2.4870	0.4373
20090331	1.2427	0.0853	0.5974	0.2119	1.0743	0.1715	0.0507	1.4500	0.2385
20090630	0.9025	0.0299	0.5655	0.1102	0.5832	0.0668	0.0157	0.6955	0.0826
20090930	1.6705	0.0677	0.9699	0.1986	1.0287	0.1479	0.0457	1.3750	0.2063
20091229	1.7017	0.0635	1.0391	0.1912	0.9289	0.1131	0.0300	1.1064	0.1483
20100331	1.3541	0.0367	0.8549	0.0955	0.6309	0.0790	0.0207	0.7261	0.0963
20100630	1.8407	0.0711	1.5325	0.2917	1.6086	0.2537	0.0804	2.0162	0.3448

4.4 Summary and Future Work

We followed the work [23] to investigate liquidity risk implied by major index market bid and ask option prices. The model calibration is based on the two-price market theory and the VGSSD model is used for the risk-neutral distribution of the underlying assets. Out-of-the-money put and call options are used for the option surface calibration. Stress levels, which could be used as an indicator of liquidity risk, are modeled as a nonlinear function of strike prices and a linear function of maturities. Results from SPX, NDX and DJX at-the-money options from 2007 to 2010 reveal that markets were more illiquid during the subprime crisis in 2008. This observation reaches the same argument in [23]. It was also observed that the minimum stress level of the whole option surface exists at a call option when the strike price is close to the spot price. The slope of the stress level on the side of OTM put options is steeper than that of the OTM call options. This suggests that markets for call options are more liquid than that of put options. In other words, more investors trade call options than put options. As discussed before, the limited downside gain for put options discourages investors to trade these options. On the other hand, the unlimited upside gain for call options encourages investors to trade these options. We may extend the work to daily calibration in order to monitor the liquidity risk. This may also be useful for stochastic liquidity trading in the future.

Appendix A

Proof of Trading Advantages of Option Spreads

Lemma A.1. *The bid price of the Bull spread is no less than the bid price of the call option on the strike K_1 minus the ask price of the call option on the strike K_2 , i.e.:*

$$K_2 - K_1 - \int_{K_1}^{K_2} \Psi(F_S(s)) ds \geq \int_{K_1}^{\infty} (1 - \Psi(F_S(s))) ds - \int_{K_2}^{\infty} \Psi(1 - F_S(s)) ds. \quad (\text{A.1})$$

Proof. The negative ask price of the call option on the strike K_2 can be written as

$$- \int_{K_2}^{\infty} \Psi(1 - F_S(s)) ds = \int_{K_2}^{\infty} (s - K_2) d\Psi(1 - F_S(s)).$$

Then, the right hand side in the equation (A.1) is:

$$\begin{aligned} RHS &= \int_{K_1}^{\infty} (1 - \Psi(F_S(s))) ds + (s - K_2)(\Psi(1 - F_S(s)) - 1)|_{K_2}^{\infty} + \int_{K_2}^{\infty} (1 - \Psi(1 - F_S(s))) ds \\ &= \infty - K_1 - \int_{K_1}^{\infty} \Psi(F_S(s)) ds - \infty + K_2 + \int_{K_2}^{\infty} (1 - \Psi(1 - F_S(s))) ds \\ &= K_2 - K_1 - \int_{K_1}^{\infty} \Psi(F_S(s)) ds + \int_{K_2}^{\infty} (1 - \Psi(1 - F_S(s))) ds. \end{aligned}$$

The left hand side which is the bid price of the Bull Spread can be written as:

$$\begin{aligned} LHS &= K_2 - K_1 - \int_{K_1}^{K_2} \Psi(F_S(s)) ds \\ &= K_2 - K_1 - \int_{K_1}^{\infty} \Psi(F_S(s)) ds + \int_{K_2}^{\infty} \Psi(F_S(s)) ds. \end{aligned}$$

We know $\Psi(F_S(s)) + \Psi(1 - F_S(s)) \geq 1$, thus, $\Psi(F_S(s)) \geq 1 - \Psi(1 - F_S(s))$.

This makes $LHS \geq RHS$. ■

Lemma A.2. *The ask price of the Bull spread is no greater than the ask price of the call option on the strike K_1 minus the bid price of the call option on the strike K_2 , i.e.:*

$$\int_{K_1}^{K_2} \Psi(1 - F_S(s)) ds \leq \int_{K_1}^{\infty} \Psi(1 - F_S(s)) ds - \int_{K_2}^{\infty} (1 - \Psi(F_S(s))) ds. \quad (\text{A.2})$$

Proof. The ask price of the Bull Spread can be written as

$$\begin{aligned} LHS &= \int_{K_1}^{K_2} \Psi(1 - F_S(s)) ds \\ &= \int_{K_1}^{\infty} \Psi(1 - F_S(s)) ds - \int_{K_2}^{\infty} \Psi(1 - F_S(s)) ds. \end{aligned}$$

Compare the above equation with the right hand side of the Equation (A.2), and with $1 - \Psi(F_S(s)) \leq \Psi(1 - F_S(s))$, we have:

$$\int_{K_2}^{\infty} (1 - \Psi(F_S(s))) ds \leq \int_{K_2}^{\infty} \Psi(1 - F_S(s)) ds.$$

Thus, $LHS \leq RHS$. ■

Lemma A.3. *The bid price of the Bear spread is no less than the bid price of the put option on the strike K_2 minus the ask price of the put option on the strike K_1 , i.e.:*

$$K_2 - K_1 - \int_{K_1}^{K_2} \Psi(1 - F_S(s)) ds \geq \int_0^{K_2} (1 - \Psi(1 - F_S(s))) ds - \int_0^{K_1} \Psi(F_S(s)) ds. \quad (\text{A.3})$$

Proof. The bid price of the Bear spread can be written as

$$K_2 - K_1 - \int_{K_1}^{K_2} \Psi(1 - F_S(s)) ds = \int_0^{K_2} (1 - \Psi(1 - F_S(s))) ds - \int_0^{K_1} (1 - \Psi(1 - F_S(s))) ds.$$

Since $1 - \Psi(1 - F_S(s)) \leq \Psi(F_S(s))$, we have :

$$\int_0^{K_1} (1 - \Psi(1 - F_S(s)))ds \leq \int_0^{K_1} \Psi(F_S(s))ds.$$

Thus, Equation (3) $LHS \geq RHS$. ■

Lemma A.4. *The ask price of the Bear spread is no greater than the ask price of the put option on the strike K_2 minus the bid price of the put option on the strike K_1 , i.e.:*

$$\int_{K_1}^{K_2} \Psi(F_S(s))ds \leq \int_0^{K_2} \Psi(F_S(s))ds - \int_0^{K_1} (1 - \Psi(1 - F_S(s)))ds. \quad (\text{A.4})$$

Proof. The ask price of the Bear Spread can be written as

$$LHS = \int_0^{K_2} \Psi(F_S(s))ds - \int_0^{K_1} \Psi(F_S(s))ds.$$

Compare the above equation with the right hand side of the Equation (A.4), and with $1 - \Psi(1 - F_S(s)) \leq \Psi(F_S(s))$, we have:

$$\int_0^{K_1} \Psi(F_S(s))ds \geq \int_0^{K_1} (1 - \Psi(1 - F_S(s)))ds.$$

Thus, $LHS \leq RHS$. ■

Lemma A.5. *The bid price of a butterfly is no less than the bid price of the put options on the strikes of K_1 and K_3 minus the ask price of the two put options on*

the strike of K_2 , i.e.:

$$\begin{aligned}
a - \int_{K_1}^{K_2} \Psi(F_S(s) + 1 - F_S(2K_2 - s))ds &\geq \int_0^{K_1} (1 - \Psi(1 - F_S(s)))ds + \\
&\int_0^{K_3} (1 - \Psi(1 - F_S(s)))ds - \\
&2 \int_0^{K_2} \Psi(F_S(s))ds. \tag{A.5}
\end{aligned}$$

Proof. The bid price of the butterfly can be written as

$$\int_{-\infty}^{\infty} cd\Psi(F_C(c)) = a - \int_0^a \Psi(F_C(K_1 + c) + 1 - F_C(K_3 - c))dc.$$

Subadditivity of the concave function $\Psi(x)$ tells:

$$\begin{aligned}
\int_0^a \Psi(F_C(K_1 + c) + 1 - F_C(K_3 - c))dc &\leq \int_0^a \Psi(F_C(K_1 + c))dc + \\
&\int_0^a \Psi(1 - F_C(K_3 - c))dc.
\end{aligned}$$

Thus,

$$\begin{aligned}
a - \int_{K_1}^{K_2} \Psi(F_S(s) + 1 - F_S(2K_2 - s))ds &\geq a - \int_0^a \Psi(F_C(K_1 + c))dc - \\
&\int_0^a \Psi(1 - F_C(K_3 - c))dc \\
&= a - \int_{K_1}^{K_2} \Psi(F_S(s)) - \int_{K_2}^{K_3} \Psi(1 - F_S(s))ds.
\end{aligned}$$

Then the left hand side in Equation (A.6) has:

$$\begin{aligned}
LHS &\geq a - \int_0^{K_2} \Psi(F_S(s))ds + \int_0^{K_1} \Psi(F_S(s))ds - \\
&\int_0^{K_3} \Psi(1 - F_S(s))ds + \int_0^{K_2} \Psi(1 - F_S(s))ds. \tag{A.6}
\end{aligned}$$

The right hand side in Equation (5) can be rewritten as :

$$\begin{aligned}
RHS &= 2K_2 - \int_0^{K_1} \Psi(1 - F_S(s))ds - \int_0^{K_3} \Psi(1 - F_S(s))ds - 2 \int_0^{K_2} \Psi(F_S(s))ds \\
&= a + \int_0^{K_1} (1 - \Psi(1 - F_S(s)))ds + \int_0^{K_2} (1 - \Psi(F_S(s)))ds - \\
&\quad \int_0^{K_3} \Psi(1 - F_S(s))ds - \int_0^{K_2} \Psi(F_S(s))ds. \tag{A.7}
\end{aligned}$$

We know,

$$\Psi(F_S(s)) + \Psi(1 - F_S(s)) \geq 1,$$

Let LHS in Equation (A.5) minus the RHS in Equation (A.5), we have:

$$\begin{aligned}
LHS - RHS &\geq \int_0^{K_1} (\Psi(F_S(s)) - 1 + \Psi(1 - F_S(s)))ds + \\
&\quad \int_0^{K_2} (\Psi(1 - F_S(s)) - 1 + \Psi(F_S(s)))ds \\
&\geq 0.
\end{aligned}$$

Thus, in Equation (A.5) $LHS \geq RHS$. ■

In order to prove the following lemmas, we first demonstrate an auxiliary lemma.

Lemma A.6. *Let $0 \leq a \leq b \leq 1$ and $0 \leq c \leq b - a$, then $\Psi(a) + \Psi(b) \leq \Psi(a + c) + \Psi(b - c)$.*

Proof. Let $\zeta(c) = \Psi(a + c) + \Psi(b - c)$. Then , we have the first derivative $\zeta'(c) = \Psi'(a + c) + \Psi'(b - c)$.

When $a + c \leq b - c$, i.e., $0 \leq c \leq \frac{b-a}{2}$, and $\Psi(x)$ is a concave function, we have $\zeta'(c) \geq 0$; when $a + c \geq b - c$, i.e., $\frac{b-a}{2} \leq c \leq b - a$, we have $\zeta'(c) \leq 0$.

Hence, the maximum of $\zeta(c)$ when $c \in [0, b - a]$ exists when $c = \frac{b-a}{2}$ and the minimum exists when $c = b - a$ or $c = 0$. Thus, we have $\zeta(0) = \zeta(b - a) = \Psi(a) + \Psi(b)$, which proves the lemma. ■

Lemma A.7. *The ask price of a butterfly spread is no greater than the ask price of put options on the strikes of K_1 and K_3 minus the bid price of the two put options on the strike of K_2 , i.e.:*

$$\int_{K_2}^{K_3} \Psi(F_S(s) - F_S(2K_2 - s)) ds \leq \int_0^{K_1} \Psi(F_S(s)) ds + \int_0^{K_3} \Psi(F_S(s)) ds - 2 \int_0^{K_2} (1 - \Psi(1 - F_S(s))) ds. \quad (\text{A.8})$$

Proof. The above statement could be reduced as:

$$\int_0^K (\Psi(F_S(s) + F_S(2K) - F_S(2K_2 - s)) + \Psi(1 - F_S(2K))) ds \leq \int_0^K (\Psi(F_S(s)) + \Psi(1 - F_S(2K - s))) ds.$$

Let K be so small that $F_S(K) < 1 - F_S(2K)$. In this case, when $0 \leq S \leq K$, we could set $b = 1 - F_S(2K - s)$, $a = F_S(s)$, and $c = F_S(2K) - F_S(2K - s)$. We have $c < b - a = 1 - F_S(2K - s) - F_S(s) = c + 1 - F_S(2K) - F_S(s)$. Apply the auxiliary lemma, we see that $\Psi(a) + \Psi(b) = \Psi(F_S(s)) + \Psi(1 - F_S(2K - s)) < \Psi(a + c) + \Psi(b - c) = \Psi(F_S(s) + F_S(2K) - F_S(2K_2 - s)) + \Psi(1 - F_S(2K))$. Hence, the inequality should take the opposite sign.

As K increases, there might be a P^* such that $\Psi(F_S(s)) < 1 - \Psi(F_S(2K))$ for $0 \leq S < P^*$ and $F_S(s) > 1 - F_S(2K)$ for $P^* < S \leq K$. In this case, when $0 \leq S < P^*$, we could set $b = 1 - F_S(2K - s)$, $a = F_S(s)$, and $c = F_S(2K) - F_S(2K - s)$.

The argument in the above case then applies and yields the inequality from the opposite sign. Now if $P^* < S \leq K$, we could set $b = F_S(s) + F_S(2K) - F_S(2K - s)$, $a = 1 - F_S(2K)$, and $c = F_S(2K) - F_S(2K - s)$. we have $c \leq b - a$ and apply the auxiliary lemma to have $\Psi(a) + \Psi(b) \leq \Psi(a + c) + \Psi(b - c)$. Therefore, we have

$$\begin{aligned} \int_0^{P^*} (\Psi(F_S(s) + F_S(2K) - F_S(2K - s)) + \Psi(1 - F_S(2K))) ds &\leq \int_0^{P^*} (\Psi(F_S(s)) \\ &\quad + \Psi(1 - F_S(2K - s))) ds. \\ \int_{P^*}^K (\Psi(F_S(s) + F_S(2K) - F_S(2K - s)) + \Psi(1 - F_S(2K))) ds &\leq \int_{P^*}^K (\Psi(F_S(s)) \\ &\quad + \Psi(1 - F_S(2K - s))) ds. \end{aligned}$$

Therefore whether or not the desired inequality holds depends on the position of P^* within the interval $[0, K]$. When K exceeds a critical value K^* such that $F_S(P_0^*) = 1 - F_S(2K^*)$ and

$$\begin{aligned} &\int_0^{P^*} (\Psi(F_S(s) + F_S(2K) - F_S(2K - s)) + \Psi(1 - F_S(2K))) ds \\ &\quad - \int_0^{P^*} (\Psi(F_S(s)) + \Psi(1 - F_S(2K - s))) ds \\ &= \int_{P^*}^K (\Psi(F_S(s) + F_S(2K) - F_S(2K - s)) + \Psi(1 - F_S(2K))) ds \\ &\quad - \int_{P^*}^K (\Psi(F_S(s)) + \Psi(1 - F_S(2K - s))) ds, \end{aligned}$$

we are going to have the desired inequality.

As K becomes so large that $F_S(2K) = 1$, we would like to set $b = F_S(s) + F_S(2K) - F_S(2K - s)$, $a = 1 - F_S(2K)$, and $c = F_S(2K) - F_S(2K - s)$. Then, $c \leq b - a$. Apply the auxiliary lemma again, we have $\Psi(a) + \Psi(b) = \Psi(1 - F_S(2K)) + \Psi(F_S(s) + F_S(2K) - F_S(2K - s)) \leq \Psi(a + c) + \Psi(b - c) = \Psi(F_S(s)) + \Psi(1 - F_S(2K))$.

The desired inequality follows. ■

Lemma A.8. *The ask price of a straddle is no greater than the sum of the ask prices of put option and call option on the strike of K , i.e.:*

$$\int_{2K}^{\infty} \Psi(1 - F_S(s))ds + \int_0^K \Psi(F_S(s) + 1 - F_S(2K - s))ds \leq \int_0^K \Psi(F_S(s))ds + \int_K^{\infty} \Psi(1 - F_S(s))ds. \quad (\text{A.9})$$

Proof. We could reduce the statement in this lemma as the following inequality:

$$\int_0^K \Psi(F_S(s) + 1 - F_S(2K - s))ds \leq \int_0^K (\Psi(F_S(s)) + \Psi(1 - F_S(2K - s)))ds.$$

Since function $\Psi(x)$ is subadditive, the inequality is concluded. ■

Lemma A.9. *The bid price of a straddle is no less than the sum of the bid prices of put option and call option on the strike of K , i.e.:*

$$K + \int_{2K}^{\infty} (1 - \Psi(F_S(s)))ds - \int_K^{2K} \Psi(F_S(s) - F_S(2K - s))ds \geq \int_0^K (1 - \Psi(1 - F_S(s)))ds + \int_K^{\infty} (1 - \Psi(F_S(s)))ds. \quad (\text{A.10})$$

Proof. We could reduce the statement in the lemma as the following inequality:

$$\int_0^K (\Psi(1 - F_S(s)) + \Psi(F_S(2K - s)))ds \geq \int_0^K (1 + \Psi(F_S(2K - s) - F_S(s)))ds.$$

Now set $a = F_S(2K - s) - F_S(s)$, $b = 1$ and $c = F_S(s)$, using the auxiliary lemma, for $0 \leq S \leq K$, we have:

$$\Psi(1 - F_S(s)) + \Psi(F_S(2K - s)) \geq 1 + \Psi(F_S(2K - s) - F_S(s)).$$

Then we conclude. ■

Bibliography

- [1] Andersen, L., and Andreasen, J. (2000) "Jump diffusion models: volatility smile fitting and numerical methods for pricing," *Review of Derivatives Research*, 4: 231-262.
- [2] A'it-Sahalia, Y. and Kimmel R. (2007) "Maximum likelihood estimation of stochastic volatility models," *Journal of Financial Economics*, 83: 413-452.
- [3] Artzner, P., Delbaen, F., Eber, J., Heath, D. (1999) "Coherent measures of risk," *Mathematical Finance*, 9: 203-228
- [4] Bachelier, L. (1900) English translation: P. Cootner, ed. *The random character of stock market prices*(MIT Press, Cambridge, MA)
- [5] Bakshi, G., N. Kapadia and B. Madan (2003) "Stock Return Characteristics, Skew Laws, and the Differential Pricing of Individual Equity Options," *The Review of Financial Studies*, 16, 101-143.
- [6] Bates, D. S. (1996a) "Jumps and stochastic volatility: the exchange rate processes implicit in Deutschmark options," *The Review of Financial Studies*, 9: 691-707.
- [7] Bernard, C., Boyle P. (2008), "Structured Investment Products and the Retail Investor", Working Paper.
- [8] Bernardo, A., Ledoit, O., (2000) "Gain, loss, and asset pricing," *Journal of Political Economy*, 108: 144-172.
- [9] Bjork, T., Slinko, I. (2006) "Towards a general theory of good deal bounds," *Review of Finance*, 10: 221-260
- [10] Black, F. (1989) "How we came up with the option formula," *Journal of Portfolio Management*, 15, 4-8
- [11] Black, F., Scholes, M. (1973) "The pricing of options and corporate liabilities," *Journal of Political Economy*, 81: 637-659
- [12] Burth, S, T. Kraus, Wohlwend H. (2001), "The pricing of structured products in the Swiss market", *The Journal of Derivatives*, 9: 30-40.

- [13] Carmona, R.(2009) *Indifference pricing theory and applications* (Princeton University Press)
- [14] Carr P., Geman H., Madan D. (2001) "Pricing and hedging in incomplete markets," *Journal of Financial Economics*, 62:131-167.
- [15] Carr P., Geman H., Madan D., Yor M., (2007) "Self-decomposability and option pricing," *Math.Finance*, 17:31-57
- [16] Carr, P., Madan, D.B. (1999) "Option valuation using the fast Fourier transform," *J. Comput. Finance*, 2: 61-73
- [17] Carr, P., Alvarez, J.J.V., Madan, D.B.(2010) "Markets, profits, capital, leverage and return," Working Paper
- [18] Cherny, A., Madan, D.B. (2009) "New measure for performance evaluation, " *Review of Financial Studies*, 22:2571-2606
- [19] Cherny, A., Madan, D.B. (2009) "Markets as a counterparty: an introduction to conic finance," *International Journal of Theoretical and Applied Finance*, to appear
- [20] Cohen, S., Elliott, R. J. (2010), "Comparisons for backward stochastic differential equations on Markov chains and related no-arbitrage conditions", *The Annals of Applied Probability*, 20: 267-311.
- [21] Cont, R., Tankov, P. (2004) *Financial modelling with jump processes* (Chapman & Hal)
- [22] Cont, R., Tankov, P. (2004), "Non-parametric calibration of jump-diffusion option pricing models," *Journal of computational finance*,7: 1-50
- [23] Corcuera, J.M., Guillaume, F., Madan, D.B., Schoutens, W.(2010) "Implied liquidity - towards stochastic liquidity modeling and liquidity trading," Working Paper.
- [24] Fang, F., Oosterlee, C.W. (2008) "A novel option pricing method based on Fourier-cosine series expansions," *SIAM Journal on Scientific Computing*, 31: 826-848.
- [25] Fang, F., Oosterlee, C.W. (2009) "Pricing early-exercise and discrete barrier options by Fourier-Cosine series expansions," *Numerische Mathematik*, 114: 27-62.

- [26] Föllmer, H., Schied, A. (2011) *Stochastic finance: an introduction In discrete time* (De Gruyter).
- [27] Hull, J. (2008) *Options, futures, and other derivatives* (Prentice Hall)
- [28] Jarrow, R. A. (2006) *Liquidity risk measurement and management: a practitioner's guide to global best practices* (Wiley Finance).
- [29] Ma, H. (2010) "Estimation of expected returns, time consistency of a stock return model, and their application of portfolio selection," Dissertation. University of Maryland, College Park
- [30] Madan, D.B. (2010) "Conserving capital by adjusting deltas for gamma in the presence of skewness," Working Paper.
- [31] Madan, D.B. (2010) "Stochastic processes in finance," *Annu. Rev. Fin. Econ.*, 2:277-314
- [32] Madan, D.B. (2010) S&P 500 index option surface drivers and their real world and risk neutral covariations, Working Paper.
- [33] Madan, D., P. Carr and E. Chang (1998), "The Variance Gamma process and option pricing", *European Finance Review*, 2: 79-105.
- [34] Madan, D.B., Eberlein, E., Schoutens, W. (2011) "Capital requirements, the option surface, market, credit and liquidity risk," Working Paper
- [35] Madan, D., Milne, F. (1991) "Option pricing with VG martingale components," *Math. Finance*, 1: 39-55
- [36] Madan, D.B., Pistorius, M., Schoutens, W. (2011) "The valuation of structured products using markov chain models," Working Paper
- [37] Madan, D., Schoutens, W. (2010), "Simple processes and the pricing and hedging of cliquets", Working Paper.
- [38] Madan, D., Schoutens, W. (2010), "Conic coconuts: the pricing of contingent capital notes using conic finance," Working Paper.
- [39] Madan, D., Schoutens, W. (2010), "Conic financial markets and corporate finance," Working paper.
- [40] Madan, D., Schoutens, W. (2011), "Tensor specific pricing," Working paper.

- [41] Madan, D., Schoutens, W. (2011), "Structured products equilibria in conic two price markets," Working paper.
- [42] Madan, D. and E. Seneta (1990), "The Variance Gamma (V.G.) Model for Share Market Returns", *Journal of Business*, 63: 511-524
- [43] McDonald, R. L. (2005), *Derivatives Markets (2nd edition)* (Addison Wesley)
- [44] Merton, R.C. (1973) " Theory of rational option pricing," *Bell J. Econ. Manag. Sci.*, 4: 141-83
- [45] Merton, R.C. (1976) " Option pricing when underlying stock returns are discontinuous," *J. Financ. Econ.*, 3:125-44
- [46] Mijatović, A. and M. Pistorius (2010), "Continuously Monitored Barrier Options Under Markov Processes", Working Paper.
- [47] O'Sullivan, C. and Moloney M. (2010) " The variance gamma scaled self-decomposable process in actuarial modelling", Working Paper in Geary Institute, University College Dublin.
- [48] Schoutens, W. (2003), *Lévy processes in finance: pricing financial derivatives* (Wiley Series in Probability and Statistics)
- [49] Seneta, E. (2004) "Fitting the Variance-Gamma model to financial data," *J. of Applied Probability*, 41: 177-187
- [50] Sharpe, W. F. (1966) "Mutual Fund Performance," *Journal of Business*, 39: 119-138.
- [51] Stoimenov, P., Simons, E. and Tistaert, J. (2004) A perfect calibration! Now what? *Wilmott Magazine*, March 2004.
- [52] Stoimenov, P., Wilkens S.(2005), "Are structured products fairly priced?", *Journal of Banking & Finance*, 29: 2971-2993
- [53] http://en.wikipedia.org/wiki/Market_liquidity#cite_note-0